

**Seb4 – an RNA-binding protein as a
novel regulator of myogenesis during early
development in *Xenopus laevis***

Dissertation zur Erlangung der Doktorwürde Dr. rer. nat.
an der Fakultät für Biologie der
Ludwig-Maximilians-Universität München

vorgelegt von Sabine Oberleitner
München, 2008

1. Gutachter: Prof. Peter Becker
2. Gutachter: Prof. Charles David

Tag der mündlichen Prüfung: 22.12.2008

Erklärung und ehrenwörtliche Versicherung:

Ich versichere hiermit ehrenwörtlich, dass die vorgelegte Dissertation von mir selbstständig und ohne unerlaubte Hilfe angefertigt ist. Es wurden keine anderen als die hier aufgeführten Hilfsmittel und Quellen benutzt.

Hiermit erkläre ich, dass ich mich anderweitig einer Doktorprüfung ohne Erfolg nicht unterzogen habe.

Danksagung

Ich danke...

Prof. Dr. Ralph Rupp für seine gute Betreuung, seine Diskussionsbereitschaft, sowie seinen Optimismus und seine wissenschaftliche Begeisterung.

Prof. Dr. Peter Becker für das hervorragende wissenschaftliche Arbeitsumfeld dieses Instituts und die Begutachtung dieser Arbeit.

Prof. Dr. Charles David für die Erstellung eines Zweitgutachtens .

Astrid Sulz für die Bereitstellung der Paraffinschnitte.

Dr. Jörn Boeke für die Hilfestellung bei den Gelfiltrations-Experimenten.

Dr. Elisabeth Kremmer für die Herstellung der monoklonalen Antikörper.

Prof. Dr. Schmidt-Zachmann für die Bereitstellung der Antikörper (co-IF)

Mein herzlicher Dank gilt meinen lieben Kollegen. Besonders Edith Mentele, Dr. Katrin Mansperger, Barbara Hölscher, Dr. Britta Linder-Stuart und Dr. Ryan Cabot danke ich für die herzliche Zusammenarbeit, ihre Hilfsbereitschaft und den vielen Spaß. Auch danke ich unserem Ärzteteam Laura Michel, Markus Nieberler und Tobias Schneider für die medizinische Beratung und die Gaudi.

Dankbar bin auch dem Salatclub für die herausragenden Kreationen, unseren Imhof-Nachbarn für die erquickenden Küchengespräche, und allen Teilnehmern der Lebensberatung und Sprechstunden bei Dr. Auerbach.

Meinen lieben Eltern danke ich für alles – vor allem aber für ihre bedingungslose Liebe und Unterstützung.

Table of Contents

Table of Contents	I-IV
Summary	1
1 Introduction	2
1.1 <i>Xenopus laevis</i> as a model organism of cell differentiation	2
1.1.1 The life cycle of <i>Xenopus laevis</i>	2
1.1.2 Developmental concepts.....	3
1.1.3 Methodological advantages of <i>Xenopus</i>	4
1.2 Mesoderm specification and myogenesis	5
1.2.1 Mesoderm induction.....	5
1.2.1.1 <i>Forming the mesoderm and its derivatives</i>	5
1.2.1.2 <i>Signalling factors involved in mesoderm induction</i>	6
1.2.2 Myogenesis.....	8
1.2.2.1 <i>Muscle formation</i>	9
1.2.2.2 <i>Signalling in myogenesis</i>	10
1.3 RNA-binding proteins and their function	13
1.3.1 The RNA recognition motif RRM.....	14
1.3.2 Post-transcriptional regulation by RRM proteins.....	18
1.3.2.1 <i>Polyadenylation</i>	19
1.3.2.2 <i>Splicing</i>	20
1.3.2.3 <i>mRNA export</i>	20
1.3.2.4 <i>mRNA stability/degradation</i>	21
1.3.2.5 <i>mRNA translation</i>	22
1.3.3 RRM proteins in differentiation.....	22
1.3.3.1 <i>RNA-binding proteins as developmental regulators</i>	23
1.3.3.2 <i>Regulation of localized RNAs in pattern formation</i>	24
1.3.4 Seb4 subfamily members in <i>Xenopus</i>	25
1.4 Objectives	28
2 Material and Methods	30
2.1 Laboratory Equipment	30
2.2 Reagents	31
2.2.1 Chemicals.....	31
2.2.2 Proteins and enzymes.....	31
2.3 Antibodies	31

2.3.1	Primary antibodies	31
2.3.2	Secondary antibodies	32
2.4	Oligonucleotides	33
2.4.1	Primers for Seb4 cloning.....	33
2.4.2	Primers for RT-PCR.....	34
2.4.3	Morpholino oligonucleotides	34
2.5	Plasmids.....	34
2.6	Biological material.....	35
2.7	Molecular biological methods	36
2.7.1	Solutions.....	36
2.7.2	Isolation of nucleic acids	37
2.7.2.1	<i>Preparation of DNA.....</i>	<i>37</i>
2.7.2.2	<i>Isolation of RNA.....</i>	<i>37</i>
2.7.3	Manipulation and analysis of nucleic acids.....	38
2.7.3.1	<i>Cloning methods.....</i>	<i>38</i>
2.7.3.2	<i>Gel electrophoresis of nucleic acids.....</i>	<i>38</i>
2.7.3.3	<i>Isolation of DNA fragments from agarose gel.....</i>	<i>38</i>
2.7.4	Polymerase chain reaction (PCR).....	38
2.7.4.1	<i>PCR amplification of DNA fragments for cloning.....</i>	<i>38</i>
2.7.4.2	<i>RT-PCR assay.....</i>	<i>39</i>
2.7.5	<i>In vitro</i> transcription	39
2.7.5.1	<i>In vitro</i> transcription for microinjection.....	39
2.7.5.2	<i>In vitro</i> transcription of digoxigenin labelled RNA probes	39
2.7.6	RNA <i>in situ</i> hybridization.....	40
2.7.7	RNA-co-immunoprecipitation	41
2.7.7.1	<i>Solutions.....</i>	<i>41</i>
2.7.7.2	<i>Coupling of antibody to ProteinG Sepharose-beads</i>	<i>41</i>
2.7.7.3	<i>Blocking of beads</i>	<i>42</i>
2.7.7.4	<i>Embryo extracts for RIP- reaction</i>	<i>42</i>
2.7.7.5	<i>Radioactive labelling via reverse transcription</i>	<i>42</i>
2.7.7.6	<i>RNA detection with autoradiography.....</i>	<i>43</i>
2.7.7.7	<i>Northern blot analysis.....</i>	<i>43</i>
2.8	Protein analysis.....	44
2.8.1	Solutions.....	44
2.8.2	Coupled <i>in vitro</i> transcription and translation	45
2.8.3	Protein extraction from <i>Xenopus laevis</i> embryos (embryo extracts).....	45
2.8.4	Nuclear preparation of <i>Xenopus laevis</i> embryos	46

2.8.5	SDS-PAGE.....	46
2.8.5.1	Western blot analysis.....	47
2.8.5.2	Coomassie-staining.....	47
2.8.5.3	Silver-staining.....	47
2.8.6	Protein-immunoprecipitation (IP).....	47
2.8.7	Gelfiltration.....	48
2.8.8	Purification of Gst-tagged recombinant Seb4 protein.....	48
2.8.8.1	Dotblot.....	49
2.9	Histological methods.....	49
2.9.1	Solutions.....	49
2.9.2	Immunocytochemistry (ICC).....	50
2.9.3	Immunofluorescence (IF).....	51
2.9.3.1	Immunofluorescence on embryo sections.....	52
2.9.3.2	Immunofluorescence on A6 culture cells.....	52
2.9.3.3	Image acquisition.....	53
2.10	Embryological methods.....	53
2.10.1	Solutions.....	53
2.10.2	Superovulation of female <i>Xenopus laevis</i>	54
2.10.3	Preparation of testis.....	54
2.10.4	<i>In vitro</i> fertilization of eggs and culture of the embryos.....	54
2.10.5	Removal of the egg jelly coat.....	54
2.10.6	Injection of embryos.....	54
2.10.7	Protein knock-down in embryos by antisense.....	
	Morpholino oligonucleotide.....	55
3	Results.....	56
3.1	Generation of antibodies against Seb4.....	56
3.1.1	Specificity of antibodies raised against Seb4.....	58
3.1.2	Defining the Seb4 antibodies.....	60
3.2	Spatial and temporal expression of Seb4.....	62
3.2.1	Developmental expression of Seb4 protein <i>in vivo</i>	62
3.2.2	Two specific Seb4 proteins.....	64
3.2.3	Seb4 is expressed in mesodermal and ectodermal derivatives.....	66
3.3	Seb4 depletion leads to reduced muscle and lens.....	69
3.3.1	Seb4 Morpholino efficiently depletes Seb4 <i>in vitro</i> and <i>in vivo</i>	69
3.3.1.1	Depletion of Seb4 causes ablation of muscle and lens.....	
	specific gene expression.....	72
3.4	Interaction partners of Seb4.....	74

3.4.1	Proteins interacting with Seb4.....	75
3.4.1.1	<i>Co-immunoprecipitation</i>	75
3.4.1.2	<i>Seb4 is not bound in a complex</i>	77
3.4.2	Seb4 – an RNA-binding protein?	79
3.4.2.1	<i>RNA-preserving-conditions ensure high protein-IP efficiency</i>	80
3.4.2.2	<i>Northern blot total RNA screen</i>	81
3.5	Localization of Seb4	84
3.5.1	Seb4 is distributed in equal amounts to the cytoplasm and the nucleus.	84
3.5.2	Seb4 is expressed in the <i>Xenopus</i> cell lines A6 and XTC	85
3.5.3	Subcellular localization of Seb4 in the embryo and in A6 cells	87
3.5.3.1	<i>Seb4 localization in different embryonic tissues is mainly nuclear</i>	87
3.5.3.2	<i>Seb4 knock-down leads to an efficient loss of Seb4 protein</i> <i>in embryonic myocytes</i>	91
3.5.3.3	<i>In A6 cells Seb4 is localized mainly to the cytoplasm</i>	92
3.5.4	Co-localization experiments by IF	93
3.5.4.1	<i>Secondary antibody compatibility tests</i>	93
3.5.4.2	<i>Markers for co-localization studies</i>	95
3.5.4.3	<i>Co-IF in embryonic myocytes</i>	97
3.5.4.4	<i>Co-IF in A6 cells</i>	98
4	Discussion	101
4.1	Molecular tools	102
4.1.1	Antibodies.....	102
4.1.2	Morpholinos	103
4.2	Spatio-temporal expression of Seb4 in <i>Xenopus</i> embryos	104
4.2.1	Seb4 is an abundant protein expressed in early development	104
4.2.2	Seb4 expression in mesodermal and ectodermal derivatives.....	106
4.3	Nuclear and cytoplasmic localization of Seb4	107
4.4	Seb4 is found as a monomer with no associated targets	110
4.5	Seb4 functions as a myogenic regulator	113
4.6	Conclusions	115
4.7	Outlook	116
	Abbreviations	118
	References	120

Summary

During vertebrate development differentiation programmes unfold stepwise and involve a multitude of signals and responses that are spatially and temporally regulated. Transcriptional control, mediated by transcription factors, is a key feature of cell differentiation, but so is regulation on the post-transcriptional level, mediated by RNA-binding proteins (RBPs). Besides having general roles in the control of RNA metabolism, RBPs have been implicated in tissue-specific processes during embryonic development. The significance of such post-transcriptional events for the regulation of cell differentiation becomes more and more evident.

Despite extensive studies in muscle differentiation, some aspects of the process are still largely unknown. This includes the signals and regulators involved in primary activation of the myogenic master regulator MyoD as well as the downstream mechanisms by which MyoD stabilizes the muscle cell fate. The discovery of our laboratory that the putative RBP Seb4 is an early MyoD target has raised the possibility that MyoD promotes muscle differentiation through post-transcriptional mechanisms.

In this study, I investigated the biochemical properties and biological function of Seb4 during early development in *Xenopus laevis*. Seb4 is an evolutionary conserved small protein, containing a single RNA recognition motif (RRM). In contrast to most ubiquitously expressed RBPs, the expression pattern of Seb4 is regulated in a stage and tissue-specific fashion in ectodermal and mesodermal derivatives. My results provide evidence that Seb4 is essential for muscle and lens differentiation in *Xenopus*. In embryonic muscle cells Seb4 protein is unexpectedly highly abundant and located in both cytoplasmic and nuclear compartments in a distinct pattern. Consistent with this, RNA-coimmunoprecipitation assays have failed to identify selective RNA-targets. Furthermore, by immunoprecipitations no specific Seb4-associated proteins were identified, confirmed by the fact that Seb4 elutes as a monomer from gelfiltration columns. Taking all these evidences in consideration, this detailed analysis revealed Seb4 as a key regulator of various differentiation programmes and suggests Seb4 to have a more general role in the RNA metabolism of differentiating cells, rather than a selective function.

1 Introduction

1.1 *Xenopus laevis* as a model organism of cell differentiation

The development of an organism is based on the formation of complex structures from differentiated cell types from a fertilized egg. To investigate this complex process experimentally, it requires easily accessible model systems.

The African clawed frog *Xenopus laevis* has been one of the most favored and best-studied model organisms for vertebrate embryology over the past decades. Major insights into early embryogenesis like signalling events important for body axis determination or germlayer formation were obtained from studies with *Xenopus*.

1.1.1 The life cycle of *Xenopus laevis*

Figure 1 illustrates an overview of the life cycle of *Xenopus laevis*. After fertilization, *Xenopus* embryos undergo cell cycles that have characteristic features (Niewkoop & Faber, 1967). During the first, 90-minute cell cycle, cortical cytoplasmic movements and male and female pronuclear fusion occur. The next eleven divisions occur at 20- to 30-minute intervals with no gap phases, while the embryo forms a blastula of 4000 cells, which encloses a fluid-filled blastocoel cavity. This mid-blastula embryo has three regions, the animal cap (which forms the roof of the blastocoel), the equatorial or marginal zone (the lateral walls and floor of the blastocoel) and the vegetal mass. Although all mid-blastula cells are pluripotent, explants of the animal cap form ectodermal derivatives in culture, while equatorial explants form mesoderm and vegetal explants form endoderm. At the end of the twelfth cycle, gap phases reappear, the cell cycle lengthens to 50min and zygotic transcription starts (this is called the mid-blastula transition, MBT; 5-6 hours post fertilization, hpf). In the 15th cycle, the dorsal lip of the blastopore forms at 9hpf, the cell movements of gastrulation begin and mitosis stops. Gastrulation converts the embryonic blastula into three layers, and establishes definitive anteroposterior and dorsoventral axes (Heasman, 2006). During neurogenesis starting 12hpf, the organs begin to form being fully developed by late tailbud stages. In regard to muscle formation, segregation of the first anterior somites begins at stage 17. Simultaneously with the segregation of an increasing number of somites from the somitic mesoderm, their cellular differentiation proceeds in a cranio-caudal direction. At stage 20 the myocoelic cavities begin to disappear. In the most anterior somites the myoblasts are

already spindle-shaped, while at stage 21 myofibrillae are formed. These myofibrillae become arranged in fusiform bundles at stage 23. At stage 24 initial motor actions can be observed. At stage 26 first spontaneous movements occur. The dorsal muscles derived from the myotomes and the ventral muscles develop further during the stages 37 and 39. At stage 51 the first indications of the formation of secondary muscles originating from the group of primary muscles appear. After metamorphosis the adult frog has developed (Nieukoop & Faber, 1967).

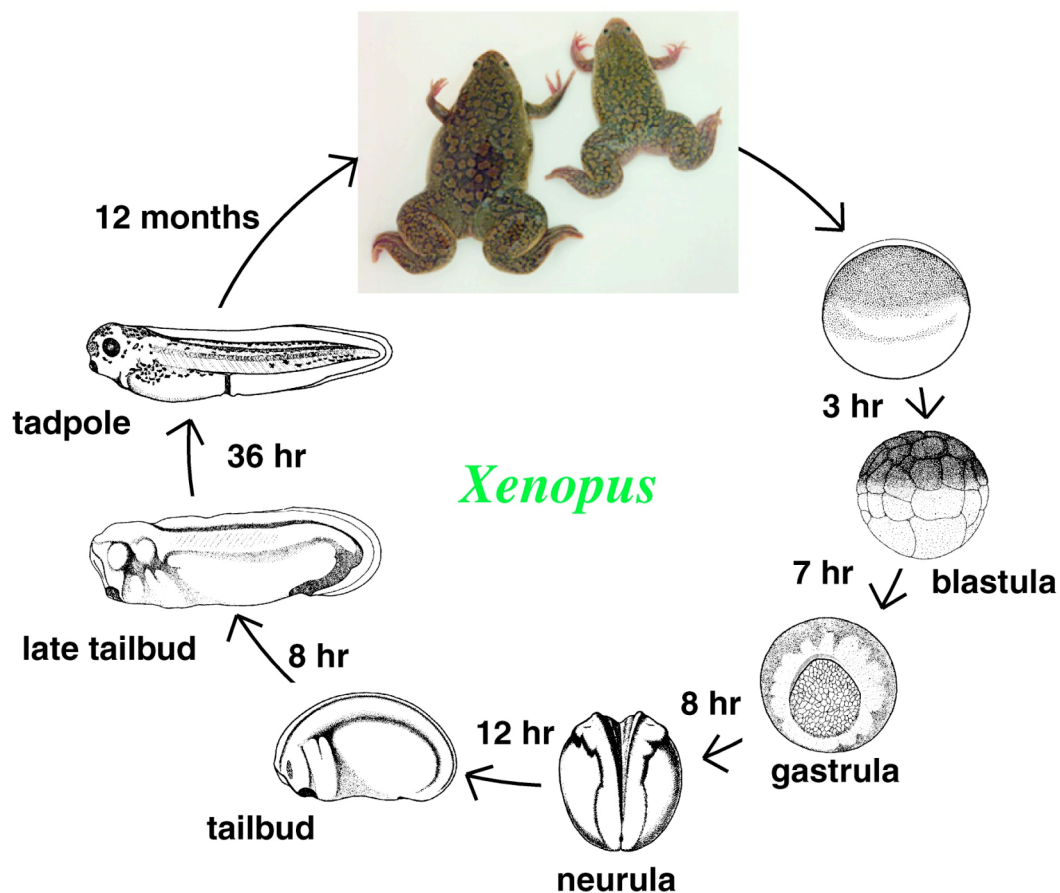


Figure 1: Life cycle of *Xenopus laevis*

All stages shown are based on the normal table of Nieukoop and Faber (Nieukoop & Faber, 1967; Nieukoop & Faber, 1994) hr: hours post fertilization (hpf); (http://www.xenbase.org/xenbase/original/WWW/Marker_pages/Xenopus_stages/Xenopus_stages.html).

1.1.2 Developmental concepts

Development results from the coordinated behaviour of cells. The major processes involved in development are cell divisions, pattern formation, morphogenesis, cell differentiation, cell migration, cell death, and growth. Since the

somatic cells in the embryo generally contain the same genetic information, the changes that occur during development are controlled by the differential activity of selected genes and maternal determinants in different groups of cells. One way of changing cell fate and directing development is communication between cells mediated by signalling molecules, e.g. morphogens. Morphogens are small, secreted proteins, which diffuse over long distances, form concentration gradients, and give the cells positional information within the embryo, which is interpreted and causes a specific response. Pattern formation, in particular the early steps after fertilization of the egg, is also regulated by maternal determinants like localized mRNAs. But also later in development cytoplasmic RNA localization is a means to create polarity by restricting protein expression to a discrete subcellular location (Wolpert, 1998).

1.1.3 Methodological advantages of *Xenopus*

Among the many advantages, the major advantages of *Xenopus laevis* over other model organisms like mouse is the extra-uterine development, the enormous size of egg clutches (several hundred up to a few thousand eggs per day), and the hormone-inducible super ovulation of female frogs. Cohorts of eggs can be fertilized *in vitro* at the same time, which allows standardization and synchronous development. This provides sufficient material to perform biochemical experiments. The embryonic development is rapid, which offers the possibility to collect different developmental stages of one batch for comparative analyses. The embryos are relatively large with 1-2mm in diameter with only little pigmentation. Therefore, they are easy to manipulate (for example by nucleic acid injection) and provide the possibility of macroscopical analysis. Furthermore, the embryos can be simply cultured in semi-sterile conditions without external growth factors.

Xenopus laevis has about the same DNA content in each of its cells as humans. It has 36 chromosomes, and the evolutionary history indicates that an ancestor of *Xenopus laevis* probably had 20 chromosomes, which were duplicated. The duplicate copies of each gene have subsequently diverged, complicating molecular analysis. For genetic analyses investigators focus their studies on a close relative of *Xenopus laevis*, *Xenopus tropicalis*, which offers the possibility of such genetic manipulations, because within the *Xenopus* genus, *Xenopus tropicalis* is the only diploid species. But the small size of the embryos limits macroscopical analyses.

Another major advantage of *Xenopus laevis* with regard to understanding the basic biology of cell determination is the utility of the animal cap-explant assay. This assay provided a valuable means for identifying the first mesoderm-inducing factors (members of the transforming growth factor signalling class β ; TGF- β) and

shed more light on endogenous signalling (Grunz et al, 1988; Rosa et al, 1988). *Xenopus laevis* became thereby the model organism with the best studied signalling pathways and the most clones isolated from it.

1.2 Mesoderm specification and myogenesis

During early vertebrate embryogenesis three germ layers, the ectoderm, mesoderm, and endoderm, are formed from pluripotent cells at the onset of gastrulation. The specification of these germ layers is substantially influenced by maternally deposited positional information. Along the animal-vegetal axis the ectoderm arises from the animal cap, the endoderm derives from the vegetal pole regions, while the mesoderm forms in the marginal zone.

1.2.1 Mesoderm induction

Mesoderm induction is one of the classical challenges in developmental biology. Various developmental biology approaches, particularly in *Xenopus laevis*, have identified many of the key factors that are involved in this process and have provided major insights into how these factors interact as part of a signalling and transcription-factor network.

1.2.1.1 Forming the mesoderm and its derivatives

Besides creating the body cavity, one of the major tasks of gastrulation is to create mesoderm. In *Xenopus*, the mesoderm induction creates a zone of mesodermal cells at the equator of the embryo (the marginal zone). Complex morphogenetic movements bring these mesodermal cells into their correct position between the endoderm and the ectoderm within the post-gastrula embryo. The fate map in Figure 2 shows how the mesoderm becomes subdivided along the dorso-ventral axis of the blastula and which tissues the mesodermal germlayer gives rise to.

The mesoderm produces a wide range of tissues including the muscles, heart, vasculature, blood, kidney, gonads, dermis and cartilage. It also has a major role in the morphogenetic movements of gastrulation and patterning the embryo.

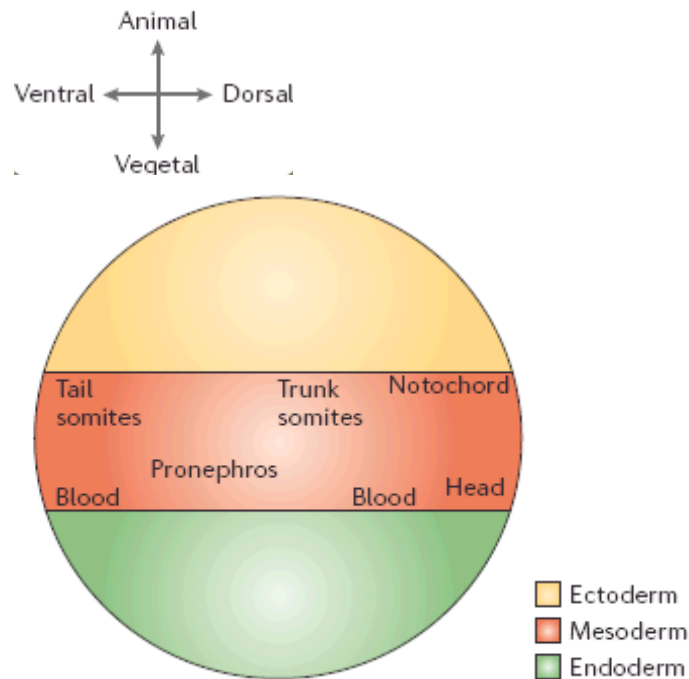


Figure 2: Fate map of the mesoderm in a *Xenopus* embryo

The figure was modified from (Kimelman & Schier, 2002).

1.2.1.2 Signalling factors involved in mesoderm induction

Simplified, the Nodal family is involved in initiating mesoderm formation, fibroblast growth factors (FGFs) and Wnt protein family members (Wnts) are involved in maintaining the mesodermal state, and bone morphogenetic proteins (BMPs) are involved in patterning the mesoderm. These factors, however, can actually do much more. For example, in various experimental models, FGFs, BMPs and Wnts have been shown to be sufficient for initiating mesoderm formation (Slack et al, 1987); (Kimelman & Kirschner, 1987), and Nodal family members have been shown to be involved in patterning the mesoderm (Birsoy et al, 2006; Gritsman et al, 2000). These results indicate that extracellular signals do not necessarily have rigidly separated functions in mesoderm induction, and instead indicate that these signals might be networking while forming and patterning the mesoderm.

In mesoderm specification the T-box transcription factor VegT (*alias* Brat, Xombi, or Antipodean) activates mesoderm induction by regulating the transcription of a large number of zygotic genes, none of which are expressed in animal cells. Additionally, VegT affects endodermal specification, dorsoventral axis formation, and convergence extension.

During oogenesis *vegT* is supplied maternally to the oocyte and is also expressed zygotically within the equatorial zone. The maternal mRNA is located

vegetally in mature oocytes and early embryos (Xanthos et al, 2001; Zhang et al, 1998). At fertilization, *vegT* transcripts are released from the vegetal pole and slowly diffuse upwards. Because the third cleavage plane passes through the equator of the embryo before the transcripts leave the vegetal hemisphere, the *vegT* transcripts are trapped there, and therefore the subsequently translated VegT protein is restricted to the vegetal half.

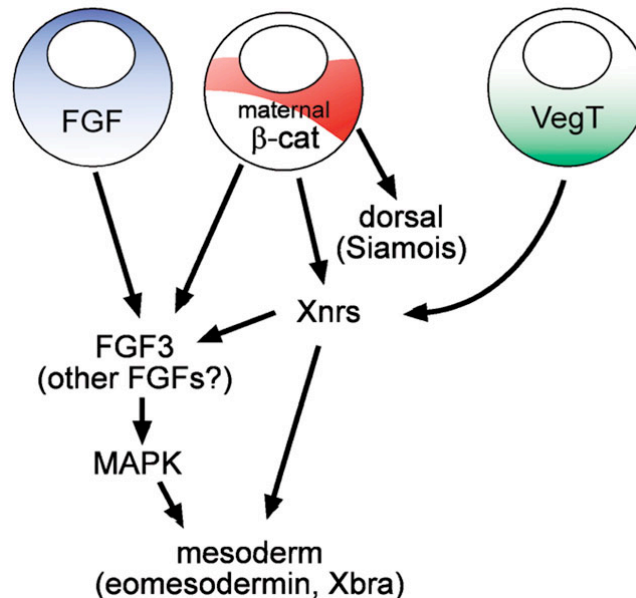


Figure 3: Early mesoderm induction in *Xenopus*

(Schohl & Fagotto, 2003)

Both β -catenin and VegT induce *Xnrs*. FGF, Xnr and β -catenin signals cooperate to induce FGF3 and, perhaps, other FGFs along the marginal zone and thus activate MAPK. The combination of Xnr and FGF/MAPK signals then activates expression of mesodermal genes such as eomesodermin and *Xbra* (Schohl & Fagotto, 2003).

In the 32-cell-stage *Wnt11* mRNA and protein is enriched on the dorsal side, presumably due to the cortical cytoplasmic rotation triggered by the sperm entry. The result of this movement is the stabilization of β -catenin, an intracellular Wnt pathway component, on the future dorsal side of the embryo. This asymmetrical stabilization of β -catenin is essential for the formation of all dorsal and anterior structures (Heasman et al, 1994; McMahon & Moon, 1989). Among the major targets of the *Wnt11*/ β -catenin/Tcf3 pathway are *Xnr3* and *siamois*, and genes that have essential roles in head formation and convergent extension movements (Lemaire et al, 1995; Smith et al, 1995).

At the start of zygotic transcription at MBT, VegT activates its targets. Many of its targets are transcription factors regulating endoderm formation, factors

that are involved in distinguishing between endodermal and mesodermal territories (*mixer*) (Kofron et al, 2004; Xanthos et al, 2001), Wnt antagonists (*chordin*, *cerberus*, *noggin* and *dickkopf*) (Xanthos et al, 2002). Another group of target genes that are directly regulated by VegT are the *Xenopus nodal related (Xnr)* genes (encoding TGF- β transcription factors) *Xnr 1, 2, 4, 5, 6* and *derriere*. High levels of Xnrs induce the Spemann's organizer in the prospective dorsal mesoderm – the main dorsalizing centre of the embryo. At gastrula stage the organizer, in turn, secretes another important group of molecules involved in mesoderm induction and patterning. These secreted molecules are antagonizing the growth factors of the BMP-, Wnt- and TGF β - pathway by binding to the growth factors in the extracellular space and prevent them from binding to their cognate receptors.

Generally, the *Xenopus nodal related (Xnr)* genes are required for the formation of bottle cells, normal gastrulation movements, and most importantly they are the inducers of mesoderm formation (Clements et al, 1999; Hyde & Old, 2000; Kofron et al, 1999).

1.2.2 Myogenesis

There are three major muscle types: cardiac, skeletal, and smooth. All of them are derived from the embryonic mesoderm during early embryogenesis. Cardiac precursor cells come from a population of cells in the anterior lateral plate mesoderm in early embryos. The heart is the first functioning organ to form during vertebrate development. Skeletal muscle arises from paraxial mesoderm that gives rise to the somites along the anteroposterior axis of the embryo. Somites become compartmentalized into the myotome, sclerotome, and dermatome, which give rise to skeletal muscle, axial skeleton, and dermis, respectively. In contrast to cardiac and skeletal muscle cells, which exit the cell cycle to undergo terminal differentiation, smooth muscle cells are highly plastic and can modulate their phenotypes between proliferative and differentiated states in response to extracellular cues. Much of our understanding of skeletal muscle gene expression regulation during development is at the level of transcription (Berkes & Tapscott, 2005).

During early embryogenesis, after mesoderm induction, the myogenic determination factors MyoD and Myf5 are activated in pre-somitic mesoderm in response to mesoderm-inducing factors. After these first inductions of the myogenic programme, forming muscles in *Xenopus* can have different destinies, some of these resulting in cell death before adulthood. In particular, during metamorphosis, the primary myotomal myofibers completely die and are progressively replaced by secondary "adult" multinucleated myofibers (Chanoine & Hardy 2003).

1.2.2.1 Muscle formation

During the development of most skeletal muscles, multinucleate myotubes are formed by fusion of many myoblasts (Youn & Malacinski, 1981). However, this does not occur during the myogenesis of the primary myotome muscle of *Xenopus laevis*. Here, myoblasts differentiate into uninucleate myocytes (Muntz, 1975; Youn & Malacinski, 1981) and later, at the onset of metamorphosis, develop into multinucleate muscle fibers. For a long time, the fate of the primary myotomal myofibers and the origin of the multinucleated secondary myotomal myofibers have been controversial (Muntz, 1975). In 1987, Boudjelida and Muntz strongly suggested that multinucleated primary myotomal fibers in *Xenopus* arise from amitotic division of the primary nuclei; hence, without cell fusion, the nuclei of the uninucleate myotomal myotubes would be polyploid up to octoploid in this species (Boudjelida & Muntz, 1987). This mechanism is mainly responsible for the multinucleation of the majority of the primary larval fibers, but it cannot be excluded that some secondary migrating myoblasts or some activated satellite cells could take part in the multinucleation process. On the other hand, some mononucleated fibers could fuse to form multinucleated secondary myotomal myofibers.

The primary myotome derives from the somites, which in turn come from mesoderm tissue that invaginated during gastrulation. Somites are formed progressively at the rate of approximately 1.5 per hour from neurula stage 17 onward. In *Xenopus*, by far the greatest part of the somite consists of myotome cells that will form muscle. A small dorsolateral part of each somite will form skin (dermatome) and only the smallest amount nearest the notochord forms the sclerotome (Nieuwkoop & Faber, 1967; Gurdon et al, 1998). In *Xenopus*, the somite cells initially orient perpendicular to the axis of the unsegmented paraxial mesoderm, then, rotate through 90 degrees to lie parallel to the axis with each primary myotome myofiber spanning the length of a single myotome (Hamilton, 1969; Youn & Malacinski, 1981).

During metamorphosis the primary myotomal myofibers die and are progressively replaced by secondary multinucleated myofibers arising from fusion of recently migrated adult-type myoblasts (Nishikawa & Hayashi, 1994). These authors reported programmed muscle cell death to be important in tail degeneration as well as in the larval-to-adult conversion of the dorsal body muscles of *Xenopus* (Nishikawa & Hayashi, 1994). As known so far, *Xenopus* is thus the only model system in which the primary body muscles die and are replaced by new adult muscles. The area of muscle cell death expands like a wave from the base of the tail to the anterior and posterior sides.

1.2.2.2 Signalling in myogenesis

In *Xenopus* the activation of the myogenic programme is initiated by the members of the MyoD family in the muscle-forming region. Then initiation of myogenesis occurs in response to mesoderm-inducing factors. Different members of the FGF, TGF- β , and Wnt protein families have been implicated in this process.

The members of the MyoD gene family, including MyoD, Myogenin, Myf5, and MRF4, encode basic helix-loop-helix (bHLH) transcription factors and contain one or two transactivation domains (at the N- and C-terminus). Remarkably, these factors are able to convert non-muscle cells to a muscle phenotype in culture. These myogenic regulatory factors (MRFs) stimulate muscle gene transcription by forming heterodimers with ubiquitous bHLH proteins, known as E proteins. These bind to E-boxes, which are DNA elements of 6bp bearing the CANNTG consensus sequence, irrespectively of the nature of the center nucleotides (Arnold & Winter, 1998).

At the initiation of myogenesis, members of the Wnt family of secreted glycoproteins are induced by BMP4 in the dorsal neural tube in mammals (Borello et al, 1999). Muscle specification during gastrulation also depends on the repression of BMP signalling, as triple depletions of Noggin, Chordin and Follistatin eliminate muscle precursor gene expression (Khokha et al, 2005). Shi et al. (2002) reported that the Wnt/ β -catenin pathway is required for regulating myogenic gene expression in the presumptive mesoderm and may directly activate the expression of the *myf5* gene in the muscle precursor cells. These Wnt proteins, in combination with low concentrations of Sonic hedgehog (Shh) from the notochord and floor plate, induce the epaxial myotome, in which the expression of Pax3, Myf5, MRF4 and subsequently MyoD is promoted (see Figure 4 upper panel). Dosch et al. (1997) showed that Myf5 expression and muscle differentiation require a low dose of BMP4, resulting from superposition of antagonizing BMP4 and noggin proteins *in vivo* (Dosch et al, 1997; Hoppler et al, 1996). This result points out the crucial role of secreted molecules involved in mesoderm patterning on MRF regional expression in gastrula embryos.

The ability to induce MyoD is under the control of linker histone proteins, which act as transcriptional inhibitors of MyoD induction (Steinbach et al, 1997). Indeed, maternal stores of the B4 linker Histone that are assembled into chromatin during the early cleavage divisions are replaced by somatic histone H1 during gastrulation. This transition in chromatin composition causes selective transcriptional silencing of regulatory genes required for mesodermal/muscle differentiation pathways (Vermaak et al, 1998).

Recent studies have established that induction is mediated by the cAMP-activated protein kinase A through the activity of the transcription factor CREB. CREB phosphorylation enables recruitment of p300. It is of interest to note that mice lacking either CREB protein or the acetyltransferase activity of p300 have impaired expression of the myogenic bHLH transcription factors, suggesting the possibility that CREB and p300, perhaps through direct interaction, might be required for activation of the myogenic programme (Chen et al, 2005; Roth et al, 2003; Sartorelli & Caretti, 2005).

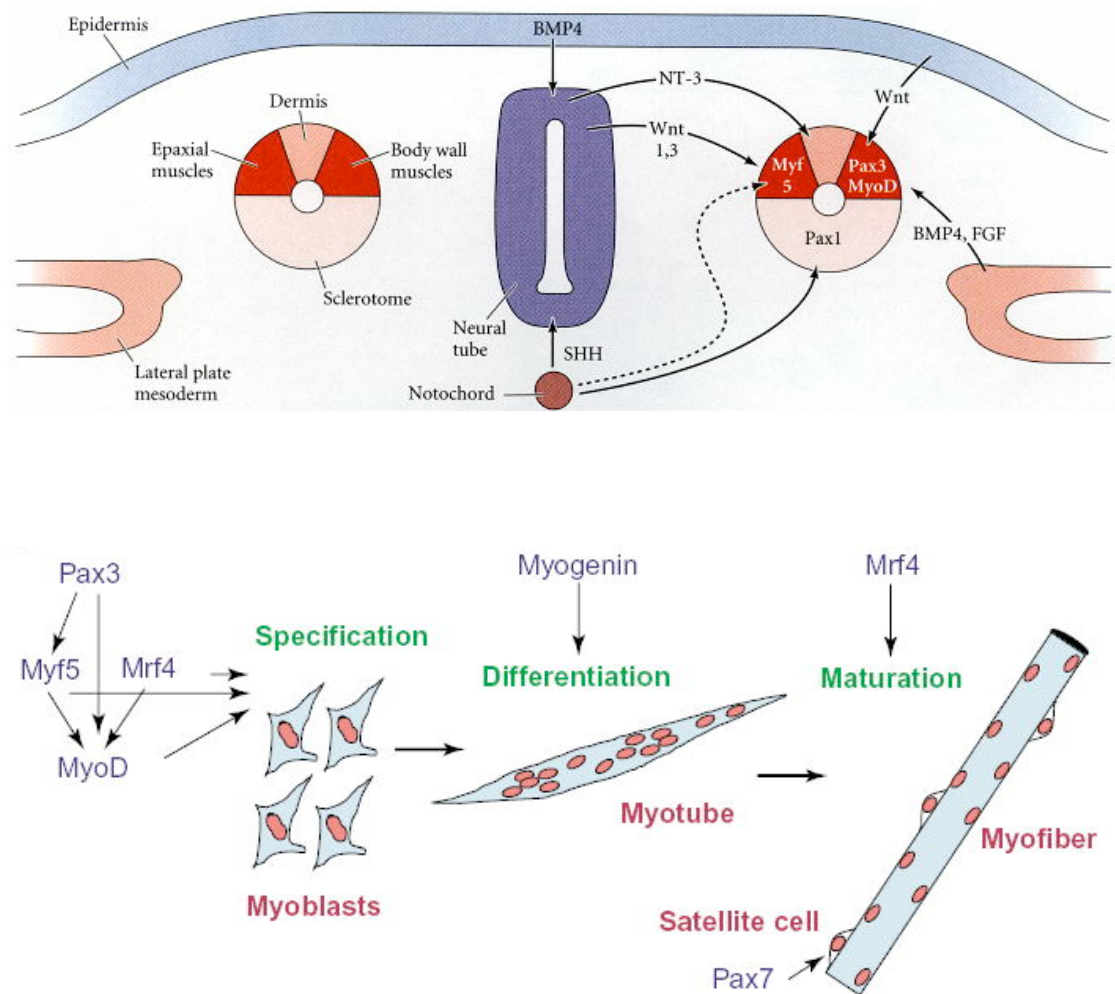


Figure 4: Models of major interactions in myogenesis

(Gilbert, 2000; Sartorelli & Caretti, 2005)

Several pathways are involved in establishing muscle precursor fates. First, FGF signalling and Xbra expression are required and maintain each other's expression. By mid-gastrulation the myogenic markers Mesp1, Myf5 and MyoD are all expressed in an equatorial omega shaped domain similar to the ring domain of

xbra and *fgf*. Depletion of FGF4, FGFR1 or *Xbra* causes severe reduction in their expression (Conlon et al, 1996; Yokota et al, 2003). Myogenin and MRF4 are hierarchically downstream of MyoD and Myf5 and are involved in muscle differentiation and myofiber formation, respectively Myf5, MRF4 and MyoD can act as specification genes, whereas myogenin is required for differentiation of specified myoblasts into myotubes, and MRF4 is involved in myofiber formation. Additionally to the role of MRF4 in terminal differentiation it seems to act earlier during determination as well. Even in the absence of MyoD and Myf5, skeletal muscle is still formed as long as MRF4 expression is not perturbed (Kassar-Duchossoy et al, 2004). Pax7 is required for satellite cell specification (Berkes & Tapscott, 2005; see Figure 4 lower panel).

Myf5 and MyoD can both be detected in pre-somitic mesoderm at the transcript level and at the protein level for MyoD (Hopwood et al, 1989; Hopwood et al, 1991; Hopwood et al, 1992; Scales et al, 1990). Myogenin expression is found later than Myf5 and MyoD. Although Myogenin expression is always associated with muscle differentiation in mammals (co-occurs with the initial appearance of transcripts of the *cardiac α -actin* gene, the first muscle structural gene to be expressed), *Xenopus* myogenesis displays the peculiar feature that Myogenin is not expressed in primary myotome, thus supporting the hypothesis that any other MRF (Myf5, MyoD, or MRF4) could play the role of myogenin during *Xenopus* primary myogenesis. In *Xenopus*, *myogenin* mRNA expression is restricted to secondary myogenesis, including the formation of new muscles in developing limbs, as well as in dorsal muscles during body remodeling occurring at metamorphosis (Nicolas et al, 1998).

Whereas extensive studies on the expression of Myf5 and MyoD during *Xenopus* myogenesis have been carried out, nothing was known about the spatio-temporal accumulation of MRF4 transcripts and protein. Whole-mount *in situ* analysis revealed the first nuclear *Xenopus* MRF4 expression in the more differentiated anterior myocytes of the embryo. *Mrf4* mRNA accumulation later extended posteriorly but was never detected in the posterior unsegmented mesoderm, in contrast to MyoD and Myf5 (Della Gaspera et al, 2006).

Muscle determination and differentiation is not an all-or-none process but one that occurs gradually and may involve a multitude of signals and responses on the transcriptional as well as on the post-transcriptional level. Recent genetic studies have demonstrated that also miRNAs are required for both proper muscle development and function, with crucial roles for miRNAs being identified in regulating

muscle cell proliferation and differentiation. Several miRNA genes, like miRNAs *miR-1*, *miR-133*, *miR-206*, and *miR-208*, are specifically expressed or highly enriched in skeletal and/or cardiac muscle (Callis et al, 2008). Beside transcription factors and miRNAs also RNA-binding proteins gain more and more importance in studying developmental processes, like myogenesis.

1.3 RNA-binding proteins and their function

In eukaryotes, transcription and translation occur in separate compartments, the nucleus and the cytoplasm, respectively. This allows eukaryotes to carry out extensive post-transcriptional processing of pre-mRNA that produces a more diverse assortment of mRNAs from its genome and provides an additional layer of gene regulation. Genome-wide studies revealed distinct programmes of RNA regulation, suggesting a complex and versatile post-transcriptional regulatory network. This network is controlled by specific RNA-binding proteins and/or non-coding RNAs. Putative RNA-binding proteins comprise 3 – 11% of the proteomes in bacteria, archaea and eukaryotes. The large number of RNA-binding proteins (RBPs) in all domains of life may merely reflect the ancient origin of RNA regulation, which is possibly the most evolutionary conserved part of cell physiology (Anantharaman et al, 2002).

RBPs play key roles in post-transcriptional control of mRNAs, which, along with transcriptional regulation, is a major way to regulate patterns of gene expression during development and adulthood. Eukaryotic cells encode a large number of RBPs (thousands in vertebrates), each of which has unique RNA-binding activity and protein-protein interaction characteristics (Glisovic et al, 2008). RBPs regulate every aspect of RNA function. This activity is mediated by a relatively small number of RNA-binding scaffolds whose properties are further modulated by auxiliary domains. Recent findings demonstrate that multiple mRNAs that encode functionally related proteins are co-regulated by one or more sequence-specific RBPs as post-transcriptional RNA operons or higher-order regulons (Keene, 2007). Ribonomic studies (systematic identification of RNAs associated with specific RBPs) have now been conducted for more than 30 specific RBPs. The results from these studies generally support and extend the proposed post-transcriptional operon model. Each of the analyzed RBPs has a unique RNA-binding spectrum comprised of 20 – 1000 distinct transcripts that often share functionally related themes. The spectra of targets overlap with other RBPs, suggesting combinatorial binding of RBPs (Halbeisen et al, 2008).

RBPs orchestrate and link the different steps of mRNA processing including polyadenylation, splicing, mRNA stability, mRNA export, localization, translation and finally degradation. In addition, RBP-RNA association is essential to recruit catalytic components to sites of RNA modification and to coordinate pre-mRNA processing with other cellular pathways.

RBPs have one or more known RNA-binding domains (RBD). Approximately one hundred types of RBDs have been described to date. Half of them are thought to have originated at early stages in evolution. Such is the K homology (KH) domain, SR domain (serin- and arginin-rich), RNA-binding Zinc finger (mainly C-x8-C-x5-C-x3-H type), RGG box, cold-shock domain (Y-box proteins), DEAD/DEAH box, Pumilio/FBF (PUF) domain, double-stranded RNA-binding domain (DS-RBD), Piwi/Argonaute/Zwille (PAZ) domain, Sm domain, etc. Others, such as the RNA recognition motif (RRM, also known as RBD or RNP domain) are mainly present in eukaryotes (Anantharaman et al, 2002; Glisovic et al, 2008).

Many RBPs have one or more copies of the same RBD while others have two or more distinct domains. Individual RBDs are separated by linker sequences of highly variable length. These linkers provide a critical determinant of binding affinity and may modulate cis versus trans binding. In many cases, individual RBDs within the same protein have different binding specificities, which suggests they may allow a single protein to bridge multiple RNAs (trans) whereas in others, multiple RBDs interact with non-specific RNA lattice to increase binding affinity (cis) (Shamoo et al, 1995).

Several RBDs are suggestive of the molecular function of their RBP; DEAD/DEAH box for RNA helicase activity, PAZ domain for short single-stranded RNA-binding in RNAi or microRNAs (miRNA) processes, and Sm domain for snRNA-binding in splicing and possibly in tRNA processing (Lee & Schedl, 2006).

1.3.1 The RNA recognition motif RRM

The RNA recognition motif (RRM), also known as the ribonucleoprotein domain (RNP) is found abundantly in all life kingdoms, although it exists at a lower abundance in prokaryotes and viruses. To date, only 85 proteins containing an RRM domain in bacteria (mostly cyano- bacteria), and six proteins in viruses have been identified (Maruyama et al, 1999). Prokaryotic RRM proteins are rather small (about 100 amino acids) and have a single copy of the RRM domain. In eukaryotes, the RNA recognition motif is one of the most abundant protein domains. The most striking development is seen in vertebrates, which have at least 30 distinct RRM-domain proteins with no orthologs in arthropods or nematodes and several

vertebrate-specific expansions within other ancient ortholog groups of RRM proteins. This diversity of RRM proteins correlates with and is probably functionally linked to the extensive utilization of alternative splicing as a means of generating protein diversity. A similar situation seems to exist in plants because over 50 plant-specific RRM proteins were detected in *Arabidopsis* (Anantharaman et al, 2002). To date, a total of 6056 RRM motifs have been identified in 3541 different proteins. In humans, 497 proteins have been identified containing at least one RRM (Finn et al, 2006). Assuming the presence of about 20000 – 25000 protein-coding genes in the human genome, the RRM would therefore be present in about 2% of gene products.

The RRM is an interaction domain, capable of association with RNA, homo-/hetero-dimerization with proteins, and rarely with DNA. This small domain is able to bind RNA with different affinities and specificities, to interact with RNA of different length and to contact several partners at the same time in a sequence and/or structure dependent manner.

RRM proteins containing up to six RRMs have been found in eukaryotic proteins. RRMs are often found as multiple copies within a protein (44%, two to six RRMs) and/or together with other domains (21%) (Maris et al, 2005). In most instances, the RRMs have some basal level of non-sequence specific RNA-binding affinity. In addition, many also have a higher affinity for a specific structure or sequence of RNA. The most conserved RRM signature sequence is an eight-residue motif called ribonucleoprotein 1 (RNP1), which has the consensus [RK]-G-[FY]-[GA]-[FY]-[ILV]-X-[FY]. A second six-residue region of homology, called ribonucleoprotein 2 (RNP2), is typically located ~30 residues N-terminal to RNP1, and has the consensus [ILV]-[FY]-[ILV]-X-N-L. Additional conserved amino acids define an ~80-residue domain that encompasses the RNA-binding function (Adam et al, 1986; Dreyfuss et al, 1988; Scherly et al, 1989).

To date, more than 30 RRM structures have been determined either by NMR or X-ray crystallography and reveal unexpected variations. All of the structures present intrinsic common features and differences in RNA recognition reflecting the remarkable adaptability of this domain in order to achieve high affinity and specificity.

The common structure of this domain is well characterized by the packing of two α -helices on a four-stranded β -sheet. However, the mode of protein and RNA recognition by RRMs is not clear owing to the high variability of these interactions. Different structural elements of the RRM are important for binding a multitude of RNA sequences and proteins. The β -sheet of an RRM remains the primary RNA-binding surface illustrated by the structures of U2AF65, 65-kDa subunit of U2 auxiliary splicing factor (three RRMs)(Kielkopf et al, 2001) and U2FA35, the small subunit

(one RRM) in Figure 5 (Kielkopf et al, 2001). Other examples for the RRM-RNA interaction via the β -sheet are the alternative-splicing factors PTB (polypyrimidine-tract binding protein, four RRMs) (Simpson et al, 2004), and SRp20 (one RRM) (Hargous et al, 2006). Interestingly, despite using the same protein surface to bind RNA, each of these proteins achieves sequence-specificity in a slightly different manner. This structure of human SRp20 recognizes only one single cytosine nucleotide sequence-specificity via the β -sheet by Glu79 and Ser81. This specificity of the SRp20–RNA interaction allows the binding of this protein to more diverse RNA sequences making the evolutionary pressure on the bound RNA weaker (Hargous et al, 2006).

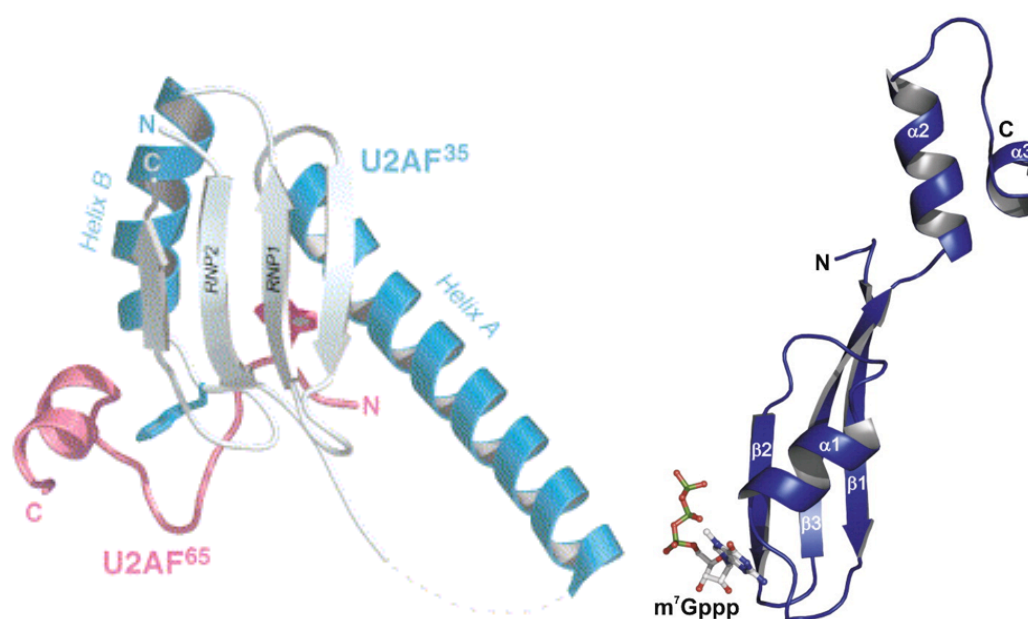


Figure 5: The RRM structure of U2AF and PARN

The U2AF35 β -sheet forms the RNA-binding surfaces of canonical RRM-containing proteins. The PARN-RRM domain with bound m^7 GTP reveals an extended shape with the two C-terminal α -helices $\alpha 2$ and $\alpha 3$ protruding from the protein core. The m^7 GTP is bound on the surface of the N-terminal part of the RRM domain involving the loops connecting $\beta 2$ – $\beta 3$ and $\beta 1$ – $\alpha 1$, respectively (Kielkopf et al, 2001; Monecke et al, 2008).

Moreover, recent structural investigations showed that the interaction of RRM with RNA is not restricted to the β -sheet surface and that the loops (especially loops 1, 3 and 5) between the α -helices and β -strands appear to be as important as the β -sheet for RNA-binding. The β -sheet surface of an RRM appears to have an inherent preference for certain RNA sequences. It is possible that a role for the loops

of RRM emerged later in evolution in order to expand the range of RNA target sequences that can be bound by an RRM.

Fox-1 (feminizing locus on X) (Auweter et al, 2006), RBMY (RNA-binding motif gene on Y chromosome) (Skrisovska et al, 2007), and PARN (Poly(A)-specific ribonuclease) (Monecke et al, 2008) are examples for single RRM proteins in which the loops between the α -helices and β -strands are crucial for RNA interactions.

Poly(A)-specific ribonuclease (PARN) is a processive 3'-exoribonuclease involved in the decay of eukaryotic mRNAs. Interestingly, PARN interacts not only with the 3'-end of the mRNA but also with its 5'-end. Still, PARN contains only one RRM domain that specifically binds both the poly(A) tail and the 7-methylguanosine (m^7G) cap (Figure 5). The interaction of PARN with the 5' cap of mRNAs stimulates the deadenylation activity and enhances the processivity of this reaction (Monecke et al, 2008).

In many RRM, a β -hairpin is present between the α 2-helix and the β 4-strand. Involvement of this β -hairpin in RNA-binding has been strongly suggested for p14, a single RRM protein operating as a subunit of the essential splicing factor 3b (SF3b) (Spadaccini et al, 2006) by NMR titration. Other structural studies show that amino acids of the β -hairpin are directly hydrogen-bonded to bases of nucleic acid targets.

In Fox-1, RBMY, U2AF35, and p14 the absence of a second RNA-binding RRM could explain the enhanced importance of the β -hairpin for interacting with RNA.

In contrast to the examples mentioned above, most RRM proteins contain multiple RRM that are thought to help achieving higher affinity and specificity considering the weak binding affinity of most RRM in isolation for their RNA targets. Indeed, biochemical data with the structure of several tandem RRM bound to RNA (Sex-lethal (Handa et al, 1999), HuD (Wang & Tanaka Hall, 2001), PABP (Deo et al, 1999)) or DNA (hnRNP A1; Ding et al, 1999) confirmed this initial hypothesis.

The combination of two or more RRM domains allows the continuous recognition of a long nucleotide sequence (8–10 nucleotides), which often drastically increases the affinity. But the individual free energies of binding of the RRM for RNA are not strictly additive. While the binding affinity of a multiple RRM containing protein might be expected to be the product of the affinities of its isolated RRM, this is not the case with all RBDs, e.g. hnRNP A1 (Shamoo et al, 1994). The linker between the RRM is an important determinant of binding affinity, with a longer length and distance decreasing the affinity immensely. Binding affinities between $10^4 M^{-1}$ and $10^6 M^{-1}$ have been observed for RBDs representative of a typical RBD

(Shamoo et al, 1995). Assuming then that each isolated RRM of a hypothetical two RRM containing protein has an affinity of 10^5 M^{-1} for a nucleic acid ligand, the overall apparent affinity is calculated for the subsequent binding of the second RRM to the ligand that is already bound by the first RRM of the same protein as follows: if the linker length is 0 residues, with a distance of 30\AA between both RRMs, the apparent affinity is calculated $2.9 \times 10^8 \text{ M}^{-1}$. However, if the linker is 120 residues long with a distance of 450\AA , the affinity is decreased to $2.0 \times 10^5 \text{ M}^{-1}$ (Clery et al, 2008; Maris et al, 2005; Shamoo et al, 1995).

Besides RRM-RNA associations, protein-RRM interactions have been found in several structures reinforcing the notion of an extreme structural versatility of this domain supporting the numerous biological functions of the RRM-containing proteins (Clery et al, 2008; Maris et al, 2005).

The p14 subunit of the essential splicing factor 3b (SF3b) within the spliceosome contains a single RRM and stably interacts with the SF3b subunit SF3b155, which also binds U2AF65. A surprising observation is that the β -sheet surface, including residues in the RNP1 and RNP2 motifs, which mediates RNA-binding in canonical RRMs, forms the binding interface with the SF3b155 peptide. Protein p14-RNA interactions are modulated by SF3b155 and the RNA-binding site of the p14-SF3b155 complex involves the non-canonical β -hairpin insertion of the p14 RRM (Spadaccini et al, 2006).

1.3.2 Post-transcriptional regulation by RRM proteins

As soon as RNA precursors are formed, RBPs associate with the nascent mRNA precursors, form ribonucleoprotein-particles (mRNPs), and mediate and couple diverse RNA processing reactions including 5'-end capping, 3'-end cleavage, polyadenylation, splicing, and editing. The transcripts are subsequently exported through nuclear pores to the cytoplasm where they may undergo localization to subcellular regions by complexes consisting of motor proteins and RBPs or by the signal recognition particle. The transcripts assemble with translation factors and ribosomes for protein synthesis, which is controlled by global or transcript-specific mechanisms (Gebauer & Hentze, 2004). Finally, mRNAs undergo exonuclease-mediated degradation by diverse decay pathways.

Surprisingly, the many different protein factors that guide mRNA modification pathways are composed of a limited number of conserved, modular RNA-binding domains. Of these, the RRM proteins with the RRM domain are by far the most abundant type of proteins.

In the following chapters some post-transcriptional events are described to illustrate the complex functions of the RRM-containing RNA-binding protein family.

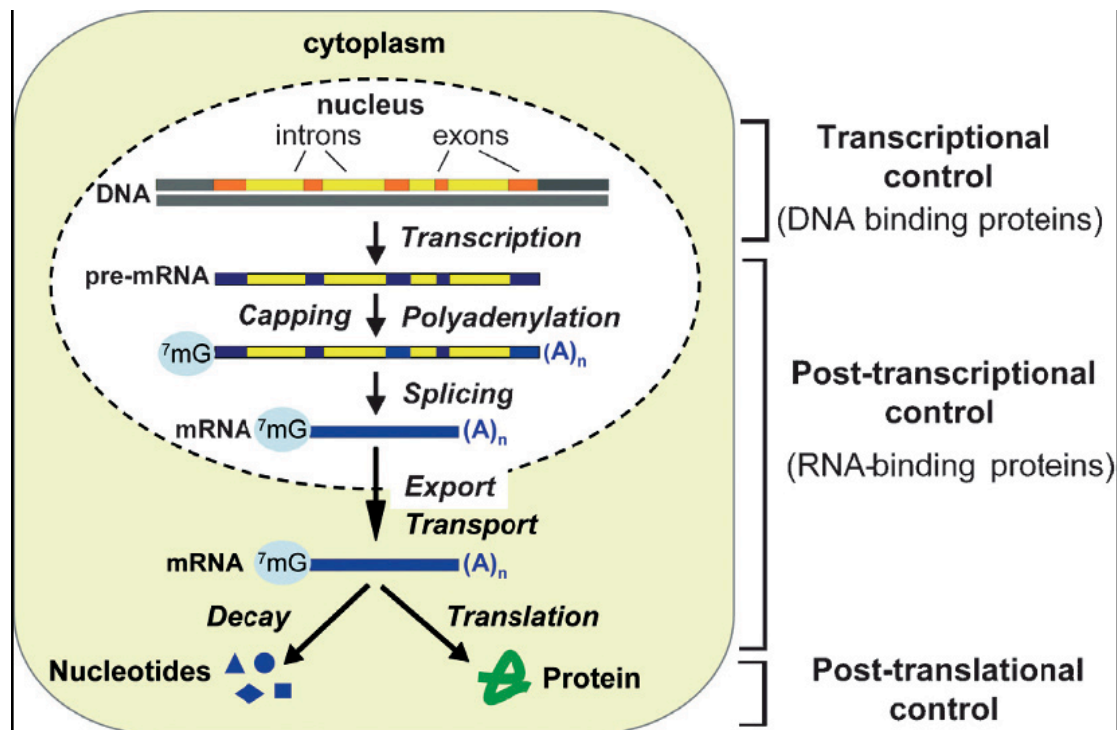


Figure 6: Control of gene expression at multiple steps

(Halbeisen et al, 2008)

1.3.2.1 Polyadenylation

Polyadenylation occurs during post-transcriptional pre-mRNA processing. It is a two-step process: cleavage and poly(A) addition. Both cis-acting elements and trans-acting factors (multiprotein complex including cleavage-polyadenylation specificity factor, cleavage stimulation factor, cleavage factor, and poly(A) polymerase) are required for this process.

The splicing factor SRp20, for example, (single RRM protein) affects recognition of an alternative 3'-terminal exon of a gene that codes for the peptides calcitonin and calcitonin gene-related peptide. SRp20 binds to splicing signals within the polyadenylation enhancer and increases exon 4 inclusion *in vivo*. This is the first indication that a canonical SR protein can influence polyadenylation and suggests that other SR proteins could play a general role in recognition of 3'-terminal exons,

thereby providing a link between the splicing and polyadenylation machineries (Lou et al, 1998).

1.3.2.2 Splicing

Pre-mRNA splicing is an essential step in gene expression that occurs co-transcriptionally in the cell nucleus. Splicing in general (and alternative pre-mRNA splicing) includes or excludes (different) portions of a nascent transcript into the final protein-coding mRNA. Splicing is catalyzed by a large number of RNA-binding protein splicing factors, in addition to core spliceosome components.

Splicing factors are localized to the nucleus in dynamic nuclear organelles (without a membrane) termed speckles. The presence of additional speckle-associated proteins is required for the release of splicing complexes from speckles, thereby affecting pre-mRNA splicing and mRNA export. Speckle structure and function is controlled by phosphorylation, where serine phosphorylation of SR proteins controls both their association with the spliceosome and their recruitment from speckles to active sites of transcription (Handwerger & Gall, 2006).

Some protein splicing factors, such as the U2 small nuclear RNP auxiliary factor (U2AF) associate with specific subsets of spliced mRNAs. U2AF is a highly conserved heterodimeric essential splicing factor, composed of a 65kDa (three RRM) and a 35kDa (one RRM) subunit, with a well-characterized role during the early steps of spliceosome assembly. U2AF transient interaction with the pre-mRNA leads to the subsequent assembly of an active spliceosome complex. Genome-wide identification of cellular mRNAs associated to U2AF65 revealed around 5000 targets encoding transcription factors and cell cycle regulators (Berglund et al, 1998; Gama-Carvalho et al, 2006; Wu et al, 1999; Zorio & Blumenthal, 1999).

1.3.2.3 mRNA export

Compared to most nuclear trafficking pathways, mRNA export is unique in employing primarily the TAP:p15 heterodimer (transcription export; TREX). The TREX complex is recruited to the mRNAs by the splicing machinery (Reed & Cheng, 2005; Stewart, 2007).

SRp20 was found not only to bind to an mRNA export element from the intronless histone H2a gene, but also enhance the export of RNAs containing the element. Further, SRp20 associates with poly(A)⁺ RNA in both the nucleus and the cytoplasm of mammalian cells. Moreover, three shuttling SR proteins can provide adapter function by recruiting the general export receptor NXF1/TAP to mRNAs (Huang et al, 2003).

Mechanisms used to transport and anchor RNAs in the cytoplasm include vectorial transport out of the nucleus, directed cytoplasmic transport in association with the cytoskeleton, and local entrapment at particular cytoplasmic sites. The majority of localized RNAs are targeted to particular cytoplasmic regions by cis-acting RNA elements; these are almost exclusively located in the 3'-untranslated region (UTR). Moreover, asymmetric distribution of RNA can also be established by the active transport of RNAs via RBP-motor protein complexes (Halbeisen et al, 2008; St Johnston, 2005).

1.3.2.4 mRNA stability/degradation

The level of an mRNA in the cytoplasm represents a balance between the rate at which the mRNA precursor is synthesized in the nucleus and the rates of nuclear RNA processing, export and cytoplasmic mRNA degradation. In eukaryotic cells, degradation of bulk mRNA occurs by two alternative pathways, both of which are preceded by removal of the poly(A) tail by deadenylases. Following this first rate-limiting step, mRNAs can undergo 3' to 5' exonucleolytic decay, which is catalysed by the exosome. The exosome activity is regulated by the SKI complex. Alternatively, after deadenylation, the cap structure is removed by the decapping enzyme DCP2, rendering the mRNA susceptible to 5' to 3' digestion by XRN1 (Houseley et al, 2006; Parker & Song, 2004).

Strikingly, all proteins that function in the 5' to 3' mRNA-decay pathway have recently been shown to localize to P bodies. P-body components dynamically exchange with the cytoplasmic pool, which indicates that decay enzymes and co-factors are not confined to P bodies. Also the exosome and SKI-complex components are not detected in P-bodies, indicating a degree of compartmentalization of mRNA-degradation pathways within the cytoplasm (Kedersha et al, 2005).

The rate of mRNA decay is regulated by the interaction of cis-acting elements, like the AU-rich elements (ARE), in the transcripts and RBPs. AREs are conserved sequences found in the 3'-UTR of nearly 5% of all human genes. These sequences are targets of many ARE-binding proteins; some of which induce degradation whereas others promote stabilization of the mRNA, such as HuR (Barreau et al, 2005).

The regulation of mRNA stability is the most well known molecular function of Hu proteins (four RRM). Hu proteins bind to the 3'-UTRs of target mRNAs and prevent their degradation, thus indirectly enhancing protein production. Numerous Hu mRNA stabilization targets have been identified (Brennan & Steitz, 2001; Pascale et

al, 2008). Hu proteins appear to stabilize target mRNAs by antagonizing the actions of destabilizing proteins, such as TTP or AUF1 (Barreau et al, 2005).

1.3.2.5 mRNA translation

Translational regulation concerns the differential recruitment of mRNA species to the ribosome for protein synthesis, which results in a lack of correlation between the relative amounts of mRNA and the amount of the encoded protein.

The 5'-cap and the poly(A) tail of the transcripts synergistically stimulate translation. The poly(A)-binding protein (PABP) contains four N-terminal RRM and requires a minimum of 12 adenosine residues to bind RNA. PABP interacts with the translation initiation factor eIF4G. This PABP-eIF4G interaction results in the circularization of an mRNA and serves as a means to confirm the integrity of a mRNA and promotes the recruitment of the 40S ribosomal subunit (Cheng & Gallie, 2007).

Stress granules, for example, are sites of translational regulation. They are specific structures in the cytoplasm that accumulate non-canonical 48S initiation complexes and contain mRNPs, 40S subunits and some initiation factors. It is proposed that TIA-1/TIAR (shuttling nucleocytoplasmic RBP containing three RRMs) forms aggregates used as a scaffold for other components of stress granules. Stress granules arise under stress conditions (e. g. heat shock, UV irradiation, energy depletion and oxidative stress) and appear as centers that sort, remodel and export specific mRNPs for re-initiation, decay or storage (Mollet et al, 2008).

The cold-inducible RNA-binding protein CIRP (hnRNP A18) contains one RRM and several repeats of the RGG motif. In response to stress CIRP migrates to the cytoplasmic stress granules, where translation initiation is stalled, and acts as a translational repressor. This migration occurs in a TIA-1 independent manner but requires methylation-dependent nuclear export of CIRP (Aoki et al, 2003; De Leeuw et al, 2007).

1.3.3 RRM proteins in differentiation

Differentiation programmes must be continuously coordinated in the embryo and adult. The activity of genes involved in differentiation direct the initial assignment of cells into specific lineages during early stages of embryonic development. The determination of different cell types (cell fates) involves progressive restrictions in their developmental potentials. Tissue differentiation occurs at later stages after cellular determination, as the cell elaborates a cell-specific developmental programme (e.g. muscle cells).

Differentiation should be able to simultaneously regulate the expression of many genes and on the other hand it should be sensitive and responsive to external cellular signals. Such requirements could be fulfilled by both transcriptional and post-transcriptional regulation. Although, differentiation programmes rely on the hierarchical expression of specific transcription factors, parts of these processes are also dependent on regulation at the level of RNA, rather than DNA. In embryogenesis this is primarily because the zygotic genome is often quiescent during the early stages. Notably, regulation at the RNA level might be beneficial in terms of the ability to respond rapidly to signals and to modulate the levels of existing RNA populations in accordance with the temporal requirements within a given tissue. Such a mechanism could therefore contribute to the selective and regulated expression of gene products whose transcription has already been activated. RBPs that direct different steps of RNA metabolism during development are often similar to ubiquitously expressed RBPs that are involved in general mRNA processing.

1.3.3.1 RNA-binding proteins as developmental regulators

One example is the ELAV (embryonic lethal abnormal visual system)/Hu protein family in *Drosophila*, human, mouse, zebrafish and *Xenopus*. ELAVs possess three RRM domains that mediate binding with high affinity and specificity to ARE-containing target mRNAs. They have been reported to target mRNAs encoding proteins important for neuronal differentiation. However, HuR regulates the stability of target myogenic mRNAs during muscle cell differentiation. HuR is initially transported to the nucleus in early myogenesis, but later accumulates in the cytoplasm where it enhances *myogenin* and *myoD* mRNA stability. The disruption of the transportin-2 (TRN2)-HuR complex at late stages of myogenesis leads to its cytoplasmic accumulation, as well as to the stabilization of *myoD* and *myogenin* messages, resulting in higher efficiency of muscle differentiation (Figuerola et al, 2003; van der Giessen & Gallouzi, 2007). An interesting feature is that without RRM3, HuR proteins cannot oligomerize on their target mRNAs, weakening their ability to prevent mRNA decay (Anderson et al, 2000; Fan & Steitz, 1998).

ElrA, a member of the ELAV family, and the *Xenopus* homologue of HuR, functions in polyadenylation and stabilization. ElrA is present at all times during *Xenopus* development and was previously shown to bind to two different maternal mRNAs in *Xenopus* embryos, polypeptide chain release factor *C12* and the activin receptor *actR* mRNAs, in a manner dependent on the presence of their embryonic-specific consensus sequences. In contrast, new findings show that ElrA binds specifically to the cyclin *E1* 3'-UTR independently of its adenylation state. ElrA has

been shown to protect the deadenylated mRNA from degradation *in vitro*, in association with the *Xenopus* cold-inducible RNA-binding protein CIRP (Aoki et al, 2003). Consistent with a role for ElrA in regulating cyclin *E1* mRNA, it was recently shown that its human homologue HuR binds to and stabilizes the mRNA encoding human cyclin E1 (Guo & Hartley, 2006; Slevin et al, 2007).

Another example is the single RRM protein ePABP2 (embryonic poly(A) binding protein) in *Xenopus*. ePABP2 is involved in poly(A) elongation, which functions as a translational switch to control the synthesis of key regulatory proteins that drive the cell cycle and promote cell-fate decisions in early embryos, such as *c-mos*, the cyclins and *wee1*. ePABP2 contains a central RRM with significant amino acid sequence identity (72%) with the RRMs of nuclear PABP2 proteins (ubiquitously nuclear expressed) from human, mouse, and *Xenopus*. Nevertheless, ePABP2 differs from the previously described nPABP2 in that it is located primarily in the cytoplasm of *Xenopus* oocytes. Both ePABP2 protein and its mRNA are detected predominantly during oogenesis and during the earliest stages of development. They decline after the onset of zygotic transcription and are later expressed in adult ovarian tissue (Good et al, 2004).

1.3.3.2 Regulation of localized RNAs in pattern formation

In *Xenopus*, only five hours after fertilization zygotic transcription commences at MBT. This means that the first patterning events occur exclusively without transcription, depending on other regulatory mechanisms, such as maternal mRNA localization.

RNA localization generally refers to the transport or enrichment of subsets of mRNAs to specific subcellular regions generating cell polarity through the spatial restriction of gene expression. Cytoplasmic RNA localization is an evolutionary ancient mechanism for producing cellular asymmetries. The maternal contribution of RNA is a special feature of RNA localization and is crucial to patterning early development; initially silent in the oocyte, these transcripts are translated after fertilization and guide the early steps of development, like germ layer formation. RNA localization can be achieved passively by local protection from degradation or through the trapping/anchoring at specific cellular locations.

RNAs are localized to the vegetal pole of *Xenopus* oocyte by three different pathways. First, the early or METRO pathway uses the mitochondrial cloud (Balbiani body) to deliver RNAs, and germinal granules (collectively called the germ plasm) to the vegetal pole in early oogenesis. Second, the late pathway operates in late oogenesis and uses microtubules and molecular motors. Third, the intermediate

pathway uses a combination of early and late pathways to deliver RNAs to the vegetal pole of the oocyte (Kloc & Etkin, 2005).

Localization of selected maternal mRNAs has been observed in other species as well. In *Drosophila melanogaster* e.g. *bicoid*, *gurken*, *nanos*, and *oskar* mRNAs are all targets of Vg1RBP/Vera and determine the body axes. Vg1RBP/Vera belongs to the VICKZ proteins, a highly conserved family of RBPs containing two RRM and four KH domains (Yisraeli, 2005). *Bicoid* and *oskar* are also targets of Staufin (RBP with double-stranded RNA binding motif), and Bruno (a single RRM protein). Bruno also interacts with *oskar* mRNA (Yisraeli, 2005). In zebrafish *vasa*, *nanos1*, and *dazl* co-localize with the mitochondrial cloud in the germ plasm and are transported to the vegetal cortex during early oogenesis (Kim-Ha et al, 1995; Kosaka et al, 2007).

A growing number of spatially localized mRNAs in *Xenopus* oocytes have been shown to be required for normal embryonic patterning, including *VegT*, *Vg1*, and *Wnt11*. *Wnt11*, for example, is localized to the vegetal pole by the early pathway. No mouse or human orthologs for *VegT* have been identified, but a *VegT* ortholog has been reported in the tunicate *C. intestinalis* (Showell et al, 2004).

In *Xenopus*, *Vg1* was the first mRNA reported to be localized at the oocyte vegetal cortex (Melton, 1987). In the late pathway of RNA localization *Vg1* is specifically recognized by Vg1RBP/Vera forming an RNP complex in the nucleus followed by export and localization (Deshler et al, 1997; Schwartz et al, 1992). Today, many different RNAs are known to be localized at the vegetal cortex such as *Vg1*; the *Xenopus* homologue of Bicaudal-C (Wessely & De Robertis, 2000), and the T-box family member *VegT* (Xanthos et al, 2001; Zhang et al, 1998) are involved in mesoderm and/or endoderm formation (see chapter 1.2.1.2.).

ElrB, another *Xenopus* ELAV family member, closely related to ElrA, binds to and translationally represses the maternal *vg1* mRNA during *Xenopus* oocyte maturation by binding to the VTE element in the 3'-UTR of *vg1* (Colegrove-Otero et al, 2005).

1.3.4 Seb4 subfamily members in *Xenopus*

In *Xenopus* several RRM proteins have been identified though in most cases their function and mechanism are still unknown. Most of these RBPs contain more than one RRM (e.g. Elav/Hu family, etc.). But there are also few proteins, that contain only a single RRM, like mentioned above, e.g. ePABP2, three homologues of CIRP, and a small evolutionary conserved subclass including Hermes, Seb4R, and Seb4 (Figure 6).

Hermes (heart RRM expressed sequence) was originally identified as a mRNA encoding a single RRM protein expressed in the developing heart, kidney, eye, and epiphysis in *Xenopus* embryos. It was demonstrated, that myc-tagged *Hermes* protein was able to associate to poly(A)⁺ RNA in oocytes. When deletion constructs of *Hermes* were tested, only the full-length *Hermes* protein could associate with poly(A) RNA *in vivo*, neither the N-terminal RRM nor the C-terminal half of the protein were sufficient enough to bind to RNA (Gerber et al, 2002; Gerber et al, 1999). *In situ* analysis revealed that embryos overexpressing *Hermes* show greatly reduced expression of the precardiac marker *nkx2-5* and myocardial differentiation markers, including *troponin (Tnlc)* and *cardiac α -actin*, whereas muscle gene expression in the somites, and overall somite morphology, was left unaffected. Overexpression of *Hermes* also led to a strong down-regulation of the kidney pre-differentiation marker, *Xpax-2* (Gerber et al, 2002).

Hermes is found, sometimes as multiple spliced forms, in many different species such as frog, fish, chicken, mouse, and human (Gerber et al, 1999; Wilmore et al, 2005), but its function remains unknown. During *Xenopus* oogenesis *hermes* mRNA and *Hermes* protein localize in the vegetal cortex of the oocyte. A subpopulation of *Hermes* protein is concentrated in a specific structure in the vegetal cortex, the germplasm, where *Hermes* protein co-localizes with *Xcat2* and *RINGO/spy* mRNAs. The overall level of *Hermes* protein decreases during meiotic maturation and is barely detected in embryos until the tailbud stage. Injection of *Hermes* antisense morpholino oligonucleotides accelerates the process of oocyte maturation and results in cleavage defects in vegetal blastomeres of the embryo (Zearfoss et al, 2004). RNA-immunoprecipitation (RIP) studies showed that myc-tagged *Hermes* protein functionally, and/or physically interacts with *RINGO/spy*, *mos*, and *Xcat2* mRNAs *in vivo*. The translation of *RINGO/spy*, *mos*, and *Xcat2* mRNAs is repressed in oocytes, an event critical to normal development. *Hermes* negatively regulates the translation of these mRNAs and therefore, plays an important regulatory role during maturation, cleavage and germ cell development (Song et al, 2007).

In 1998, Heinrich Jasper from our laboratory identified a cDNA coding for the *Xenopus* orthologue of mouse SEB4 (named after the Staphylococcal aureus enterotoxin B) as a direct target of MyoD in a suppression PCR-screen for novel MyoD targets (Jasper, 1998). Overexpression studies revealed that *Seb4* induced efficiently ectopic skeletal muscle gene expression in uninduced animal cap explants. In 2000, *seb4b* the non-allelic gene copy of *seb4a* was cloned and characterized by Ingrid Fetka (Fetka et al, 2000). The *seb4a* and *seb4b* gene copies encode each a

single RRM-containing protein with the Seb4a protein encompassing 225 and the Seb4b protein encompassing 227 amino acid residues. *Xenopus* Seb4 shares 65% identity with mouse Seb4 and 62% with its human counterpart (RNPC1) and 43% identity with *C. elegans* T22B2.4. *Xenopus* Seb4 transcripts are present at all stages from the oocyte to the late tadpole. By RT-PCR it was shown that before zygotic transcription is initiated, *seb4* mRNA is maternally contributed to the early embryo. In the early gastrula embryo Seb4 is expressed in the paraxial mesoderm that is fated to give rise to the somites. *Seb4* mRNA expression is also found in the heart, the lens and the otic vesicle (Fetka et al, 2000).

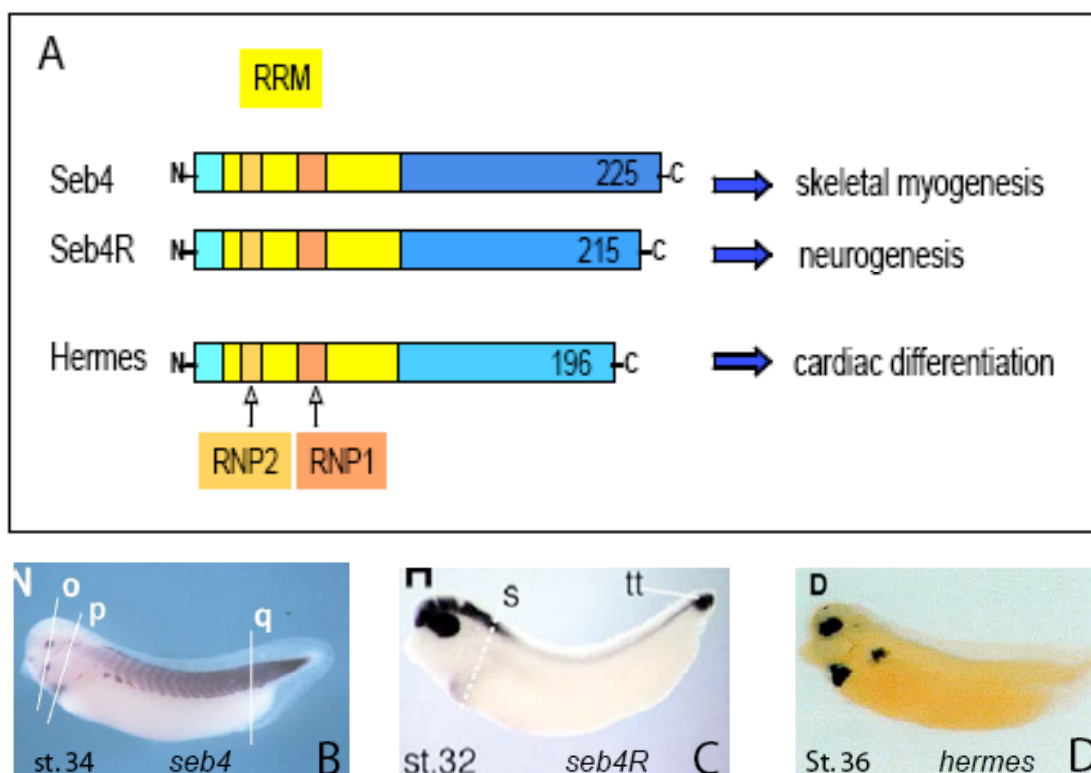


Figure 7: Seb4 subfamily

(A) Model of the Seb4 closest related single RRM proteins illustrating the conserved motifs and their suggested function. (B-D) *In situ* hybridization in *Xenopus* embryo against (B) *seb4* (Fetka et al, 2000), (C) *seb4R* (Boy et al, 2004), and (D) *hermes* (Gerber et al, 1999).

In 2004, a Seb4-related protein Seb4R was characterized in *Xenopus* as a putative RBP with a single RRM. Seb4R exists as a maternal protein, as well as a zygotic protein. Seb4R transcripts are present at all stages from the oocyte to the late tadpole. Maternal Seb4R is localized to the vegetal pole. Recently, it was found that ectopic Seb4R acts as a positive regulator of *vegT* mRNA stability and

translation leading to a role for maternal Seb4R in endoderm and mesoderm formation (Souopgui et al, 2008).

At gastrula stage (st. 10.5), zygotic Seb4R expression is exclusively restricted to the mesoderm. At stage 20, Seb4R expression clearly follows the formation of the central nervous system, including the expression in the area designated to form the eye, olfactory placodes, forebrain, midbrain, hindbrain and spinal cord. In stage 32 embryos, Seb4R is strongly expressed in the central nervous system, and particularly in the subventricular zone of the neural tube, an area containing specified neuroblasts (Boy et al, 2004). Overexpression experiments of ectopic Seb4R demonstrated a pro-neural effect of Seb4R on all neuronal tissues promoting early neural differentiation. Blocking Seb4R function using Morpholino oligonucleotides leads to the opposite effect. Seb4R is found to be upregulated by the pro-neural marker Neurogenin and the differentiated marker NeuroD, but inhibited by the Notch/Delta signal transcription cascade (Boy et al, 2004).

Seb4 and Seb4R contain a single RRM in the N-terminal part and two additional conserved domains in the C-terminal part of the protein. Seb4 shows an overall amino acid sequence similarity to Seb4R of 73% and an RRM similarity of 98%. Despite the high degree of similarity of Seb4 to Seb4R on the sequence level, Seb4 is clearly distinct from Seb4R in its expression pattern. Yet, when Seb4 was ectopically overexpressed in the retina, it was even found to cause the same effects in the retina as Seb4R did (Boy et al, 2004).

The functions of Seb4, in particular in muscle, still remain elusive.

1.4 Objectives

Global coordination of gene expression not only depends on transcriptional regulation, but also to a large extent on post-transcriptional events. Besides general roles in the control of RNA metabolism RRM-containing proteins have been implicated in different tissue-specific processes during embryonic development and the significance of post-transcriptional mechanisms for the regulation of cell differentiation becomes more and more evident.

Despite extensive studies in muscle formation, some aspects of the myogenic specification process are still largely unknown. This includes the signals and regulators involved in primary activation of the myogenic master regulators

MyoD and Myf5, as well as the downstream mechanisms by which MyoD and Myf5 stabilize the muscle cell fate.

The discovery, from our laboratory, that the RNA-binding protein Seb4 is an early MyoD target raises the possibility that MyoD promotes muscle differentiation through post-transcriptional mechanisms. This view has also been substantiated by the finding that Seb4 is capable of inducing ectopic skeletal muscle.

The main goal of this work was to analyze Seb4 in *Xenopus* embryos biochemically and biologically in the context of myogenesis. A biochemical characterization of Seb4 has not been shown to date and should be supported by the generation and use of specific antibodies against Seb4 for protein detection supporting many different experimental approaches. The search of interacting proteins and RNA targets could also shed more light on its biological function. Another important issue that should be investigated was protein expression pattern and the cellular localization of Seb4.

The biological characterization included the generation of Seb4 mutant phenotypes by depletion of endogenous Seb4 protein levels in the embryo and the analysis of affected marker genes to find out more about Seb4 and its role in muscle differentiation.

2 Material and Methods

2.1 Laboratory Equipment

The subsequent laboratory equipments were used. The companies are put in brackets.

CCD camera: ProGres C14 (Zeiss)

Centrifuges: Eppendorf centrifuge 5417C (Eppendorf); Omnifuge 2.0 RS (Haereus); Sorvall RC-5B (Du Pont), Micro 22R (Hettich Zentrifugen), Optima MAX-E Ultracentrifuge (Beckman), PicoFuge (Stratagene)

Developer: Curix-60 (Agfa)

Glass injection needles: Glass 1BBL W/FIL 1.0 mm (World Precision Instrument).

Injector: Pli-100 (Digitimer Ltd.)

Incubator: Driblock DB1 and DB20 (Teche)

Microneedle Puller: P-87 (Sutter Instrument).

Micromanipulator: Mm-33 (Science Products)

Microscopes: Stereomicroscopes Stemi SV6, Stemi SV11 (Zeiss), MZFCIII (Leica), Axiophot (Zeiss), Axiovert 200M (Zeiss)

Nylon membrane: Hybond™ N (Amersham)

pH-Meter: pH-Meter 761 Calimatic (Knick)

Pipetes: Pipetman, Gilson (2µl, 20µl, 200µl, 1000µl)

Software: Photoshop CS2 (Adobe); Illustrator CS2 (Adobe); MacVector 7.1 (Oxford Molecular Group); Office 2004 for Mac (Microsoft), Endnote 9.0 (Thomson), QCapture Imaging (Zeiss/Axiophot), BASreader and Aida Image analyser415 Software (Phospho-Imager)

Sonicator: Bioruptor™ (Diagenode), Branson Sonifier

Spectrophotometer: GeneQuant II (Pharmacia Biotech), Nanodrop ND-1000 (PeqLab)

Thermocycler: Primus 96 plus (MWG), Gene Amp PCR System 9700 (Applied Biosystems)

UV-crosslinker: (Stratagene)

2.2 Reagents

2.2.1 Chemicals

Agar (Difco); Agarose (Gibco/BRL); Ampicillin, Streptomycin, Bacto trypton, Yeast extract (Difco); Chicken serum, lamb serum (Gibco/BRL); Human chorionic gonadotropin (Sigma); Levamisol (Vector Laboratories); QIAzol (QIAgen).

The fine- and bio-chemicals were ordered at the following companies: Fluka, Merck, Sigma-Aldrich, Roth, Biomol.

2.2.2 Proteins and enzymes

The following proteins/enzymes were ordered at the companies put in brackets:

Alkaline phosphatase (Roche); BSA fraction V, Chymostatin, Leupeptin, Pepstatin (Sigma); DNase I (Stratagene); Klenow enzyme (Roche); RevertAid™ M-MuLV Reverse Transcriptase (Fermentas); Restriction endonucleases with 10x restriction buffer system (NEB, Roche, Fermentas); RNaseA (Sigma); RNasin (Promega); T3, T7 and SP6 RNA polymerase with 5x incubation buffer (Promega); Taq DNA polymerase with 10x PCR buffer (NEB); Proteinase K (Sigma); RNase free DNase I (Promega); Precision Plus Protein Prestained Standard (Biorad).

2.3 Antibodies

2.3.1 Primary antibodies

The rat monoclonal antibodies were generated in collaboration with Dr. Elisabeth Kremmer, GSF München. The polyclonal rabbit antibodies against Seb4 were generated at BioGenes GmbH, Berlin.

The SF3b155, X DRSP, X NO-66, X NO-38 and X AND-1 antibodies were kind gifts from Prof. Marion Schmidt-Zachmann, deutsches Krebsforschungszentrum dkfz, Heidelberg.

antibody	host species, subclass	marker for	application, dilution
X Seb4 6E5	mono rat serum, IgG2a	striated muscle, lens, heart	ICC: 1:1000, WB: 1:10, IF: undiluted, IP
X Seb4 8B3	mono rat serum, IgG2a	—	—

X MyoD 7F11	mono rat serum, IgG2a	striated muscle	WB: 1:10, IP
X PGDS 7D12	mono rat serum, IgG2a	β -Catenin	WB: 1:10, IP
hu Serin 2	mono rat serum	RNA Polymerase II (active)	IF: 1:10
X Seb4 7600	poly rabbit serum	striated muscle, lens, heart	ICC: 1:1000, WB: 1:8000
X Seb4 7601	poly rabbit serum	—	—
SF3b155	guinea pig	splicing speckles	IF: 1:100-200
X DRSP	guinea pig	splicing speckles	IF: 1:500
X NO-66	mono mouse ascytes	nucleolus	IF: 1:500
X NO-38	mono mouse ascytes	nucleolus	IF: 1:3000-5000
X AND-1	mono mouse ascytes	nuclearplasm	IF: 1:500
X Lamin	mono mouse ascytes	inner nuclear envelope	IF: 1:1000
α -Tubulin	mono mouse ascytes, sigma	microtubuli, cytoplasm	IF: 1:100, WB: 1:1000
hu WG16	mono mouse serum	RNA Polymerase II (active and inactive)	IF: 1:10, WB: 1:50
Histone H3	rabbit, Abcam	H3 core region	WB: 1: 1000

2.3.2 Secondary antibodies

antibody	conjugate	company	dilution
sheep anti-digoxygenin fab	alkaline phosphatase	Roche	ISH: 1:2500
sheep anti-mouse IgG	alkaline phosphatase	Chemicon	ICC: 1:1000
anti-rabbit IgG Fc	alkaline phosphatase	Promega	ICC: 1:1000
goat anti-rat IgG + IgM	alkaline phosphatase	Dianova	ICC: 1:1000
goat anti-mouse IgG	peroxidase	Dianova	WB: 1:10000
goat anti-rat IgG + IgM	peroxidase	Dianova	WB: 1:5000
goat anti-rabbit IgG	peroxidase	Dianova	WB: 1:10000
rabbit anti-rat IgG	Alexa-fluor 488	Invitrogen	IF: 1:100
goat anti-mouse IgG	Alexa-fluor 594	Invitrogen	IF: 1:200
donkey anti-guinea pig IgG	Cy-2	Dianova	IF: 1:200
donkey anti-rat IgG	Rhodamin red X	Dianova	IF: 1:100
donkey anti-mouse IgG	Cy-2	Dianova	IF: 1:200
donkey anti-mouse IgG	Rhodamin red X	Dianova	IF: 1:200

2.4 Oligonucleotides

Primers were synthesized by Biomers (<http://www.biomers.net/de>) and Morpholino oligonucleotides were ordered from Gene Tools (<http://www.gene-tools.com/vivomorpholinos>).

2.4.1 Primers for Seb4 cloning

Seb4 full length: HJ37 + HJ40

HJ37 for; EcoRI, XhoI, start

5'-CGAATTCAGCTCGAGGGCAAG**ATGCACACCA**-3'

HJ40 rev; XbaI, stop

5'-GGTCTAGACTAAGCGCTATTGCATGCGGT-3'

Seb4 subcloning:

RR175 for; XhoI, start

5'-CCGCTCGAGGGCAAGATGGCAAATGTGAATCTTHGCATA-5'

RR176 rev; stop, XbaI

5'-GGTCTAGACTATGCTCCCAGGTATGCAAG-3'

SO3 rev, stop, XbaI

5'-AGATCTCTACTTCCTGAGGCTGGA-3'

SO4 for; EcoRI

5'-GAATTCATCCAGCCTCAGGAAG-3'

SO5 rev; stop, XbaI

5'-AGATCTCTAAGCTCTGTCTGCCAT-3'

SO6 for; EcoRI

5'-GAATTCAATGGCAGACAGAGCT-3'

construct 12: HJ37 + SO3; product size 93bp

construct 34: SO4 + SO5; product size 117bp

construct 56: SO6 + RR176; product size 96bp

construct 14: HJ37 + SO5; product size 206bp

construct 36: SO4 + RR176; product size 197bp

delta C: HJ37 + RR176; product size 290bp

delta N: RR175 + HJ40; product size 446bp

2.4.2 Primers for RT-PCR

Random Hexamer:

RR13: 5' - NNNNNC -3' (N = G, A, T or C)

Oligo (dT)₁₈:

5'-TTTTTTTTTTTTTTTTTTT-3'

XHistone H4; annealing temperature 55°C, 23 cycles

for 5' - CGGGATAACATTCAGGGTATCACT -3'

rev 5' - ATCCATGGCGGTAAGTGTCTTCCT -3

XGAPDHb; annealing temperature 55°C, 23 cycles

for 5'- TGAGCGGTAAAGTTCAAGTCGTC -3'

rev 5'- CACTACATACTCGGCACCAGCATC -3'

XSeb4R; annealing temperature 58°C, 28 cycles

for 5'-GGAACCTGCAGAGCGCATTACTA-3',

rev 5'-GTCAGGCTGGAGCTGTTGAGGCTG-3',

XSeb4 HJ 26/27; annealing temperature 58°C, 28 cycles

for 5'-GGGCTATGGCTTTGTCACAATGGCAGAC- 3'

rev 5'-GCTGAACACCAAATGCAAACCTGGCTG -3'

2.4.3 Morpholino oligonucleotides

Seb4 MO: 5'-AAGATGCACACCACACAGAAGGACA-3'

Standard control MO: 5'-CCTCTTACCTCAGTTACAATTTATA-3'

2.5 Plasmids

pBS (Stratagene)

pCS2+ (Rupp et al, 1994)

pCS2+MT6 (Rupp et al, 1994)

pCS2+ FLAG (Cabot, R.)

pET-M30 (Novagen)

pGEX 4T3 (Pharmacia)

pGEM-T (Promega)

pCS2+XSeb4 (Jasper, H.)
pCS2+mut-XSeb4 (Cabot, R.): seven nucleotide substitutions downstream of ATG start codon; position 4-10 WT sequence of CACACCA is deleted and substituted by GCAGGAG
pCS2+XSeb4-flag (Cabot, R.)
pCS2+mut-XSeb4-flag (Cabot, R.)
pGEXGst-XSeb4 (Mansperger, K.)
pCS2+MT6-Seb4 construct 12 (Oberleitner, S.)
pCS2+MT6-Seb4 construct 34 (Oberleitner, S.)
pCS2+MT6-Seb4 construct 56 (Oberleitner, S.)
pCS2+MT6-Seb4 construct 14 (Oberleitner, S.)
pCS2+MT6-Seb4 construct 36 (Oberleitner, S.)
pCS2+MT6-Seb4-delta C (Authaler, A.)
pCS2+MT6-Seb4-delta N (Authaler, A.)
pCS2+XSeb4R (Boy et al, 2004)
pCS2+XMyoDb (Rupp et al, 1994)
pCS2+TCF1-flag (Mansperger, K.)
pBluescript-KS-XMLC35 (Theze et al, 1995)
pBluescript-Nrp1 (Richter et al, 1990)
pGEM-T- α -crystallin (Winkler, M.)
pBluescript-SK-Troponin (Drysdale et al, 1994).
EF1 α (Frydenberg et al, 1991)

2.6 Biological material

***E. coli* strains:**

BL21(DE3): B F- dcm ompT hsdS(rB- mB-) gal (DE3); (Novagen)

XL1Blue: F'⁺::TN10 proA⁺B⁺lacI^q Δ (lacZ)M15/recA1 end A1 gyrA96(Nal^R) thi hadR17 (rK-mK-) glnV44 relA1 lac; (Stratagene)

***Xenopus laevis* (Nasco, *Xenopus* Express):**

Adult wild-type *Xenopus laevis* frogs were used. The frogs were kept in tap water with a temperature of 17-19°C and a population density of one frog per 5l water. The animals were fed three times per week with Pondsticks Premium brittle (Interquell GmbH, Wehringen).

XTC and A6 culture cells (ATCC, LGC-Promochem):

Cells were cultured in DMEM medium, 15% ddH₂O, 15% fetal bovine serum, at 26°C in 26mm Petri dishes. A6 cells were subcultured with 0.25% trypsin and 0.03% EDTA for cell detachment. Medium was renewed twice per week, when cells were split in a dilution 1: 1 or 1: 2 according to their confluency.

2.7 Molecular biological methods

2.7.1 Solutions

Antibody solution: 80% TBSX, 15% heat-inactivated lamb serum, 5% *Xenopus* egg extract

Staining solution: BM-Purple solution (Boehringer) ready to use;

BCIP 5-Bromo-4-Chloro-Indolylphosphate, (Biomol)

NBT Nitroblue Tetrazoliumchloride (Biomol)

3.5µl BCIP (in 100% Dimethylformamide, stored at -20°C) and 4.5µl NBT (in 70% Dimethylformamide, stored at -20°C) added to 1ml AP-Buffer

Egg extract: Homogenate of equal volumes of dejellied *Xenopus* eggs and PBS, centrifuge twice for 10min at 4°C at 10000rpm in HB4 or SS34 rotor until extract is clear, aliquots of 0.75ml stored at -20°C

AP-Buffer: 100mM trichlorethane Tris/HCl 9.5; 100mM NaCl; 50mM MgCl₂

Bleaching solution: 1% H₂O₂; 5% Formamid; 0.5x SSC

DEPC-H₂O: ddH₂O with 0.1% Diethylpyrocarbonat (DEPC) agitated at 23°C o/n and autoclaved afterwards.

10mM digoxigenin labelled NTP mixture: 10mM CTP, GTP, ATP, 6.5mM UTP and 3.5mM dig-11-UTP (Roche).

Hybridization solution: 5x SSC, 50% formamide, 1% Boehringer block, 0.1% Torula RNA, 0.01% Heparin, 0.1% Tween-20, 0.1% CHAPS, 5mM EDTA.

Lamb Serum: Heat-inactivated lamb serum (30min with 56°C), stored at -20°C

MEMFA: 0.1M 3-(N-Morpholino)-propanesulfonic acid (MOPS), 2mM EGTA, 1mM MgSO₄, 3.7% formaldehyde (pH 7.4 at 23°C)

Paraformaldehyde: 4% paraformaldehyde in PBSw (pH 7.5 at 23°C), stored at -20°C

PBS: 137mM NaCl, 2.7mM KCl, 8mM Na₂HPO₄, 1.7mM KH₂PO₄ (pH 7.2 at 23°C)

PBSw: 1xPBS, 0.1% Tween-20

Proteinase K: 10µg/ml Proteinase K in PBSw

20xSSC: 3M NaCl, 0.3M sodium citrate (pH 7.0 at 23°C)

TBS: 50mM trichloroethylene (Tris)/HCl, 150mM of NaCl (pH 7.5 at 23°C)

TBSX: 1xTBS, 0.1% Triton X-100 (pH 7.5 at 23°C)

TE: 1mM EDTA, 10mM of Tris/HCl (pH 8.0 at 23°C)

TBE: 100mM Tris/HCl, 83mM borate, 0.1mM EDTA (pH 8.6 at 23°C)

2.7.2 Isolation of nucleic acids

2.7.2.1 Preparation of DNA

Plasmid DNA preparations were carried out using mini-, midi- or maxi preparation kits (QIAGEN): QIAprep Spin Miniprep Kit (250), Cat. No. 27106; QIAprep Plasmid Midiprep Kit (25), Cat. No. 12143; QIAprep Plasmid Maxiprep Kit (25), Cat. No. 12163.

2.7.2.2 Isolation of RNA

Embryos were collected at the required developmental stage according to the normal table of Nieuwkoop and Faber (Nieuwkoop & Faber, 1967), (5 embryos per tube). Buffer was removed and QIAzol (QIAGEN) was added (600µl per 5 embryos per tube; for RIP experiments: 50 embryos per 30µl sepharose beads / 300µl QIAzol). Samples were stored at -80°C, or if used immediately they were shock frozen with liquid nitrogen, then thawed on ice, and vortexed for 30sec at rt.

Cell debris was removed by centrifugation for 10min at 12000xg at 4°C. 0.2 vol chloroform was added to the supernatant, shaken by hand, incubated for 3min at rt and finally centrifuged for 15min at 12000xg at 4°C. Supernatant was mixed with 0.5 vol (of starting volume) of isopropanol, incubated for 10min at rt followed by centrifugation at 12000xg for 10min at 4°C. RNA pellets were then washed twice with 70% ethanol and air-dried for about 10min at rt. The RNA was dissolved in DEPC-treated H₂O (15µl for RIP-material, and 30µl for other material) on ice, 10min at 56°C, and then stored at -80°C.

2.7.3 Manipulation and analysis of nucleic acids

2.7.3.1 Cloning methods

The desired DNA fragments were amplified by PCR with appropriate primers containing specific restriction sites. The PCR products were subcloned into pCR2-TOPOII-vector (Invitrogen) and sequenced by MWG. Further, the constructs were digested with the appropriate endonucleases, separated on an agarose gel and purified. Subsequently, the DNA fragment was ligated into the desired (dephosphorylated) vector.

2.7.3.2 Gel electrophoresis of nucleic acids

DNA was isolated in horizontal agarose gels. Depending upon fragment size, 1-2% TBE agarose gels were used. After electrophoresis the gels were photographed. 1kb or 100bp DNA ladder (Fermentas) was used as size standard. RNA was separated in 1.5% denaturing formaldehyde agarose gels (1x MOPS).

2.7.3.3 Isolation of DNA fragments from agarose gel

In order to isolate DNA fragments after electrophoresis from agarose gel, the appropriate bands were cut out under long-wave UV light. The DNA was extracted from the gel with QIAquick Gel Extraction Kit (250), Cat. No. 28706 (QIAGEN).

2.7.4 Polymerase chain reaction (PCR)

2.7.4.1 PCR amplification of DNA fragments for cloning

The reaction was carried out in a total volume of 50µl. The reaction mixture contained 100ng template DNA, 25pmol each primer, 0.5mM dNTPs, 1U Advantage Taq Polymerase (Invitrogen) or Taq polymerase (NEB) and 1x of the supplied buffer. The programme was 95°C 30 sec, 58°C (for all Seb4 constructs) 30sec, 72°C 1min,

30 cycles. The PCR products were subcloned into pcR2-TOPOII-vector (Invitrogen) and sequenced by MWG.

2.7.4.2 RT-PCR assay

In the RT-PCR assay, 0.5-1µg total cellular RNA was reverse-transcribed in a volume of 20µl with RevertAid™ M-MuLV Reverse Transcriptase (Fermentas) and random hexamer primer under RNA-preserving conditions (by adding RNasin) according to the manufacturer's protocol to generate cDNA. The cDNA templates were amplified by Taq DNA polymerase standard (NEB). The cDNA samples were mixed with polymerase, 1x buffer and H₂O in one tube that was split before adding the different primer pairs used. The samples were normalized by PCR amplification of housekeeping genes, such as H4 (Histone H4) or GAPDH, and the desired target cDNA species were amplified using specific primers. The PCRs were carried out in the exponential phase of amplification. This was pre-tested by determining the specific cycle number (from three different cycle rounds), at which an unsaturated product signal was generated (detected by agarose gel electrophoresis). Last, the PCR samples were loaded side by side in an agarose gel to compare their intensity.

2.7.5 In vitro transcription

2.7.5.1 In vitro transcription for microinjection

For microinjection capped mRNAs were *in vitro* transcribed with DNA dependent RNA polymerase (Promega). Reactions were set up as following: in a total volume of 50µl, 2µg linearized plasmid DNA, 1x of the supplied transcription buffer, 0.5mM dNTPs, 2.5mM G(ppp)G RNA Cap Structure Analogue (NEB), 10mM DTT, 20U RNasin and 40U Sp6 or 60U T3 or T7 RNA Polymerase. The reaction was incubated for 4 hours at 37°C. Subsequently, the template DNA was digested with 10U RNase free DNaseI for 30min at 37°C. The RNA was purified with the RNeasy Kit, Cat. No. 74104 (QIAGEN). The concentration of the RNA was determined with a NanoDrop ND-1000 spectrophotometer (Peqlab) and the quality was controlled by electrophoretic gel analysis.

2.7.5.2 In vitro transcription of digoxigenin labelled RNA probes

Plasmids were linearized and antisense RNA was generated by *in vitro* transcription with a DNA dependent RNA polymerase (Promega). The reactions were set up in a total volume of 50µl as following: 2µg linearized plasmid DNA, 1x of the supplied transcription buffer, 0.35mM digoxigenin labelled UTPs (DIG-11-UTP; Roche), 0.65mM UTP, and 1mM each ATP, GTP and CTs, 20U RNasin and 20U

SP6, T3 or T7 RNA Polymerase. The reactions were incubated at 37°C for 4h and purified with the RNeasy Kit (Qiagen). The quality was controlled by electrophoretic gel analysis.

2.7.6 RNA *in situ* hybridization

The embryos were fixed in fresh MEMFA for 1.5-2 hours at rt under rotation and washed afterwards with PBS 3x5min. The dehydration of the embryos was performed over a period of one hour by replacing the PBS with 100% ethanol. The lipid membranes were dissolved by storing the embryos at -20°C in 100% ethanol at least for 16h. The embryos were rehydrated through a 75, 50, 25% ethanol series in PBSw. Each ethanol step was incubated for 5min at rt. Afterwards 3 washes for 5min with PBSw were performed. The solution was then changed to Proteinase K in PBSw (10µg/ml) and incubated for 20min at 17°C, followed by a short rinse with PBSw. Again two washes for 5min were performed with PBSw. After the Proteinase K digest the embryos were refixed with 4% paraformaldehyde for 20min. A short rinse with PBSw was performed followed by five subsequent washes in PBSw for 5min. The PBSw was replaced with hybridization solution (50% PBSw: 50% hybridization solution; 100% hybridization 3min each step). 0.5ml of fresh hybridization solution was added to each vial and incubated at 65°C for 1h to inactivate endogenous phosphatases. The embryos were then prehybridized at 60°C for 2-6h. To 100µl of hybridization solution 30-50ng of RNA probe was added and incubated at 95°C for 2-5min, cooled immediately afterward on ice and added to the embryos in prehybridization solution. The RNA probe was hybridized to the mRNA over night at 60°C. To remove excess of non-hybridized RNA probe, the embryos were washed after the hybridization as follows: 2xSSC; 0.1% CHAPS short rinse; 2xSSC; 0.1% CHAPS for 20min; short rinse with 0.2xSSC; 0.1% CHAPS; twice for 30min at 60°C in 0.2xSSC; 0.1% CHAPS. Prior to the binding of the antibodies the embryos were transferred into TBSX (short Rinse in 50% TBS: 50% 0.2xSSC; 0.1% CHAPS), washed in TBS for 5min and rinsed in TBSX. To block unspecific antibody binding sites, the embryos were incubated in antibody buffer (0.5ml per vial) for 2h at 4°C. In parallel, AP-conjugated anti-DIG antibody (1/5000 diluted in antibody buffer) was preabsorbed against *Xenopus* proteins present in antibody solution. 0.5ml of preabsorbed antibody solution was added to the embryos and incubated o/n at 4°C. After antibody binding, the embryos were briefly rinsed with TBSx and washed six times for 1h in TBSX. Embryos were shortly rinsed in AP buffer and equilibrated for 15min. AP-buffer was replaced with 0.5ml staining solution and incubated o/n at 17°C in the dark. The staining reaction was stopped when the specific stain

appeared saturated by washing twice in PBS for 10min. Unspecific staining background of the embryos (if occurred) was removed by washing the embryos in 75% ethanol in PBS for 20min. The stain was fixed in MEMFA o/n. The embryos were bleached in bleaching solution on a light box for roughly 2h. The bleach solution was washed out with PBS three times for 5min. For long-term storage, the embryos were transferred to PBSw containing 0.2% Na-azide and stored at 4°C.

2.7.7 RNA-co-immunoprecipitation

All experimental steps were performed under RNA preserving conditions. This includes: Sterile, disposable plasticware is generally free of RNase activity. Glassware was either treated by baking at 200° C o/n or was washed with RNaseAway (Roth); always wearing gloves; all experiments were performed on ice or by 4°C; clean bench using RNaseAway (Roth).

2.7.7.1 Solutions

DEPC-H₂O: ddH₂O with 0.1% Diethylpyrocarbonat (DEPC) agitated at 23°C o/n and autoclaved afterwards

10x MOPS: 41.8 g 3-[N-morpholino] propanesulfonic acid (MOPS), 6.8 g Sodium acetate, 20ml 0.5 M EDTA, add H₂O to 1000 ml, store at 4°C in the dark, no autoclavation

20xSSC: 3M NaCl, 0.3M sodium citrate (pH 7.0 at 23°C)

RIP- buffer: 50mM Tris/HCL, 100mM NaCl, 1.5mM MgCl₂, 100mM sucrose, 0,1% NP-40, 0.5mM DTT, 10mM Vanadyl complex (NEB), 50U/ml Supersasin, protease inhibitors (pH 7.5 at 4°C)

NB hybridization solution: 1xDenhardtts, 2xSSC, 2% 5.2mg/ml salmon DNA

2.7.7.2 Coupling of antibody to ProteinG Sepharose-beads

Specific antibodies used for RIP were coupled to ProteinG-Sepharose beads by incubating 100µl beads with 10ml antibody containing tissue culture supernatant o/n at 4°C under rotation. Beads with bound antibodies were centrifuged at 110rcf at 4°C, tissue culture supernatant was collected, and beads were washed twice with 0.2M sodium borate (pH 9.0 at 23°C). The coupling reaction (+5mg/ml dimethylpimelimidat; 20mM) was incubated for 30min at rt under rotation. The

reaction was stopped by washing with 0.2M ethanolamin (pH 8.0 at 23°C), and then by incubating with 0.2M ethanolamine for 2h. Beads were stored in PBS at 4°C.

2.7.7.3 Blocking of beads

The blocking procedure was tested (IP with embryo extract, on Coomassie gel) with several blocking conditions (time and temperature) and components (in different concentrations), like *E.coli* t-RNA, yeast RNA type III, 10-20% BSA, and salmon sperm DNA leading to the final protocol: 100µl antibody-coupled or uncoupled ProteinG-Sepaharose beads were blocked by adding 1ml 20% BSA + 25µl *Salmon* sperm (5.2mg/ml) DNA for 2h at rt under rotation.

2.7.7.4 Embryo extracts for RIP- reaction

For the RIP-reaction I established a RIP protocol. Per experimental condition ca. 50 neurulae were collected in a 15ml falcon tube and homogenized with 3ml RIP-buffer by pipetting with a 1000µl tip and sonication with the Bioruptor 3x30sec at high level. Cell debris was removed by 3300rcf centrifugation at 4°C for 10min.

The embryo lysate was precleared with 20µl blocked (uncoupled) beads for 1h at 4°C. Beads were centrifuged for 1min at 4°C at 110rcf and discarded. Subsequently, the precleared lysate was incubated with 40µl blocked and antibody-coupled beads for 2h at 4°C (RIP-reaction).

After binding of the desired protein to the antibody-coupled beads, the beads were washed several times with increasing salt concentrations (2x RIP-buffer with 100mM NaCl, 2x RIP-buffer with 200mMNaCl, 1x RIP-buffer with 300mMNaCl) each step 5min long with 2 min centrifugation at 110rcf at 4°C.

Bound protein material was eluted by RIP-buffer containing 0.2% sarcosyl (without NP-40 or MgCl₂) for Western blotting. Associated RNA material was precipitated by RNA isolation with QIAzol.

2.7.7.5 Radioactive labelling via reverse transcription

The reaction mixture of template RNA (0.5µg RNA; 2µl RNA from RIP experiments, after QIAzol-RNA preparation), 1µl oligo(dT)₁₈ primer (0.5µg/l) or 1.5µl random hexamer primer (0.2µg/µl) were filled up with DEPC-treated H₂O to 8µl, mixed gently and spun down in a microcentrifuge for 3 sec. The mixture was then incubated at 70°C for 5min, chilled on ice and briefly centrifuged. The following components were added: 4µl 5xreaction buffer, 1µl RNasin (20u/µl), 1µl mix of 10mM dGTP, dATP, dTTP. After incubation at 37°C for 5min (if oligo(dT) primer was used), or at 25°C for 5min (if random hexamer primer was used), finally 1µl [α^{32} p]dCTP

(10mCi/ml) and 1 μ l RevertAid M-MuLV Reverse Transcriptase (200u/ μ l) were added. The RevertAid™ M-MuLV Reverse Transcriptase (RT) possesses an RNA-dependent and DNA-dependent polymerase activity and a ribonuclease H activity specific to RNA in RNA-DNA hybrids. The DNA polymerase activity of the RT lacks a 3' - 5' exonuclease activity. The mixture was incubated at 42°C for 60min (if random hexamer primer was used, 10min incubation at 25°C additionally and before the 42°C step). The reaction was stopped by adding 5 μ l of 0.5M EDTA. 25 μ l of 0.6N NaOH were added and incubated at 70°C for 30min (final hydrolysis of RNA from the RNA-cDNA hybrid). Unincorporated dNTPs were removed by purification with G-50 quick spin columns (Roche), according to the manufacturer's protocol.

2.7.7.6 RNA detection with autoradiography

Radioactively labelled cDNA derived from RIP-RNA-material, was loaded on vertical 6% PAA TBE gels, and separated by gel eletrophoresis. Gels were dried on Whatman paper at 80°C for 1h and exposed to a phospho-imager screen. Screens were analyzed with a phospho-imager apparatus FujiFilm Fla-3000 and the according software (BASreader control software for FujiFilm BAS and FLA scanners and Aida Image Analyser415).

2.7.7.7 Northern blot analysis

For the purpose of hybridizing radioactively labelled cDNA probes (derived from the RIP-material) to total *Xenopus* RNA, I adapted the procedure based on the basic protocol for Northern blot hybridization of current protocols in molecular biology as follows (Terry Brown et al., 2004). Equal amounts (20 μ g RNA/lane) of total RNA (isolated from neurula embryos) were loaded on a horizontal 1.5% denaturing formaldehyde agarose gel (1xMOPS) and were size-separated by electrophoresis (3h, 80-100V). Blotting the size-separated RNA to a nylon membrane was accomplished by capillary force in a 10xSSC buffer bath o/n at 4°C. After blotting, the membrane was washed twice briefly with 2xSSC, backed for 15min at 80°C, and UV crosslinked with 1200 Joule. The membrane then was cut into single lane stripes, and put into 15ml falcon tubes and washed with 6xSSC for 5min, followed by prehybridization at 68°C for 2h with 5ml hybridization solution per tube under rotation. The radioactivity of the labelled cDNA probes was monitored by measuring the counts per minute (cpm) via scintillation. (e.g., n=1; RIP-Seb4: 14070cpm, RIP-beads: 23309cpm, RIP- β Cat: 7410cpm, EF1- α cDNA: 187827cpm, neurulae cDNA: 31373cpm, -cDNA: 5001cpm, mock: 27cpm). To hybridize the radioactively labelled cDNA probes to total *Xenopus* RNA, 100 μ l probe was incubated for 5min at 95°C,

added to 1ml hybridization solution and applied on to the membrane strips. After hybridization o/n at 68°C under rotation, the membrane strips were washed twice for 5 min at rt with 2xSSC; 0.1% SDS, and twice for 20min at 42°C with 0.5xSSC; 0.1%SDS, and once briefly with 2xSSC. The membrane was exposed to a phospho-imager screen and subsequently analyzed.

2.8 Protein analysis

2.8.1 Solutions

3x Lämmli buffer: 150mM Tris/HCl (pH6.8 at 23°C), 300mM DTT, 4% SDS, 30% glycerol

Embryo lysis buffer for WB: 20mM Tris/HCl (pH7.5 at 23°C), 100mM NaCl, 1mM EDTA, 1% Triton X-100, 10% glycerol, 3mM CaCl₂, 3mM MgCl₂, β-mercaptoethanol 1:1000, protease inhibitors

E1-buffer: 110mM KCl, 50mM Tris/HCl (pH7.4 at 23°C), 5mM MgCl₂, 0.1mM spermine, 0.1mM EDTA, 2mM DTT, 0.4mM PMSF

Nuclear-buffer: 25% glycerol, 25mM Tris/HCl (pH7.4 at 23°C), 70mM KCl, 5mM MgCl₂, 0.2mM EDTA, 2mM DTT, 0.4mM PMSF

Embryo-lysis-buffer for gelfiltration: 20mM Tris/HCl (pH7.5 at 23°C), 100mM NaCl, 1mM EDTA, 10% glycerol, 3mM CaCl₂, 3mM MgCl₂, protease inhibitors

BC-100 column buffer (gelfiltration): 100mM NaCl, 25mM Hepes (pH 7.6 at 23°C), 1mM MgCl₂, 0.5 EGTA, 0.1mM EDTA, 10% glycerol, protease inhibitors

BC-200 column buffer (gelfiltration): 200mM NaCl, 25mM Hepes (pH 7.6 at 23°C), 1mM MgCl₂, 0.5 EGTA, 0,1mM EDTA, 10% glycerol, protease inhibitors

Chemiluminescence reagents (ECL):

Luminol solution: 0.44g luminol in 10ml DMSO, frozen in 1ml aliquots, stored at -20°C; p-coumaric acid: 0.15g in 10ml of DMSO, frozen in 0.44ml aliquots, stored at -20°C;

solution 1 (100ml): 10ml 1M Tris/HCl (pH 8.5 at 23°C), 1ml luminol, 0.44ml p-coumaric acid;

solution 2 (100ml): 10ml 1M HTris/Cl (pH 8.5 at 23°C), 60µl 30% ddH₂O₂

HEG buffer: 50mM Hepes pH7.6, 10% glycerol, 1mM EDTA, 1mM DTT, 1% TritonX-100, 1mM PMSF, 2.5µg/ml Leupeptin, 10µg/ml Aprotinin, 0.7µg/ml Pepstatin

HEG150: HEG buffer with 150mM NaCl

HEG300: HEG buffer with 300mM NaCl

1x HEMG: 25mM Hepes pH7.6, 0.1mM EDTA pH8, 12.5mM MgCl₂, 10% glycerol

GST-lysis-buffer: 1xHEMG, 0.5M NaCl, 0.1% NP-40, 1mM PMSF, 2.5µg/ml Leupeptin, 10µg/ml Aprotinin, 0.7µg/ml Pepstatin

GST-washbuffer I: 1xHEMG, 0.7M NaCl, 0.1% NP-40, 1mM PMSF, 2.5µg/ml Leupeptin, 10µg/ml Aprotinin, 0.7µg/ml Pepstatin

GST-washbuffer II: 1xHEMG, 0.7M NaCl, 0.01% NP-40, 1mM PMSF, 2.5µg/ml Leupeptin, 10µg/ml Aprotinin, 0.7µg/ml Pepstatin

GST- urea-elutionbuffer: 1xHEMG, 8M Urea

Lysozyme solution: 0.5g/10ml GST-lysis-buffer

Developer solution (silverstaining): 7.5g Na₂CO₃ in 250ml ddH₂O, add 125µl 37% formaldehyde

2.8.2 Coupled *in vitro* transcription and translation

In vitro translations of proteins were performed with the TNT® SP6 Quick Coupled Transcription/Translation System (Promega) according to the manufacturer's protocol.

2.8.3 Protein extraction from *Xenopus laevis* embryos (embryo extracts)

Embryos were collected at the required developmental stage according to the normal table of Nieuwkoop and Faber (Nieuwkoop & Faber, 1967) (5 embryos

each tube). 50µl embryo-lysis-buffer for Western blot analysis was added to each embryo (250µl starting volume/ tube/ 5 embryos). Embryos were lysed and homogenized by pipetting (with a 200µl tip) and sonication, using the Bioruptor 3x30sec at high level. Cell debris was removed by 10min centrifugation at 4°C at full speed. 250µl 1,1,2-Trichlorotrifluoroethane were added to the supernatant, vortexed and centrifuged for 10min at 4°C at full speed. After separating the organic from the aqueous phase, the upper phase containing the proteins was kept and precipitated by Wessel-Flügge-precipitation. The samples were mixed with 1 vol ddH₂O, 2 vol methanol, 1 vol CHCl₃, vortexed and centrifuged for 5min at full speed at 4°C. After removing the upper phase subsequently 3vol of methanol were added to the interphase and vortexed. After centrifugation the white protein pellet was air-dried and resolved in 3x Lämmli buffer, incubated for 10min at 95°C, shock frozen with liquid nitrogen and stored at -80°C.

2.8.4 Nuclear preparation of *Xenopus laevis* embryos

Around 100 embryos were collected at the required developmental stage according to the normal table of Nieuwkoop and Faber (Nieuwkoop & Faber, 1994) in 15ml falcon tubes and washed 3x with 1ml E-1 buffer containing 0.2% NP-40 and 0.25M sucrose. Embryos were lysed and homogenized by pipetting in E-1/0.25M sucrose (20µl per 5 embryos). Additional E-1/0.25M sucrose buffer was added to a volume of 40µl per 5 embryos, followed by vortexing with another 200µl E-1 with 0.05% NP-40 and 2.2M sucrose. The homogenate was layered on a 10µl cushion of E-1/2.2M sucrose in a 5x20mm centrifuge tube (Beckman) and spun at 130000xg for 2h at 4°C in an Beckman ultra-centrifuge Optima MAX-E (TLA-55 rotor). Yolk and lipid supernatant were separated from the cytoplasmic fraction. The nuclear pellet was resuspended in 250µl nuclear buffer. Then the nuclei were spun down on a 10µl cushion of 80% glycerol for 10min at 4000rcf in a microfuge at 4°C. The supernatant was removed and the nuclear proteins were extracted with the protein extraction protocol (see 2.8.3).

2.8.5 SDS-PAGE

SDS-PAGE (SDS-polyacrylamide gel electrophoresis) was carried out according to standard protocols (Sambrook et al, 1989), with 10%, 12% or 15% PAA gels according to the size of the protein of interest.

2.8.5.1 Western blot analysis

Western blot analysis was carried out according to standard protocols (Sambrook et al, 1989), and signals were detected by enhanced chemiluminescence solution in a relation of 1:1. The signals were exposed to a Super-RX Fuji medical X-ray film and developed according to the manufacturer's protocol.

2.8.5.2 Coomassie-staining

SDS-PAA gels were incubated o/n at rt in 0.4g of Coomassie blue R350 dissolved in 200ml of 40% (v/v) methanol in water, and destained in 60% ddH₂O, 30% methanol and 10% acetic acid for roughly 4h, and exchanging the destain-solution 2-4 times.

2.8.5.3 Silver-staining

The silver-staining reaction is based on the use of silver nitrate to bind proteins at a weakly acidic pH and subsequent reduction of silver ions to metallic silver by formaldehyde at an alkaline pH. This procedure is >100 times more sensitive than traditional Coomassie Brilliant Blue staining and allows for superior detection of low abundance proteins (> 100pg) and nanogram quantities of DNA and RNA. There are several disadvantages of this method including a lack of linearity, non-stoichiometric staining of proteins, a lack of compatibility with the microchemical preparation of proteins for identification by mass spectrometric techniques, and a highly subjective assessment of the staining endpoint.

SDS-PAA gels were washed twice for 10min in 50% methanol, once 10min in 5% methanol, once 15min in 33µM DTT in ddH₂O, and once 15min in 0.1% AgNO₃. Afterwards the gels were flushed 3x with ddH₂O, then briefly washed in developer solution and then developed in fresh solution for about 5min. When protein bands became visible the developer solution was poured off and the gels were washed twice with ddH₂O. Finally, the reaction was stopped by adding solid citric acid.

2.8.6 Protein-immunoprecipitation (IP)

ProteinG-Sepharose beads were coupled with specific antibodies of interest and blocked as described in 2.7.6.2 and 2.7.6.3. The embryos were lysed in 50-100µl HEG500 per embryo with a 200µl Pipetman tip and incubated on ice for 20min. The lysate was cleared via centrifugation at 4°C for 10min at full speed. The supernatant was transferred into a new siliconized tube. One sample equivalent was put aside as the input sample. 25µl of blocked and antibody incubated ProteinG-Sepharose beads-slurry was added to the samples and incubated o/n

under rotation at 4°C. The sepharose was pelleted by centrifugation at 100xg for about 10sec. The supernatant was carefully removed and discarded. The beads were washed under rotation lasting 15min at 4°C with the following buffers: 2xHEG150, 2xHEG300. After the last step, as much washing buffer as possible was removed. The beads were incubated in 20µl 3xLämmli buffer for 5min at 95°C. The IP samples including input dilutions were loaded on a SDS-PAGE.

2.8.7 Gelfiltration

Gelfiltration chromatography was performed at 4°C using a Superose6 column with an Amersham Biosciences UPC-900 monitor and pump system, equilibrated with BC-200 buffer. The system was monitored and controlled by methods run by the UNICORN control system (Version 5.01). The Superose6 column was calibrated with blue dextran (2 MDa), thyroglobulin (669 kDa), apoferritin (443 kDa), β-amylase (200 kDa), alcohol dehydrogenase (150 kDa), albumin (66 kDa), and carbonic anhydrase (29 kDa; Sigma MWGF 1000 molecular weights kit). Three different methods for protein extraction were performed and compared. (A) 100 embryos at st. 24 were collected and lysed in 1.5ml and (B) 200 embryos at st. 24 were collected and lysed in 12ml embryo lysis buffer, which was adapted to the requirements for gelfiltration (no detergents, no denaturing reagents). Both extracts were sonicated 3x30sec in the Bioruptor at high level and cleared by centrifugation. Extract (B) was precipitated with 0.3g ammoniumsulfate per ml lysate, dialysed and resuspended in BC-100. Extract (C) is a modified extract (A), using a douncer instead of the Bioruptor for homogenization. Protein concentrations from all extracts were measured with the Bradford reagent (Biorad). Embryo extracts (about 1.3mg protein) were applied to the column in a volume of 500µl and eluted at a flow rate of 0.150 ml/minute. Fractions (500µl) were collected, precipitated (after Wessel-Flügge) and analyzed by Western blotting.

2.8.8 Purification of Gst-tagged recombinant Seb4 protein

The expression vectors were transformed into *Escherichia coli* strain BL21. A starter culture was grown over night at 37°C. The starter culture was diluted 1:100 and grown at 37°C to an OD₅₉₅ of 0.6. Optimal Gst-Seb4 expression was observed upon induction with 0.4mM IPTG for 2h at 30°C (standard conditions of 1mM IPTG, 2h at 37°C were optimized for Gst-Seb4). The cells were harvested at 4000xg for 20min and the supernatant was discarded. The pellet was resuspended in 15ml GST-lysis-buffer per 1l culture volume. 200µl lysozyme solution were added per

1l culture volume and rotated for 30min at 4°C. Afterwards the lysate was frozen in liquid nitrogen and thawed at 37°C for three times. To shear the genomic DNA, the lysate was sonicated 3x30sec with an amplitude of 50% with a microtip (Branson sonifier). Warming up was avoided by putting the tube on ice. The lysate was cleared via centrifugation for 30min at 15.000rpm, 4°C. Prior to the GST purification, the glutathione sepharose beads-slurry was washed with 5-10 vol of GST-lysis-buffer. 300µl beads-slurry were added to 20ml of crude lysate and rotated for 1h at 4°C to allow binding of GST-fusion protein to glutathione beads. Afterwards the beads were washed three times with 5ml GST-washbuffer I and three times with 5ml GST-washbuffer II for 15min at 4°C. The GST-fusion protein was eluted off the beads with GST-urea-elutionbuffer for 2h at rt. A second elution was performed o/n at rt. Both eluates were compared by SDS PAGE and Coomassie staining, whereby the first eluate made up the majority, of approximately 90%, as expected. Afterwards both eluates were combined and dialysed in PBS o/n. Aliquots of all steps were analyzed by SDS-PAGE.

2.8.8.1 Dotblot

In vitro translations of the deletion constructs were performed with the TNT® SP6 Quick Coupled Transcription/Translation System (Promega) according to the manufacturer's protocol. 5µl of of the TNT lysates containing the translated myc-tagged Seb4 deletion proteins were pipetted directly onto a nitrocellulose membrane and analyzed by Western blotting and autoradiography. The autoradiograph served as a protein expression control. The TNT protein amounts were represented by comparable protein signals, because they were subcloned into the pCS2+myc-tag vector. Every construct contained six methionin residues derived from the six aligned myc-tags, while the remaining portions of Seb4 protein contain either none or one additional methionin or cystein residue. Thus, the theoretical labelling efficiencies differ by less than 15%, while the actual specific activity reflects also the efficiency of translation of each of the clones.

2.9 Histological methods

2.9.1 Solutions

AP buffer: 100mM Tris/HCl (pH 9.5 at 23°C), 50mM MgCl₂, 100mM NaCl, 0.1% Tween 20, 5mM Levamisole

AP staining solution: 3.5 μ l 5-Bromo-4-Chloro-Indolylphosphate (Biomol) (in 100% Dimethylformamide, stored at -20°C) and 4.5 μ l Nitroblue Tetrazoliumchloride (in 70% Dimethylformamide, stored at -20°C) added to 1ml AP-Buffer

A-PBS: 103mM NaCl, 2.7mM KCL, 0.15mM KH₂PO₄, 0.7mM NaH₂PO₄ pH7.5

A-PBS-T: APBS with 0.1% Tween20

Blocking buffer: PBT plus 10% heat inactivated serum

Citrate buffer: Stock A: 0.1M citrate monohydrate (10.5g for 500ml solution)

Stock B: 0.1M Trisodiumcitrate-dihydrate (14.7g for 500ml solution)

Working Sol.: 9ml A with 41ml B to 450 ml ddH₂O

DAPI: Hoechst dye (1mg/ml) 1:1000 in APBS-T

Dent's Fixative: 80% methanol, 20% dimethyl sulfoxide (DMSO)

Elvanol: 2.4g of MOWIOL 4-88, 6 g of glycerol, 6ml of H₂O, 12ml of 0.2M Tris (pH8.5), 2.5% w/v DABCO (1,4,-diazobicycli-(2.2.2)-octane)

2.9.2 Immunocytochemistry (ICC)

The vitelline membrane was manually removed with forceps Dumont No.5 from the embryos. Subsequently, the embryos were fixed in MEMFA for 1-2h at rt under rotation and rinsed afterwards with PBS. PBS was gradually replaced with methanol. The embryos were incubated in methanol at -20°C for at least 16h. They were rehydrated by 80%, 50%, 0% methanol in PBS for 5min each, followed by a 1x5min rinse with PBS and one washing step in PBT for 15min. The embryos were incubated in PBT plus 10% heat inactivated goat serum, blocking unspecific antibody binding sites at rt for 1h. The primary antibody was diluted in the blocking buffer and incubated over night at 4°C. Afterwards the embryos were washed six times with PBT for 1h. The secondary antibody coupled with alkaline phosphatase was diluted 1:1000 in blocking buffer. The embryos were incubated in secondary antibody solution over night at 4°C. Subsequently, the embryos were washed six times with PBT for on hour. Prior to staining, the embryos were equilibrated twice in AP buffer for 30min. The endogenous alkaline phosphatases were inactivated by addition of Levamisol to the AP buffer. The embryos were stained in 1ml staining solution in the

dark for 30 to 120min at rt, until the specific stain appeared saturated. The staining reaction was stopped by rinsing the embryos in PBS. The stain was fixed in MEMFA o/n. The embryos were bleached with bleaching solution (1% H₂O₂; 5% Formamid; 0.5x SSC) for 2h on a light box.

2.9.3 Immunofluorescence (IF)

Both, the embryonic tissue and the single cells were fixed (not live), either by crosslinking and/or precipitating fixatives, formaldehyde and methanol or acetone and methanol respectively. Crosslinking fixatives, e.g. formaldehyde, act by creating covalent chemical bonds between proteins in tissue. Precipitating (or denaturing) fixatives (e.g. methanol, acetone) act by reducing the solubility of the proteins and by disrupting the hydrophobic interactions which give many proteins their tertiary structure. The proteins of these samples are therefore denatured but preserved from decay and mechanically stabilized for the IF procedure.

The fluorophores chosen for the immunofluorescence experiments were excited by light of one wavelength, and emitted light of a different wavelength in the visible spectrum, shining green or red. Alexa Fluor 488 (absorption at 488nm and emission at 540nm), and Cyanine Cy2 (absorption at 492nm and emission at 510nm), fluoresce green, and Alexa Fluor 594 (absorption at 594nm and emission at 640nm), and Rhodamine Red-X RRX (absorption at 570nm and emission at 590nm), fluoresce red. For nuclear detection DAPI staining was performed. DAPI was excited with ultraviolet light. When bound to the minor groove of double-stranded DNA its absorption maximum is at 358 nm and its emission maximum is at 461 nm. This emission is fairly broad and appears blue. DAPI also binds to RNA (around 500 nm), though it is not as strongly fluorescent.

The Alexa Fluor dyes (Molecular Probes by Invitrogen) were synthesized through sulfonation of rhodamine and cyanine dyes. Sulfonation makes Alexa Fluor dyes negatively charged and hydrophilic. Alexa Fluor dyes are very photostable, bright, and less pH-sensitive than common dyes of comparable excitation and emission. Rhodamine Red-X conjugates also contain a spacer arm (from aminohexanoic acid), which extends the dye out from the surface of the protein. Consequently, proteins conjugated with Rhodamine Red-X are significantly brighter than others and are particularly recommended from the producing company (Dianova) for double labelling along with Cy2 (Dianova). All secondary antibodies used were affinity purified and guaranteed to have minimal cross reaction with other species.

2.9.3.1 Immunofluorescence on embryo sections

The following protocol is based on Kunz et al. (2004) with modification for paraffin sections. The embryos were fixed under rotation in MEMFA for 1h at rt. Afterwards they were transferred into ice-cold Dent's Fixative o/n at -20°C. Prior to embedding, the embryos were rehydrated for 30min in 100mM NaCl, 100mM Tris/HCl pH7.4. Embryos were again dehydrated with an ascending ethanol series of 50%, 70%, 80%, 96% and 100% for 2h each. The ethanol was replaced by incubating the embryos twice for two hours in Xylene. Then they were soaked in paraffin at 55°C twice for two hours. The embryos were placed in paraffin and the blocks of paraffin were hardened on a cooling plate. The embryos were sectioned with an electrical microtome to slices of 4µm and dried for 2h at 37°C. The paraffin was removed by the following steps: 2x10min Rotihistol (Roth), 2min 100% Ethanol, 2min 96% Ethanol, 2min 80% Ethanol, 1min 70% Ethanol, 1min 50% Ethanol, briefly in ddH₂O. After a short rinse with citrate buffer, the antigen was renatured by boiling the slides in citrate buffer in the microwave twice for seven minutes with a 2min break. The sections were cooled down to rt for at least 20min. A short rinse with ddH₂O followed. Prior to immunostaining, unspecific antibody binding sites were blocked by incubation for one hour at rt in APBS-T with 20% heat inactivated lamb serum. The slides were incubated with the primary antibody o/n at 4°C in APBS-T with 10% heat inactivated lamb serum. Subsequently, the slides were washed the following: 2x5min in APBS-T, 5min in APBS-T with 0.3M NaCl, 2x5min in APBS-T. The secondary antibody was again incubated over night at 4°C in APBS-T with 10% heat-inactivated lamb serum. Since the secondary antibody was labelled with a fluorescent dye the sections were kept in the dark from this step on. Afterwards the slides were washed the following: 2x5min in APBS-T, 5min in APBS-T with 0.3M NaCl. The DNA was stained for 10min with DAPI. The slides were washed for the last time for 5min in APBS-T. Afterwards they were dried and embedded in Elvanol. The cover slipedges were sealed with colorless nail polish. The sections were analyzed with fluorescence microscopy.

2.9.3.2 Immunofluorescence on A6 culture cells

The protocol used for IF on A6 cells is based on the protocol of Prof. Schmidt-Zachmann. A6 cells were cultured on cover slips in 12-well plates o/n until confluency was reached (an adherent epithelium). Culture medium was removed, cells were washed once briefly with ice-cold PBS and fixed by washing 7min in -20°C methanol, followed by 30sec -20°C acetone. After 15min air-drying, the cells were rehydrated in PBS. The cells were then incubated for 25min in the primary antibody

solution (in APBS-T with 10% heat inactivated lamb serum). Subsequently, the cells were washed twice 5min with PBS, followed by incubation for 25min with the secondary antibody in APBS-T with 10% heat inactivated lamb serum, and two repeated washing steps (2x5min PBS). The DNA was stained with DAPI for 10min with one washing step afterwards. The cover slips were dried and placed upside down on slides with one drop of Elvanol. The cover slips were fixed with colorless nail polish. The sections were analyzed with fluorescence microscopy.

2.9.3.3 Image acquisition

Images were obtained using a Zeiss Axiophot or Leica MZFCIII microscope fitted with 5x, 10x, 20x, 40x and 60x objectives and AxioCam or ProGres Zeiss digital cameras. For digital image acquisition and processing, Qcapture (Zeiss) or ProGres C14 (Zeiss) were used. All image acquisition settings of one experiment were adapted to the according background control. Final arrangement of all images was performed using Adobe Photoshop and Adobe Illustrator, adjusting the levels of one image in the linear range.

2.10 Embryological methods

2.10.1 Solutions

Cystein: 2% L-Cystein in 0.1xMBS (pH7.8 at 23°C, adjusted with 5M NaOH)

Human Chorionic Gonadotropin (HCG): 1000 I.U./ml HCG in ddH₂O

MEMFA: 0,1M 3-(N-Morpholino)-propanesulfonic acid (MOPS), 2mM EGTA, 1mM MgSO₄; 3.7% formaldehyde (pH 7.4 at 23°C)

1x Modified Barth's Saline (MBS): 5mM HEPES, 88mM NaCl, 1mM KCl, 0.7mM CaCl₂ (before use), 1mM MgSO₄, 2,5mM NaHCO₃ (pH 7.6 at 23°C)

MBS/high salt: 1xMBS with 50mM NaCl

0.1xMBS/Gentamycin: 0.1xMBS, 10µg/ml Gentamycin

MBS/CS: 0.8xMBS high salt with 20% chicken serum, 200U Penicillin/ml, 200µg/ml streptomycin stored at -20°C

2.10.2 Superovulation of female *Xenopus laevis*

Xenopus laevis females were stimulated to lay eggs by injection of 500-800 units of human chorionic gonadotropin (Sigma) into the dorsal lymph sac and incubation at 18-20°C over night. Egg laying started about 12-18h later.

2.10.3 Preparation of testis

A male frog was anaesthetized in 0.1% 3-Aminobenzoic acid-ethyl-ester in ddH₂O for 30min, cooled down in ice-cold water, and killed by decapitation. The two testes were taken from the abdominal cavity by pulling out the yellow fat body, with which they are connected by connective tissues. Until use, the testes were stored in MBS/CS for maximal 7 days.

2.10.4 *In vitro* fertilization of eggs and culture of the embryos

For *in vitro* fertilization a piece of testis was minced in 1xMBS and mixed with freshly laid eggs. Afterwards the embryos were cultured in 0.1xMBS at 16-23°C in 110mm Petri dishes.

2.10.5 Removal of the egg jelly coat

One hour after fertilization or later, the egg jelly coat was removed in 2% cysteine solution pH 7.8 for about 5min with gentle agitation in a conical glass flask. Embryos were washed three times with 0.1xMBS and cultured further in 0.1xMBS+10µg/ml gentamycin at 16-23°C.

2.10.6 Injection of embryos

Injection needles were pulled from glass capillaries (World Precision Instrument, Inc.; glass thin wall W/Fil 1.0mm, 4IN) with the Microneedle Puller (setting: heat: 800; pull: 35; vel: 140; time: 139; Sutter Instrument, model P-87). It was placed into the holder of the injection equipment (Medical System, model Pi-100). The tip of the injection needle was broken with Dumont tweezers (No 5); the opening was calibrated until an injection pressure of 30psi produced an injection volume of 5nl in a defined injection duration (30ms-1s). The needle was filled with 1-2µl antisense Morpholino oligonucleotide containing solution shortly before the injection. 10nl nucleotide solution was injected into each embryo. Embryos were injected at the two-cell stage unilaterally twice in one blastomere or once/twice in both blastomeres. After injection, the embryos were incubated in 0.1xMBS containing gentamycin at 16-23°C until the desired developmental stages in a 60mm Petri dish

covered with 1% agarose in 0.1xMBS. The saline was changed every day to increase the survival rates of the embryos.

2.10.7 Protein knock-down in embryos by antisense Morpholino oligonucleotide

Antisense Morpholino oligonucleotides are nonionic DNA analogs available from Gene Tools. The optimal target is a 25-base sequence that lies within the region from the 5' cap through the first 25-bases of coding sequence, has a ~50% GC content for high target affinity and has little or no secondary structure. The Morpholino oligonucleotide should not have stretches of four or more contiguous G so that it remains water-soluble (see Genetools; <http://www.genetools.com//vivomorpholinos>).

Due to complementary binding of the antisense Morpholino oligonucleotide to its target RNA, translation of this protein is efficiently blocked (Heasman, 2002; Heasman et al, 2000). Depending on the turnover of Seb4 protein, after a certain time the pool of existing protein is degraded and the knock-down of Seb4 becomes effective, because *de novo* translation is inhibited.

Embryos were injected with 10nl antisense Morpholino oligonucleotide at the two-cell stage. After injection, the embryos were incubated in 0.1xMBS containing gentamycin at 16-23°C until tadpole stage.

3 Results

Besides the general role of RNA-binding proteins (RBPs) in cellular processes, RBPs can play major roles in development by operating at different steps of differentiation or in concert with tissue-specific regulators controlling gene expression on the post-transcriptional level. The putative RNA-binding protein Seb4 is a novel factor that might mediate its suggested role in muscle differentiation by post-transcriptional regulation.

The experiments presented here aimed to investigate the biochemical characterization and biological role of Seb4 during *Xenopus* development.

3.1 Generation of antibodies against Seb4

Specific antibodies are a major tool to analyze protein characteristics *in vitro* and *in vivo*. For broader application options we chose to generate both specific monoclonal and polyclonal antibodies against Seb4 protein. For this purpose a glutathione-S-transferase (Gst)-Seb4-fusion construct was cloned and recombinant Seb4 was expressed in *E.coli* cells. After purification of the Gst-Seb4-fusion protein with glutathione-Sepharose, the eluted full-length protein and in a small percentage its degradation products were analyzed by SDS-PAGE with subsequent Coomassie staining and were evaluated against a BSA standard (Figure 8A). As often reported in the literature, the *E.coli* host protein DnaK (Hsp70; molecular chaperone homologue migrating at 70kDa) was co-purified along with Gst-Seb4 (migrating at 50kDa) (Baneyx, 1999). The monoclonal antibodies were raised in cooperation with the laboratory of Elisabeth Kremmer (GSF München) using rats for immunization. Positive primary hybridoma cell supernatants were pre-screened by the Kremmer laboratory concerning their specificity to bind the Seb4-antigen, but not to the GST-fusion part (or DnaK). Two additional sera of polyclonal antibodies were generated by BioGenes, by immunizing rabbits with the Gst-Seb4-fusion protein. Two monoclonal antibodies Seb4 8B3 and Seb4 6E5 and the two polyclonal sera 7601 and 7600 were then further analyzed by Western blotting to test their antigen specificity and to evaluate their signal/noise ratio (Figure 8B and C). 6E5 specifically recognizes *in vitro* translated Seb4, whereas 8B3 does not (Figure 8B). After the second boost of immunization the specificity against *in vitro* translated and endogenous Seb4 (migrating at 25kDa) increases in the polyclonal serum 7600,

accompanied with unspecific binding in the higher molecular range. The polyclonal serum 7601 does not recognize endogenous Seb4 in embryo extracts.

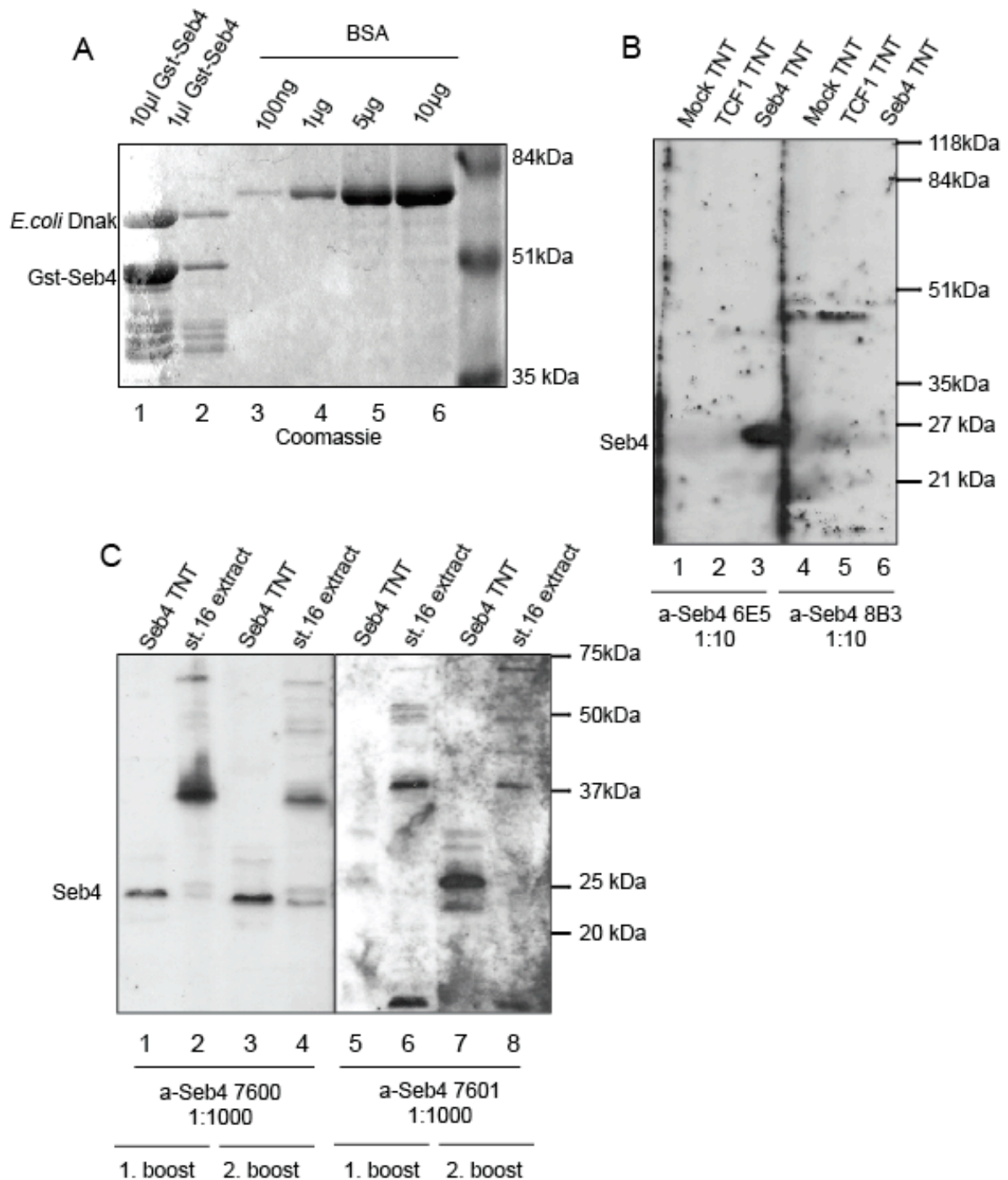


Figure 8: Generation of Seb4 monoclonal and polyclonal antibodies

(A) Quantitation of bacterially expressed and purified Gst-Seb4 against BSA protein. (B) Western blot analysis testing the rat monoclonal 6E5 and 8B3 antibody against *in vitro* translated (TNT) Seb4 and TCF1 as an unspecific protein control (antibody dilution 1:10; 5min exposure time). (C) Western blot analysis testing the rabbit polyclonal sera 7600 and 7601 against *in vitro* translated (TNT) Seb4 and embryo protein extracts (from st. 16 embryos) comparing 1st and 2nd boost of immunization (antibody dilution 1:1000; 10sec exposure time).

3.1.1 Specificity of antibodies raised against Seb4

Seb4a protein (Jasper, 1998) and its non-allelic gene copy encoding Seb4b (Fetka et al, 2000) have a very high sequence similarity and are of approximately similar molecular weight due to their amino acid sequence of 225 amino acids (aa) and 227aa, respectively (Figure 9). Seb4R protein is smaller in size with 215aa and has less sequence similarity, but is still closely related (Boy et al, 2004). The N-terminus which contains the RRM domain is highly conserved in all three proteins, whereas the C-termini are more diverse, as one can see in the sequence alignment in Figure 9.

Since both the monoclonal and polyclonal antibodies were raised against the full-length Seb4a protein the antigenic regions could be present in a conserved region on all three proteins mentioned above. In order to use the generated antibodies as a reliable tool for Seb4a characterization, first of all their specificity had to be tested and furthermore the appropriate dilution factor had to be titrated.

In the Western blot analyses shown in Figure 9B, C and D the polyclonal (7600) and the monoclonal (6E5) antibodies with the highest antigen specificity (Figure 8) are tested against endogenous protein extracts from embryo lysates of tadpole stage 26 or 37, respectively, and *in vitro* translated proteins (Seb4a and Seb4R). The different embryo stages used here exhibit no protein differences in quantity of endogenous Seb4. *In vitro* translated Seb4a protein (Seb4 TNT) migrates at 25kDa, which correlates with the estimated molecular weight of 24,750Da (lane 1 in B and C). Interestingly, when endogenous protein from embryo lysates is analyzed, both antibodies detect a double band (lane 2 in B and C) at around 25kDa. As illustrated by the schematic representation of the banding patterns in panel B and D, the lower band (lane 2 in B and C) migrates at the same size as the *in vitro* translated Seb4 protein (lane 1 in B and C), at the expected molecular weight of 25kDa.

Interestingly, *in vitro* translated Seb4R (Seb4R TNT; lane 4 in B and C) is also recognized by both polyclonal and monoclonal antibodies, but shows decreased mobility compared to its theoretical molecular weight of 23,650Da. Seb4R is detected at a size of around 25,5kDa, and therefore migrates slower than Seb4. The endogenous protein detected as the upper band (around 26kDa; lane 2 in B and C), however, does not correlate with the same size of the *in vitro* translated Seb4R protein (lane 4 in B and C). Side by side comparison of *in vitro* translated Seb4 and Seb4R protein (lane 3 in B and C) demonstrates the different migration behaviour between the TNT and the endogenous proteins detected by the antibodies. The

molecular nature of endogenous protein represented by the upper band (lane 2 in B and C), is currently unclear.

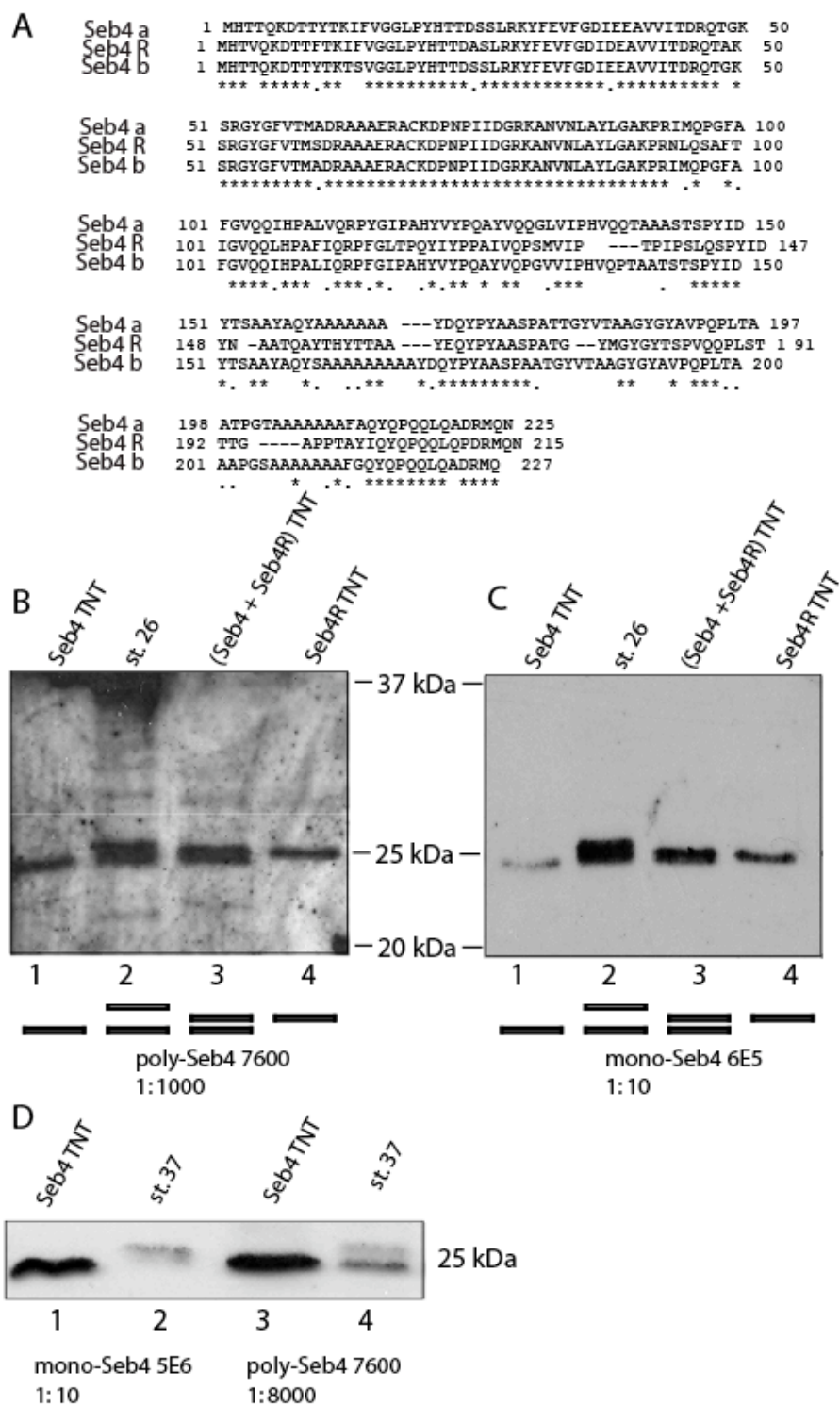


Figure 9: Comparative analysis of specific polyclonal (7600) and monoclonal (6E5) antibodies against Seb4. (A) Sequence alignment of Seb4 gene copies and Seb4R. (B), (C), (D) Endogenous (from st. 26 embryos) and *in vitro* translated (TNT ³⁵S-cys+met labelled) Seb4 and Seb4R in Western blots (B and C on one film, exposure time 3min; D exposure time 1min) with Seb4 antibodies in different concentrations, as indicated. Black bars depict protein migration pattern.

In regard to the specificity, both antibody sera detect endogenous and *in vitro* translated Seb4 and *in vitro* translated Seb4R. The polyclonal antibody serum 7600 also recognizes multiple unspecific proteins in the embryo extract and in the reticulocyte lysate after *in vitro* translation (lane 2 and 3 in B), but with lower signal intensity than the specific Seb4 signal. With an optimal dilution of 1:10, the monoclonal antibody 6E5 (Figure 9C) detects exclusively specific signal. Using a higher dilution (1:8000) of the polyclonal antibody serum a comparable (to the monoclonal antibody) selectivity for Seb4 can be achieved (Figure 9D). *In vitro* translated Seb4 protein serves as a reference, which co-migrates with the lower endogenous band. The relative intensities varied from experiment to experiment and can be neglected.

3.1.2 Defining the Seb4 antibodies

Seb4 and Seb4R are highly similar in their amino acid sequence. Both proteins are expressed tissue and stage-specifically, whereby Seb4R is mainly expressed in the nervous system, and in contrast, Seb4 mainly in striated muscle. As shown in 3.1.1 both the polyclonal as well as the monoclonal antibodies recognize endogenous Seb4 but also *in vitro* translated Seb4R.

To define the properties of the antibodies in more detail, the location of the epitopes were mapped. For this reason several deletion constructs of Seb4 were cloned, which are schematically shown in Figure 10A. The new constructs and the proteins, which they encode, are named after the numbered PCR primer pairs used to generate them. In an initial experiment the constructs delta C (containing the RRM) and delta N (the C-terminal half) were *in vitro* translated and tested for 6E5 antibody recognition by Western blot analysis, with the result that only delta C was detected (data not shown). Subsequently, I generated new constructs 12, 34, 56, 14 and 36 representing different portions of the RRM domain. In a dotblot, duplicates of native, *in vitro* translated and ³⁵S-methionin/cystein labelled protein constructs (from Figure 10A) were spotted on a membrane and tested for 6E5 antibody recognition. Due to the subcloning into the pCS2+myc-tag vector, every construct contains six methionin residues upstream of every myc-tag and either none or one additional methionin or cystein residue. Thus, the specific labelling activities differ less than 15% from each other. Therefore, the autoradiograph serves as a protein expression control. As a control for specificity I used a monoclonal antibody against β -Catenin, (PGDS) which is of the same subclass (IgG2a) as the monoclonal Seb4 antibody 6E5.

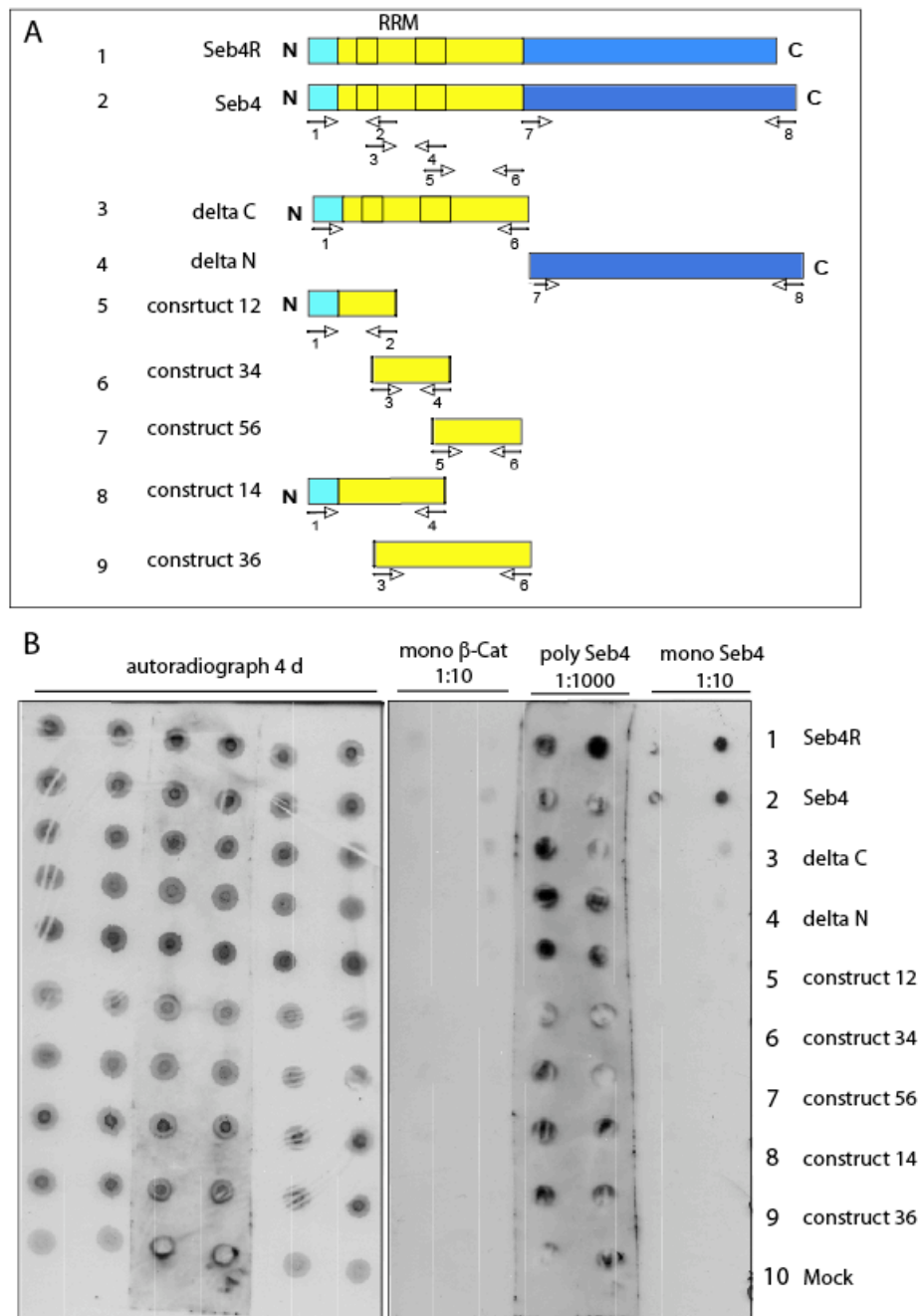


Figure 10: Epitope characterization of antibodies raised against Seb4

(A) Overview of Seb4 deletion constructs, cloned with numbered primer sets (arrows) shown underneath. Construct names (numbers) derive from primer numbers. Shaded boxes show different protein domains, as marked in Figure 7A. (B) Right panel; dotblot of *in vitro* translated Seb4 deletion constructs (^{35}S -cys+met labelled), as depicted in (A) on a nitrocellulose membrane, detected with antibodies against proteins as indicated (PGDS, poly-7600, mono-6E5). Left panel; autoradiograph.

The signals show clearly that the monoclonal Seb4 antibody 6E5 recognizes only the native Seb4R (lane 1) and Seb4 (lane 2) full-length proteins and, unexpectedly, none of the native deletion mutants. Interestingly, endogenous Seb4R

is not recognized but as an *in vitro* translated protein, native or denatured, it is. Furthermore, the delta C deletion protein is recognized in its denatured form, but not as a native peptide. As expected, the polyclonal antibody serum against Seb4 recognizes many epitopes located in many different regions spanning the whole protein length. Except for construct 34 (lane 6), all mutant proteins are recognized by the 7600 serum.

The experiments to define the 6E5 antibody revealed that the epitope is located in the highly conserved N-terminus (mainly the RRM). This observation explains why both sequence-homologues, Seb4 and Seb4R, are recognized. Unfortunately, the exact location of the epitope could not be mapped. The epitopes of the polyclonal serum are distributed all over the protein from the N- to the C-terminus, as expected. The polyclonal serum may be useful when used at higher dilutions (1:8000; compare Figure 10B to D).

Taking all antibodies' characteristics in consideration, the monoclonal 6E5 antibody against Seb4 provides a powerful tool, because its high specificity results in minimal background. Additionally, it may be useful to have two specific antibodies with diverse properties, a monoclonal and a polyclonal serum, recognizing epitopes in different locations, and having different host specificities.

3.2 Spatial and temporal expression of Seb4

Characterization of gene expression patterns is a crucial part of understanding the molecular determinants of development. Gene expression in a developing embryo occurs in a time-specific manner (temporal patterns) with subsets of differentially expressed genes in spatial patterns, which leads to the differentiation of cell fates. The expression pattern *per se* at a specific time point or developmental stage and in a specific tissue gives a lot of information about the character and function of a gene or protein and is mostly the fundamental step on which further experiments are built on.

3.2.1 Developmental expression of Seb4 protein *in vivo*

To date, no protein data of Seb4 is available. Seb4 mRNA is present continuously from the unfertilized egg until at least late tadpole stages with a low point during gastrulation (Jasper, 1998; Fetka et al, 2000). Our newly generated Seb4 antibodies were used to assess the corresponding protein expression pattern of endogenous Seb4 during embryonic development.

Protein extracts from different developmental stages between the unfertilized egg and tadpole stages were analyzed by Western blot analysis. In the unfertilized egg Seb4 protein is already present and remains at the same level until early neurula stage (Figure 11A lane 1 to 5). During neurogenesis (between stage 13 and 19) protein expression increases strongly (compare lane 5 and 6). Strikingly, in all stages Seb4 migrates as a double band at 25kDa (see Figure 9) of comparable abundance, and Seb4 protein never disappears or decreases.

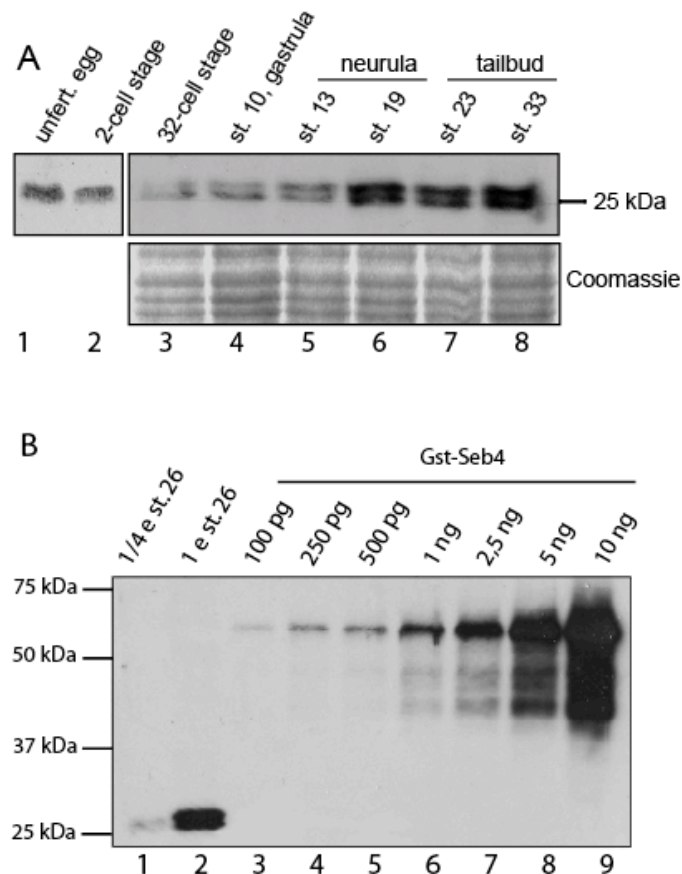


Figure 11: Endogenous Seb4 protein expression *in vivo*

(A), (B) Western blots against Seb4 using the monoclonal antibody 6E5 diluted 1:10. Equivalents of 2 embryos loaded per lane in A, or as indicated in B (1e: one embryo; 1/4e: one quarter of an embryo). (A) Endogenous Seb4 protein levels in different developmental stages. Lower panel: Coomassie stained SDS-gel serves as loading control. (B) Seb4 protein quantitation comparing different amounts of recombinant Gst-Seb4 fusion protein with endogenous Seb4 protein levels of embryo extracts.

To determine the abundance of Seb4 protein in the embryo, Western blot signals from lysates were compared to the signals from a titration series of recombinant Seb4 protein (Figure 11B). This results in the conservative estimate that

one embryo stage 26 contains approximately 1ng soluble Seb4 protein. (One quarter of an embryo is approximately equivalent to 100pg of recombinant Gst-Seb4, and the Seb4 signal of one embryo equals the signal of 1ng recombinant Seb4). Assuming that such an embryo consists of approximately 10^6 cells (Mohun et al, 1984), of which up to 10% express Seb4 mRNA/protein, Seb4 protein is present at 10^5 copies per cell. According to this estimation, Seb4 belongs to the class of very abundant proteins in the cell expressed throughout early larval development.

3.2.2 Two specific Seb4 proteins

Since Seb4a/b and Seb4R are very similar in sequence, but expressed in different tissues, it was essential to rule out that endogenous Seb4R was also detected by the Seb4-specific antibodies. As described in chapter 3.1.1 and 3.2.2 the antibodies raised against Seb4 detect a double band at the estimated molecular weight of Seb4 at 25kDa. It was of interest to identify the proteins represented by these two bands and to distinguish between the putative candidates Seb4a, Seb4b and Seb4R proteins. In embryo extracts, the lower protein band correlates with Seb4, whereas the upper band could not be attributed to any of the proteins mentioned above. Additionally to Seb4, the antibodies recognize *in vitro* translated Seb4R, as shown above (3.1.1), which migrates slower than expected from its theoretical molecular weight. One explanation for the discrepancy in migration behaviour may be a post-translational modification.

Subsequently, the Seb4 protein expression was investigated further *in vivo*. First, knock-down experiments using specific Morpholino oligonucleotides against Seb4 were performed (Figure 12A, B). Due to complementary binding of the Morpholino to the *seb4* target mRNA, translation of Seb4 protein is efficiently blocked (see below, chapter 3.3.1). The Morpholino oligonucleotide (target region shown in Figure 12A; position -3 until +22) was designed against the *seb4b* clone instead of the *seb4a* clone, because of better solubility characteristics (compare *seb4b* position 11 to 13 CAC, and Seb4a position 11 to 13 CCC; see 2.10.7). In spite of one mismatch at position 12, the Seb4 antisense Morpholino oligonucleotide (MO) targets both mRNAs, *seb4a* and *seb4b*. The corresponding region of *seb4R*, however, contains seven mismatches in the stretch of 25 nucleotides and should not be targeted by the Seb4 MO (Figure 12A).

Next, the Seb4 MO was injected into 2-cell stage embryos, lysed at early neurula stage 14 and analyzed for the endogenous Seb4 protein levels by Western blot analysis (Figure 12B). With increasing amounts of injected MO against Seb4, the Seb4 protein represented by the double band signal decreases (in comparison to the

uninjected control signal) and has almost disappeared with the highest dose of 40ng MO per embryo (Figure 12B lane 3).

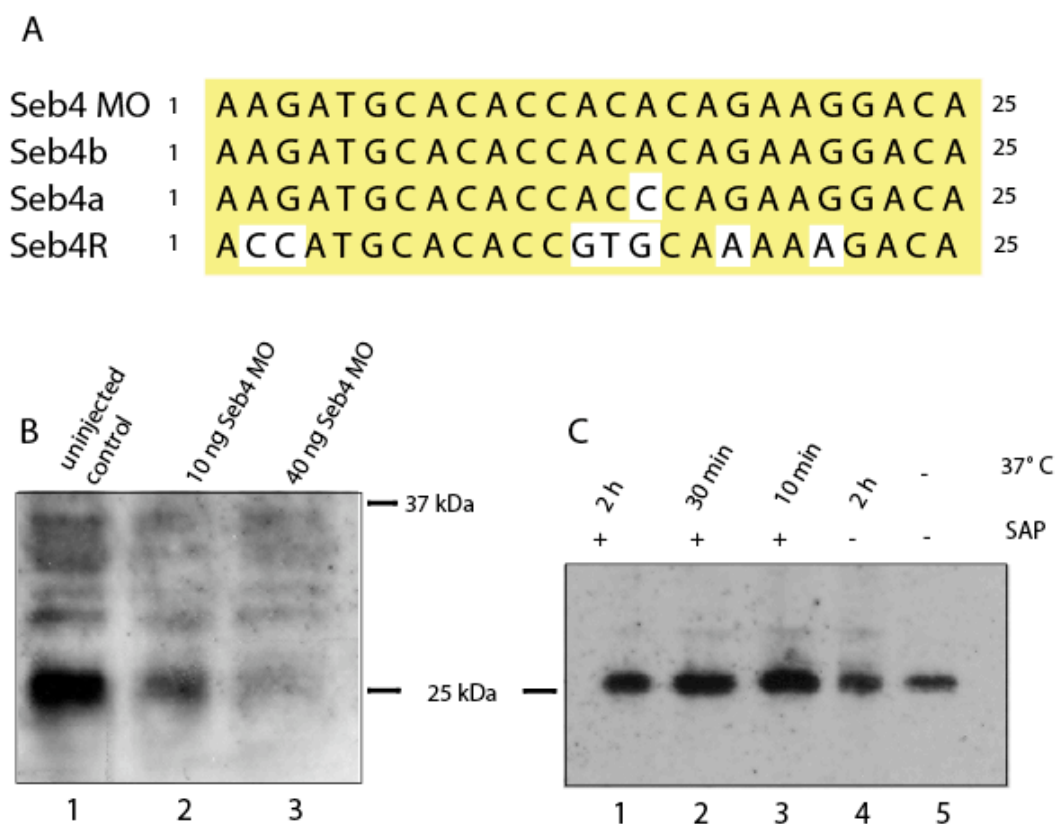


Figure 12: Seb4a/b protein is not phosphorylated

(A) Sequence of Morpholino oligonucleotide aligned with Seb4 gene copies and Seb4R. (B) Seb4 Morpholino injected embryos lysed at stage 27, Western blot against Seb4 with 6E5 antibody, diluted 1:10. (C) Embryo extracts stage 27 treated with shrimp alkaline phosphatase (SAP) for different time periods, as indicated; Western blot against Seb4 with 6E5 antibody, diluted 1:10.

The second question concerning the unexpected migration behaviour potentially as a result of a post-translational modification was addressed next. Since phosphorylation is one of the most common post-translational modifications, Seb4a/b were tested for phosphorylation to be the cause of the slower migrating protein (represented by the upper band). For this reason, embryo extracts from stage 27 embryos were treated with shrimp alkaline phosphatase (SAP) for several time points (10min, 30min, 2h), as indicated in Figure 12C, and analyzed by Western blot analysis against Seb4. Both signal bands were still detectable after 2h of SAP treatment; the protein pattern has not changed.

These results indicate that the monoclonal antibody 6E5 recognizes endogenous Seb4 but not Seb4R *in vivo*, although *in vitro* translated Seb4R can be detected by 6E5. The Seb4a/b protein migrates as a double band at 25kDa. Phosphorylation as a post-translational modification of Seb4a/b can be excluded.

3.2.3 Seb4 is expressed in mesodermal and ectodermal derivatives

Analysis of the spatial and temporal *in situ* expression pattern of a factor can shed light on its biological function in many ways. For example overlapping expression domains can give information about potential interaction partners, or upstream/downstream regulation.

Seb4 was shown to be a direct target of MyoD (see 1.3.4; (Jasper, 1998)), so, first of all the RNA expression pattern of both factors were compared by RNA *in situ* hybridization (ISH; Figure 13A).

In blastula stage embryos (st. 9), zygotic *myoD* expression is not significantly induced yet, but a basal, maternal, ubiquitous *myoD* expression exists. The same is true for *seb4*, low, maternal RNA expression is detectable by RT-PCR (Fetka et al, 2000), but not by ISH yet. The *myoD* expression is induced in prospective myoblasts in the gastrula stage (st. 11) in an omega-shaped pattern around the blastopore, excluding the organizer region above the dorsal lip. Zygotic *seb4* is induced in two small regions within the *myoD* expression domain flanking the dorsal lip/organizer. Neurula stage embryos (st. 18) show an identical *myoD* and *seb4* expression pattern in the unsegmented, paraxial mesoderm consisting of presumptive myoblasts. In tailbud stage embryos (st. 30), *myoD* is expressed in the myotome and begins to be down-regulated in postmitotic, differentiating myocytes. *Seb4* is likewise expressed in the myocytes of the myotome, but also in the myocardium and in ectodermal derivatives like the lens, the ventral part of the otic vesicle, some cranial placodes and developing lateral line primordia (Schlosser & Northcutt, 2000).

In the next experiment, the developmental Seb4 expression was followed *in situ* on the RNA level (ISH; 1-8) as well as on the protein level by immunocytochemistry (ICC; 1'-8') in comparable embryonic stages (Figure 13B). In the early blastula (st. 7; Figure 13B1) the maternal RNA contribution of *seb4* is located in the animal hemisphere. Seb4 protein is also localized in low amounts in the animal half of an early blastula embryo (B1').

In the gastrula stage embryo (B2), zygotic *seb4* transcription is induced in two small domains flanking the organizer region around the blastopore.

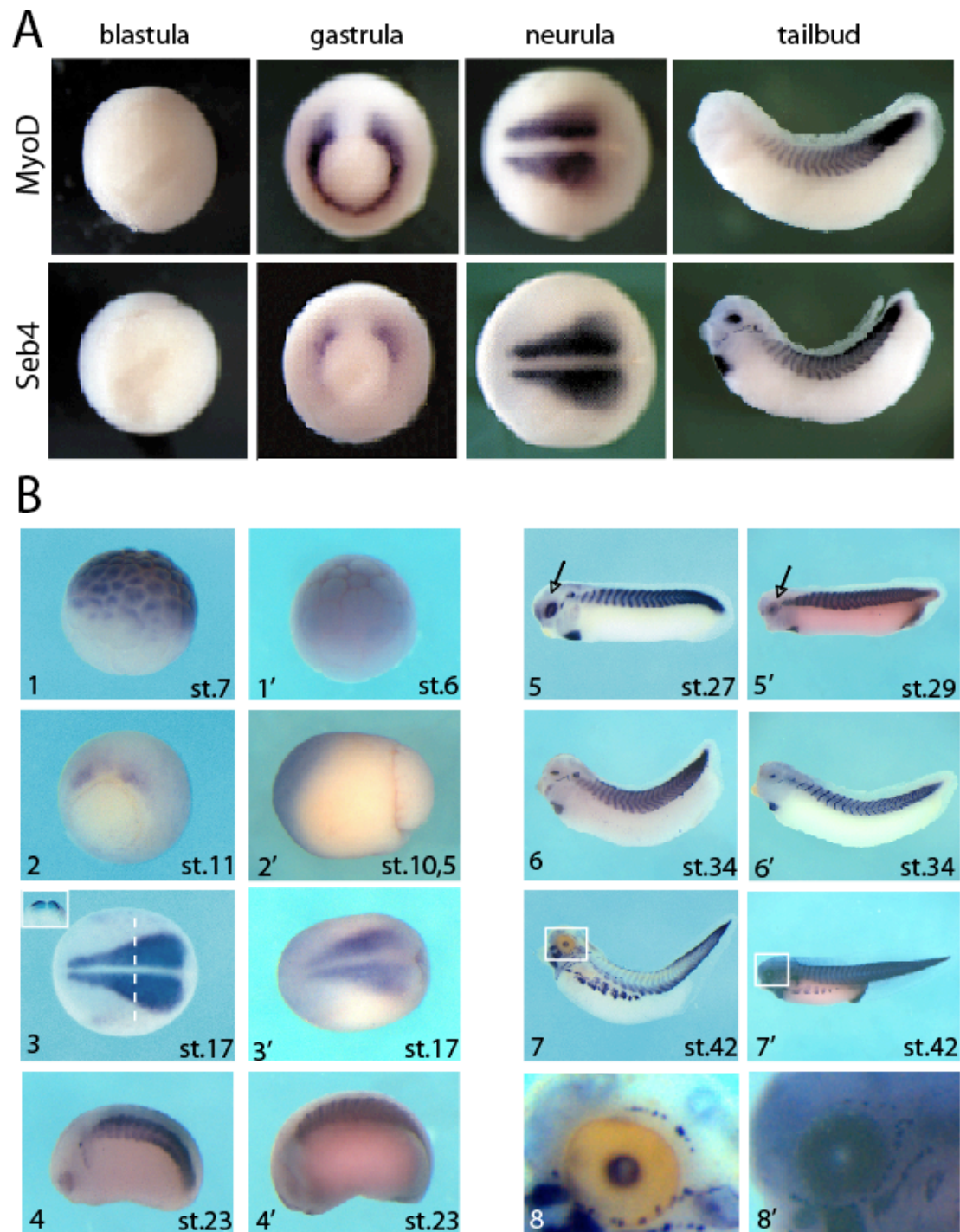


Figure 13: *In situ* expression pattern of Seb4 in *Xenopus laevis* embryos analysing the RNA and protein level. (A) *Seb4* and *myoD* RNA *in situ* hybridization in blastula, gastrula, neurula and tailbud stages. (B) Comparative analysis between *Seb4* RNA (1-8) and protein (1'-8') expression/localization in several stages by ISH (1-8) and ICC (1'-8'), respectively. Panels B1, 2', 4-8' lateral view; 1' animal view; 2 posterior view; 3, 3' dorsal view. Inlay in panel 3: crosssection perpendicular to A-P axis as indicated by white dashed line. Arrows in 5, 5' point at the retina and lens, respectively. White squares in 7, 7' are shown as enlargements in 8, 8'.

At this stage the protein is still distributed over the animal half; no distinct protein domains are visible yet (B2').

In neurula stage embryos (B3, 3') the RNA and protein expression domains are located in the paraxial mesoderm and correlate with each other. In early tailbud stages, *seb4* RNA expression is induced in the retina and in the otic vesicle (auditory vesicle; ear), whereas Seb4 protein cannot be detected yet in these ectodermal derivatives (B4, 4').

Seb4 expression in the myoblasts correlates on the RNA and protein level. In later tailbud stages (B5, 5') *seb4* mRNA is expressed strongly in the retina (arrow) as well as in the myocardium. Seb4 protein is now also found in the eye, where it is expressed in the lens (arrow) and absent from the retina. The same is true for the proctodeum, where Seb4 protein is present, but Seb4 mRNA cannot be detected. Heart muscle and skeletal muscle in the somites show both Seb4 RNA and protein expression. In even later stages, after 2d of development (st. 34; 6 and 6'), the expression pattern of *seb4* RNA and protein correlate in all tissues: striated muscle, heart muscle, lens and otic vesicle. Seb4 protein that was earlier (and later; see below) found in the anal region, has disappeared at stage 34. After 3d (st. 42; 7 and 7') *seb4* RNA expression begins to be down-regulated in the dorsal myocytes, whereas the protein is still detectable. At this time Seb4 is strongly expressed in the differentiated ventral body wall muscle. The ventral muscles have migrated ventrally and retain segmental identity, by the lack of fusion between the adjacent myotubules (Martin & Harland, 2001). Here, Seb4 protein appeared again in the anal region, whereby Seb4 mRNA seems absent.

Seb4 expression is also induced in the head in some cranial and facial placodes, in cells around the eye belonging the developing lateral line primordia, epibranchial placodes and trigeminal placodes (Schlosser & Northcutt, 2000). Most strikingly, *seb4* RNA expression in the eye is still restricted to the lens, whereas Seb4 protein is clearly localized to the retina, and excluded from the lens (8 and 8').

Altogether, Seb4 is expressed in a distinct tissue specific pattern in mesodermal and ectodermal derivatives. Including the neurula stages, its mesodermal expression domain mainly overlaps with the expression domain of *myoD*. At tailbud stages Seb4 is expressed not only in the somites like MyoD but is also found in the lens, the ear, and the heart. Seb4 expression correlates on the RNA and protein level in the myoblasts. Exceptions to this rule occur in the anal region and during eye differentiation in early tailbud and late tadpole stages.

3.3 Seb4 depletion leads to reduced muscle and lens

To find out more about the function of a protein a major method of a biologist is to create mutant embryos and to analyze their phenotypes. In contrast to gain-of-function (G-o-F) experiments, only loss-of-function (L-o-F) studies can reveal the essential functions of a protein. For the L-o-F approach antisense Morpholino oligonucleotides were utilized as a means to investigate gene function *in vivo* in the embryo — a method well established in *Xenopus* (Heasman et al, 2000). Additionally, the specificity of the endogenous Seb4 expression pattern analyzed in 3.2.3 can be confirmed by the lack of Seb4 protein upon Seb4 knock-down. Analysis of Seb4 mutant phenotypes can also lead to conclusions about the requirement of Seb4 for a specific tissue. Nevertheless, the technique applied here in this study (see 2.10.7) only targets the zygotic, and not the maternal Seb4 protein.

For the L-o-F experiments I generated a Seb4 knock-down by injecting antisense Morpholino oligonucleotides (MO) directed against *seb4* and thereby blocking *seb4* translation. After protein ablation, the morphology of the developing mutants can be described and further investigated by marker analysis.

3.3.1 Seb4 Morpholino efficiently depletes Seb4 *in vitro* and *in vivo*

Before the generation of Seb4 knock-down mutant embryos, the specificity of the exogenous flag-tagged Seb4 MO and the efficiency to block translation had to be initially tested. In several experiments this was successfully accomplished. First of all, the MO was tested in reticulocytes lysate assays, next it was confirmed *in vivo* by blocking the translation of Seb4 protein (data not shown). Finally the MO was used *in vivo* to efficiently deplete endogenous Seb4 protein.

In the *in vitro* approach, first of all, the MO specificity and dose-dependency was tested by comparison of the *Xenopus* Seb4 MO to a human standard control MO. Secondly, the Seb4 MO was tested for its target specificity for wildtype *seb4* but not for a mutant *seb4*, which contains seven nucleotide substitutions downstream of the ATG start codon.

The reaction was performed in reticulocytes lysates, which provide every component needed for protein synthesis (SP6 RNA-polymerases, nucleotides, ribosomes, amino acids, etc.) from plasmid DNA. The inhibition of translation was controlled by applying the MOs in two doses (with 10x fold difference) to the reaction expressing either wildtype or mutant *seb4* cDNA plasmids. The samples were loaded on a SDS-PAGE and analyzed by Western blotting against Seb4 (Figure 14). As expected, in presence of the unrelated control MO neither the mutant nor the

wildtype Seb4 protein synthesis is altered (compare lane 1, 5 and 2, 6). If adding the specific Seb4 MO, the mutant Seb4 protein is still expressed, whereas the wildtype Seb4 translation is strongly reduced (compare lane 3, 7 to 4, 8). With a 10x higher dose of the Seb4 MO the wildtype Seb4 expression can be blocked almost completely (lane 8) proving that the Seb4 MO works in a specific and efficient manner.

In the next step the blocking efficiency and specificity was tested *in vivo*. Therefore embryos were injected in the 2-cell-stage into both blastomeres with a total of 20ng MO per embryo. The embryos were collected at the time points indicated past the injection procedure (e.g. at 6h, 30h and 54h). The total protein of the embryos was extracted and Seb4 was analyzed by SDS-PAGE and Western blotting (Figure 14B). The lanes were equally loaded, as judged by Ponceau S staining (data not shown). The uninjected control group of embryos (lane 1, 4 and 7) as well as the standard MO injected group (lane 2, 5 and 8) show ascending Seb4 protein levels as development proceeds. In contrast, Seb4 MO injected embryos show descending Seb4 protein levels at the given times (lane 3, 6 and 9) and Seb4 protein expression is decreased to a large extent after 54h (compare lane 7, 8 and 9).

After the specificity and the efficiency of the Seb4 MO had been confirmed, the Seb4 expression pattern was investigated *in situ* upon Seb4 MO knock-down and the mutant phenotypes and their penetrance was analyzed.

Unilateral injections offer several advantages. The uninjected body half serves as an internal control to the mutant body side. Another advantage is that higher doses of a specific MO can be tested in unilaterally injected embryos, because the wildtype side can compensate the phenotypic perturbation effect to some extent.

In Figure 14C, both sides, the uninjected (4, 5, 6) and the MO-injected (4', 5', 6') side of Seb4 depleted embryos are shown. Excitingly, the typical striated muscle structure of the aligned myocytes is lost in the injected body half. Only very few cells still express Seb4 protein after injection of 20ng/e MO (4-4''). Injection of 30ng/e of MO (5-5'') results in an even stronger decrease of Seb4 expression. A total lack of Seb4 protein can be observed in the embryo in panel 5'' in the trunk region of the skeletal muscle. Only low amounts of Seb4 protein are still present in the muscle of the tailbud tip (5').

With an increase of the injected dose of Seb4 MO, the body is increasingly reduced in length, with malformations of the head (microcephaly) and a shortened tailbud tip. These developmental defects on the mutant side consequently lead to the curvature of the embryo towards the injected side.

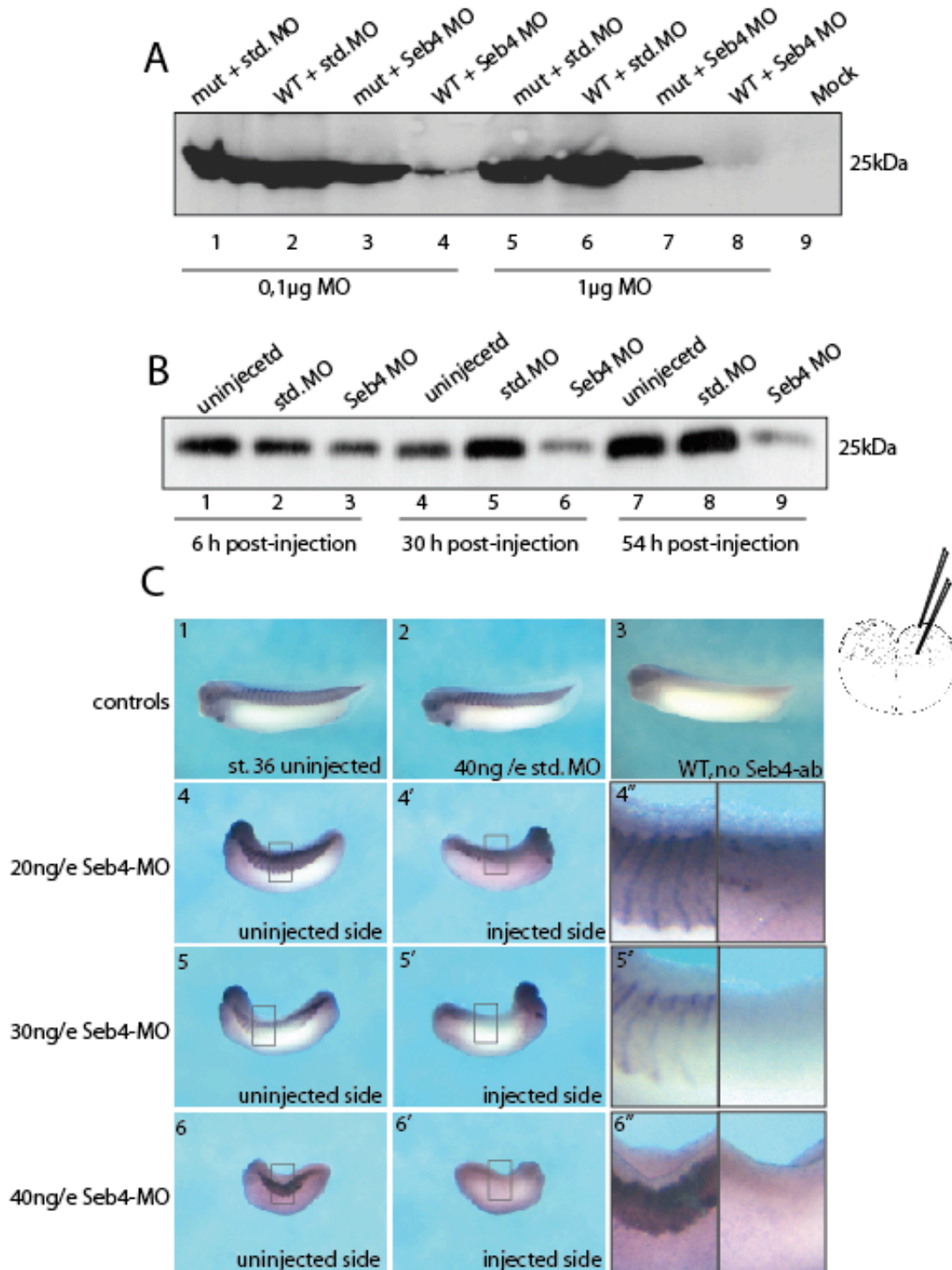


Figure 14: *In vivo* knock-down of endogenous Seb4 protein reduces muscle tissue (A) Western blot against Seb4 using 6E5 (1:10); TNT reticulolysate assay. (B) Western blot against Seb4 using 6E5 (1:10); depletion of endogenous Seb4 protein in embryos by injection of 20ng MO per embryo in the 2-cell-stage into both blastomeres. (C) Unilateral Seb4-MO injected embryos were analyzed at stage 36 by ICC with the 6E5 antibody diluted 1:1000. (C1-3) controls; (1) uninjected WT embryo; (2) 40ng/e standard MO injected twice into both blastomeres; (3) ICC control uninjected WT embryo without 6E5 ab; (4), (5), (6) uninjected control side, (') double unilateral injected side of same embryo, concentrations are as indicated; (') Somites of both embryo sides in detail.

The highest dose of injected MO (40ng/e; 6-6'') causes a very severe phenotype. Under this condition Seb4 protein is not detectable anymore in the myotome, heart and eye. The body size is reduced to 50%, the axis is shortened, and the head/eyes and tailbud/fin are reduced drastically (6'). Also the uninjected side is affected in its Seb4 expression. The myocytes do not align in their proper manner anymore; the myotome appears compressed and unstructured leading to the suggestion of Seb4 being involved in myogenesis as a factor regulating structure, alignment and adhesion of myocytes.

The L-o-F experiments strikingly show that injections of increasing concentrations of Morpholino against Seb4 lead to a loss of Seb4 expression, which causes reduced muscle tissue, diffuse and unstructured myocytes, reduced body size, head and tailbud ablations and a loss of tissue on the mutant side causing a bend in the body axis towards the injected side.

3.3.1.1 Depletion of Seb4 causes ablation of muscle and lens specific gene expression

The characterization of the mutant Seb4 phenotype was completed by substantiated marker analysis *in situ*, which identified the altered tissues and pathways involved (Figure 15). According to the Seb4 expression pattern supported by the pattern of the mutants lacking Seb4, several marker genes were selected for RNA *in situ* hybridization (ISH) to reveal the phenotypic consequences of Seb4 ablation. Since Seb4 is mainly expressed in the somites, the first tissue analyzed was paraxial mesoderm and skeletal muscle. As described in chapter 3.2.3, the *seb4* expression domain in the neurula embryo matches completely with the expression pattern of *myoD*. Therefore, the gene expression of *myoD* was investigated as an early master regulator of skeletal muscle (Hopwood et al, 1989). As a late muscle marker, *myosin light chain mlc35* (alias *MLC1f/3f*) was analyzed, designating differentiated myocytes in the somitic muscle (Theze et al, 1995).

To test whether neural tissue was affected by Seb4 depletion, *nrp1* (nervous system-specific RNP protein-1) gene expression was investigated, Nrp1 is specifically expressed in the nervous system, including brain, spinal cord and eye, beginning at the stage of neural plate formation, where cell proliferation takes place (Richter et al, 1990). Furthermore, markers for heart and lens were tested, due to Seb4 expression in both tissues in late tailbud stages (see Figure 13B). Troponin (cardiac troponin Ic) expression is restricted to the heart at all stages of *Xenopus* development (Drysdale et al, 1994). *α -crystallin* belongs to the family of crystallins, which are very abundant structural components of the lens. The antisense probe

against α -crystallin serves as a molecular indicator of lens differentiation (Brunekreef et al, 1997).

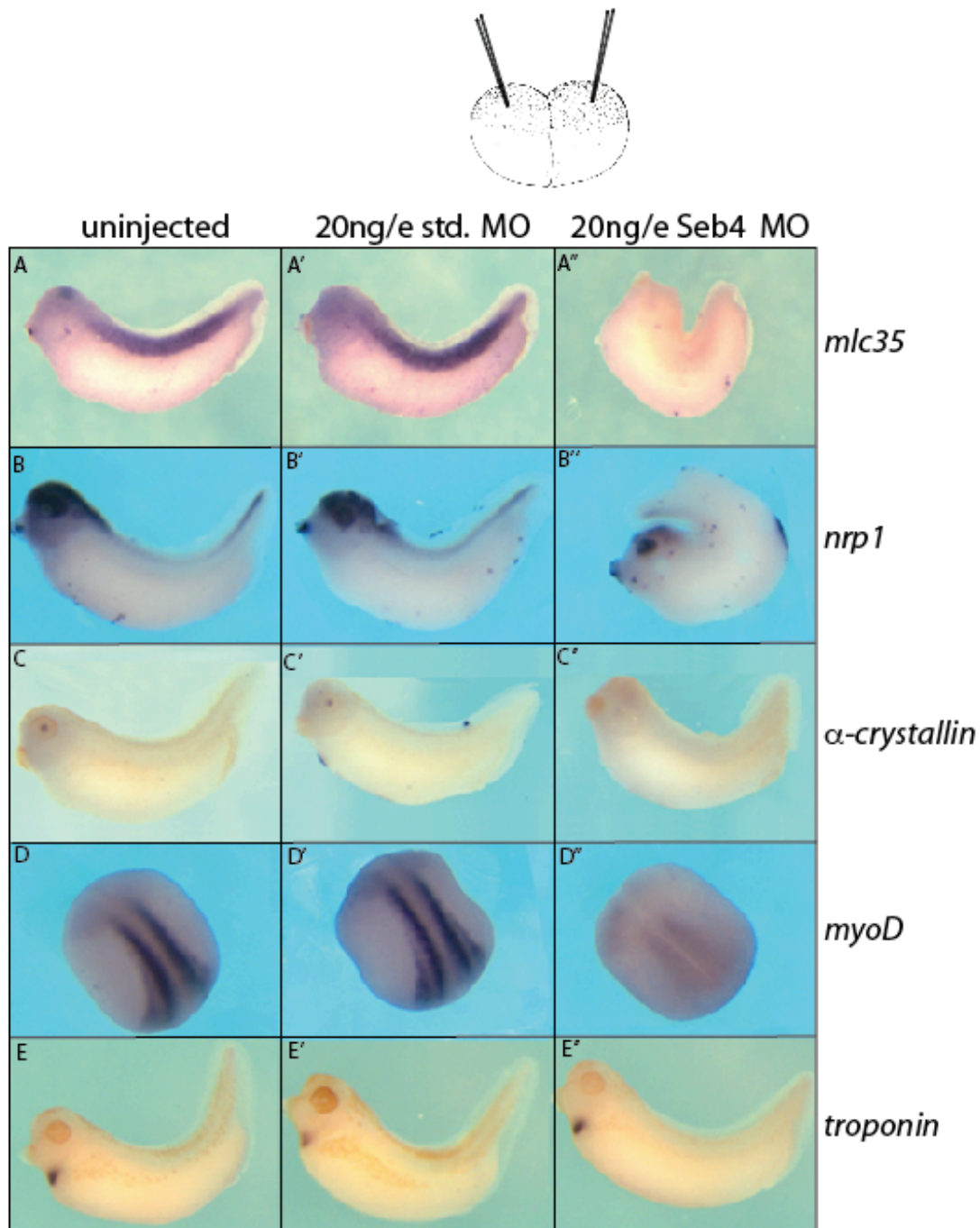


Figure 15: Seb4 protein depletion reduces skeletal muscle and lens specific gene expression. Injection of 20 ng/e Seb4 MO into two blastomeres at the 2-cell-stage. Embryos were analyzed at the neurula (st. 15) and tailbud stage (st. 34) by ISH (digoxigenin labelled antisense probes against *myosin light chain 35*, *nrp1*, α -crystallin, *myoD*, *troponin*). (A-E) Uninjected control embryos; (A'-E') 20ng/e standard MO injected control embryos; (A''-E'') 20ng/e Seb4 MO injected embryos.

The experiment was carried out by injecting 20ng/e of Seb4 MO into both blastomeres in the 2-cell-stage and following analysis of the manipulated embryos in the stage according to the optimal expression of the marker gene (Figure 15). Consistent with the morphological perturbation of the larval musculature (described in chapter 3.3.1), *mlc35* is completely abolished upon Seb4 depletion (15A''). The lack of *mlc35* expression (15A'') implies that no differentiated myocytes are formed anymore. *Nrp1* expression, in contrast, appears only weakly impaired by Seb4 depletion (15B''). *Nrp1* is still strongly expressed in the eye, brain and spinal chord. The little reduction in global *nrp1* expression is possibly due to a secondary effect caused by the ablation of muscle tissue. In panel 7C-C'' is shown that the expression of *α-crystallin* in the lens is strongly down-regulated after Seb4 knock-down indicating that Seb4 is required for proper lens differentiation. By contrast, the absence of Seb4 protein in the myocardium does not influence *troponin* expression (15E''). Thus, Seb4 expression is not essential for heart development. Intriguingly, the expression of *myoD*, one of the direct upstream regulators of Seb4, is decreased immensely upon Seb4 depletion (15D'').

Concluding from the results illustrated in Figure 15, Seb4 ablation leads to reduced expression of skeletal muscle and lens specific genes implying an important regulatory role for Seb4 in the differentiation programmes of these tissues. However, Seb4 appears to be dispensable for heart muscle differentiation, despite strong expression of Seb4 in the heart. Seb4 depletion also leads to an extensive reduction of *myoD* expression, one of the key regulators of the myogenic lineage, suggesting a regulatory feedback loop between Seb4 and MyoD.

3.4 Interaction partners of Seb4

Most proteins act in concert with others. Protein-protein and protein-RNA interactions are of central importance for virtually every process in a living cell. Information about these interactions improves our understanding of the coordination of biochemistry, signal transduction networks and can provide the basis for understanding the function of a protein.

After analysis of the Seb4 expression *in vivo* and *in situ* the next aim was to identify any associated factors to Seb4. Due to its protein sequence and domain composition Seb4 has the potential to bind to protein and RNA. First of all, I searched by general means for an interacting protein partner of Seb4 and secondly, I adapted an RNA-immunoprecipitation assay to find associated target RNAs.

3.4.1 Proteins interacting with Seb4

3.4.1.1 Co-immunoprecipitation

Co-immunoprecipitation (co-IP) is considered to be a major assay to detect protein-protein interactions, especially when it is performed with endogenous (not overexpressed and not tagged) proteins. The protein of interest is isolated with a specific antibody. One way is to separate the antibody-antigen complex from the other proteins and cellular components by using sepharose beads coupled to antibodies, which bind the complex.

To adapt the method of co-IP to Seb4 protein, the individual steps of the co-IP were optimized to meet the necessary requirements for optimal specificity and efficiency. The specific antibody (6E5) was covalently coupled to proteinA sepharose beads before blocking the unoccupied positions. This offered several technical advantages. The antibody can be easily removed from the coimmunoprecipitated material after “pulling-down” Seb4 with its associated factors. More stringent washing conditions can be applied to the sample without losing material but gaining a higher specificity. Higher and more stable beads-occupancy also led to reduced background and higher efficiency. The co-immunoprecipitated proteins were subsequently visualized by silver staining (Figure 16).

In an initial experiment, the IP conditions concerning the antibody-beads association (before and after the coupling process) were tested and compared in a Coomassie stained SDS gel (Figure 16A lane 3, 5 and 4, 7). When the antibody is not covalently coupled to the beads, the antibody is dissolved in the Lämmli buffer or IP-eluate, respectively, resulting in two extra protein signals of the heavy and light chain after Coomassie-staining (the light chain migrates at 25kDa, and the heavy chain at 55kDa) (16A lane 3, 7). The strong signals of the heavy and light chain are very dominant (the light chain migrates at the same size as Seb4), superimposing the faint IP-signals (16A lane 7). After coupling the antibody covalently to the beads, the antibody remains stably associated and can be removed (lane 4). In the IP-eluate, subsequently no antibody proteins are found (16A lane 5, 6) and, thus, the antibody signals are not disturbing the detection of proteins of similar molecular weight. The IP-efficiency is analyzed by Western blotting (Figure 16B). Seb4 is not unspecifically bound to the beads (16B lane3). Antibody dependent, Seb4 protein is immunoprecipitated with high efficiency (far above 10%), because after a 5sec exposure of the IP-band the same signal intensity is reached as the 10% input band after 3min).

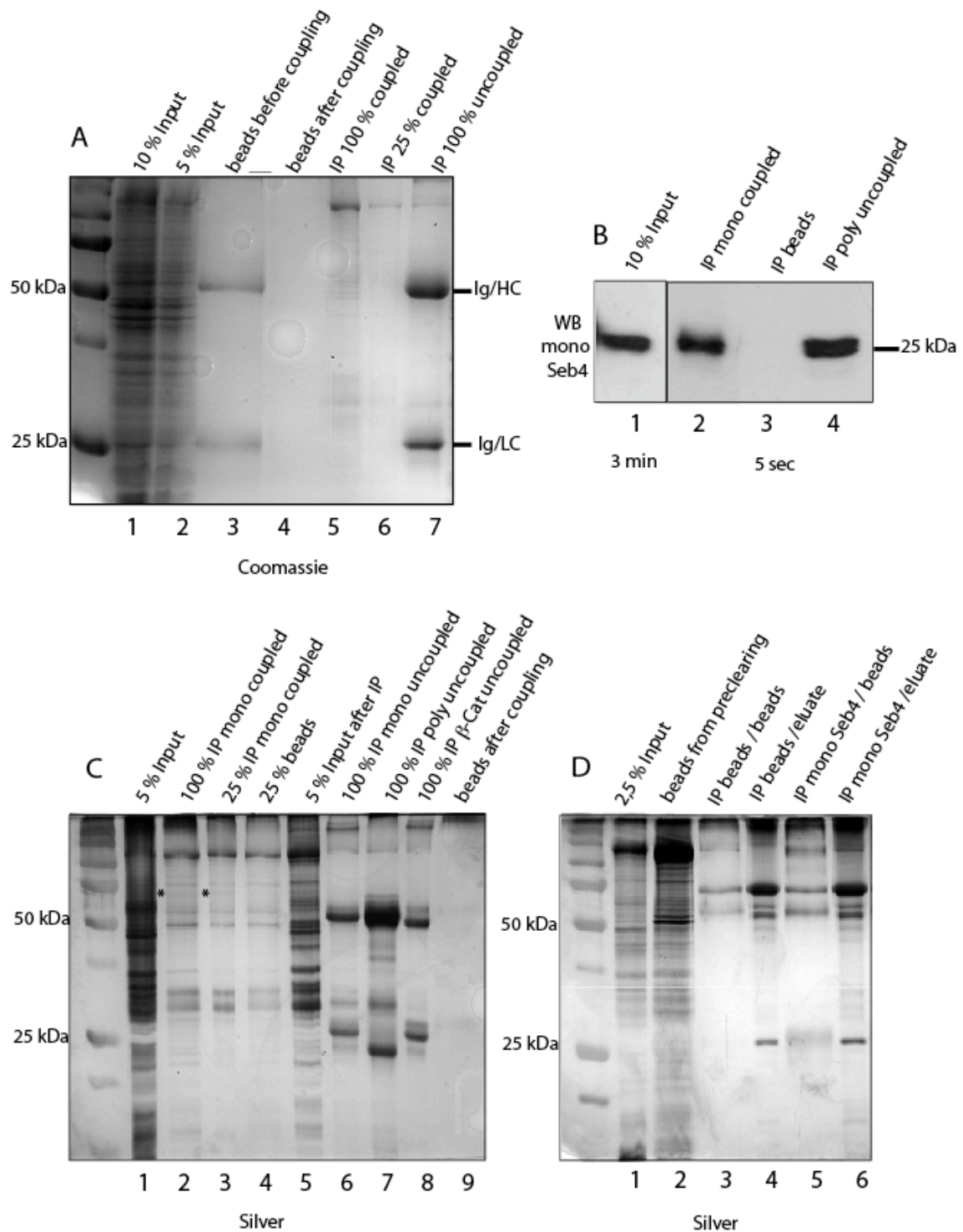


Figure 16: Efficient co-immunoprecipitation of Seb4 detects no interacting proteins. (A) and (B) were accomplished under „normal“ (not RNA-preserving) conditions, whereas (C) and (D) were performed under RNA-preserving conditions. (A), (C), (D) Coomassie- or silverstained SDS-PAGE. (B) IP efficiency shown by a Western blot against Seb4 with 6E5 diluted 1:10. Exposure times are indicated. (D) Elution of immunoprecipitated material with 0.2% sarcosyl. Percentage of the input or immunoprecipitated material loaded per lane is indicated. Antibodies used, are either covalently coupled or not coupled to the beads, as indicated.

Both antibodies, the monoclonal 6E5 (coupled to the beads, 16B lane 2) and the polyclonal 7600 (uncoupled to the beads, 16B lane 4), have the potential to immunoprecipitate Seb4 with equal high efficiencies.

Since the polyclonal Seb4 antibody recognizes many epitopes, most likely also some on other proteins, I preferred the monoclonal 6E5 antibody for the IP experiments in order to reduce unselective background. In regard to the putative role of Seb4 to bind RNA, the IPs were performed under RNA-preserving conditions. In case Seb4-RNA interaction serves as a platform for protein-protein interaction, the RNA-preserving conditions supported the chance of detecting interacting proteins dependent on Seb4-RNA association.

In the following experiments, the IP samples were either directly dissolved in Lämmli buffer or eluted with sarcosyl detergent and then resolved by SDS-PAGE (16C, D). The gels were subsequently stained with silver, because this procedure is compatible with mass spectrometry analysis of proteins. The Seb4-immunoprecipitated material (16C lane 2, 3) shows the same protein band pattern than the control reaction without an antibody control (beads alone; 16C lane 4), which leads to the conclusion that the protein bands visualized by silver-staining are actually not immunoprecipitated, but unspecific background. Interestingly, one protein detected at 70kDa (asterisks; 16C lane 2 and 3) is specifically enriched after Seb4-IP.

In the next experiment, the immunoprecipitated material is recovered from the beads-ab-complex by elution with 0.2% sarcosyl (Figure 16D). Unfortunately the protein of approximately 70kDa detected before (16C lane 2, 3) cannot be reproduced with this method. The eluate and the removed beads of the control IPs (lane 3, 4) and the Seb4-IPs (lane 5, 6) show no Seb4-specific enrichment.

Despite the high sensitivity of the method applied here (silver-staining detects low abundance proteins > 100pg), no protein interaction partners of Seb4 were detected.

3.4.1.2 *Seb4 is not bound in a complex*

Another option to investigate if Seb4 is bound in a complex of protein interaction partners is size exclusion chromatography. Gelfiltration is a chromatographic method in which particles in an aqueous solution (BC-200 buffer) are transported through a stationary phase (superose6) in a column and are separated based on their hydrodynamic volume. This results in the separation of a solution of proteins based on size. The filtered solution (eluate) was collected in different fractions, precipitated and analyzed.

Protein extracts from embryo lysates of neurula stage embryos, were homogenized under different conditions and analyzed by Western blotting against Seb4 (Figure 17A). The embryos were either homogenized with a glass douncer (extract 1, lane 1' and 1 in 17A) or by Bioruptor-lysis (ultrasonic waterbath; extract 2, 3 in 17A).

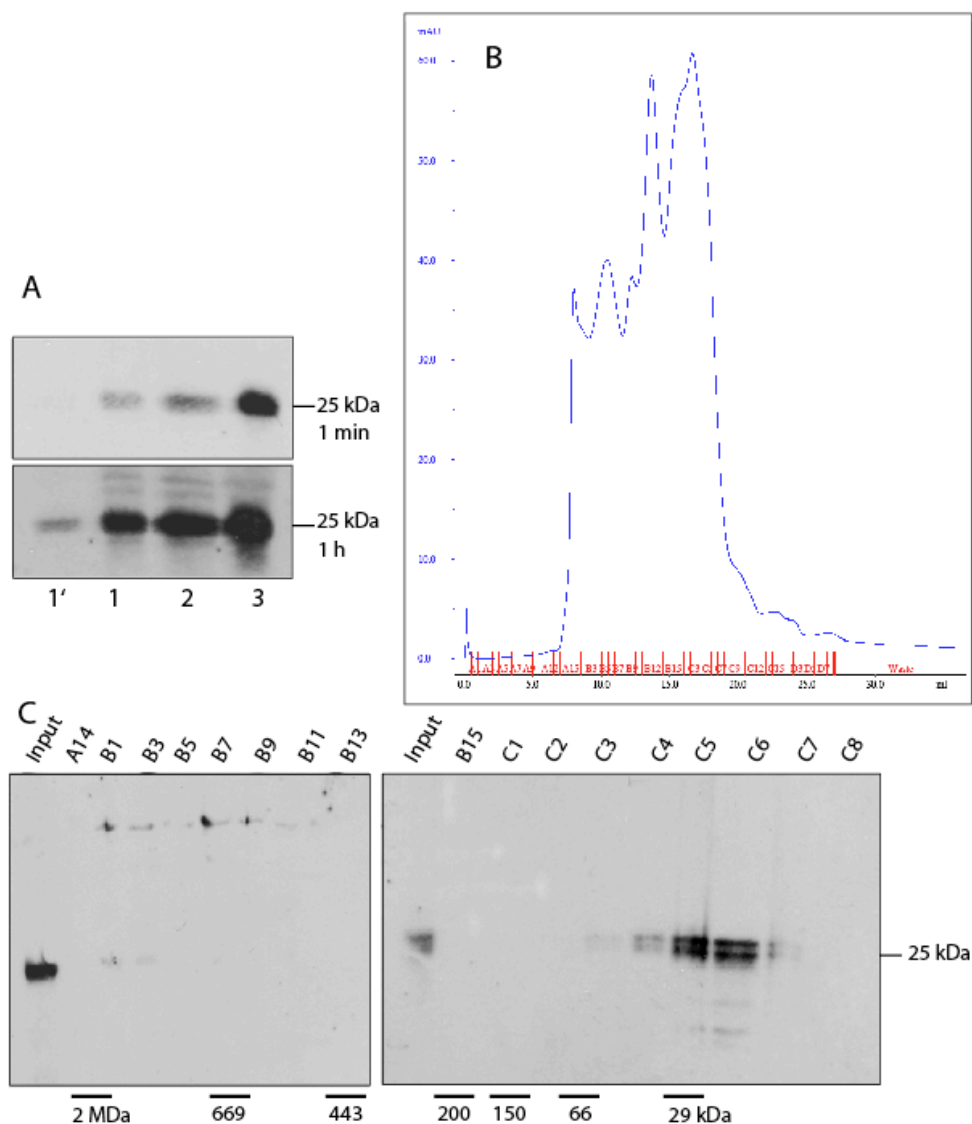


Figure 17: Seb4 elutes as a monomer by gelfiltration.

(A), (C) Western blots against Seb4 with 6E5, diluted 1:10. (B) UV absorbance of extract 2 used for gelfiltration. (B) Comparison of different extract conditions. Extract 1: douncer, no detergent, 1' = $\frac{1}{4}$ of 1; extract 2: bioruptor, no detergent; extract 3: bioruptor, + 1 % triton. (C) Collected fractions after gelfiltration.

Extract 3 (17A lane3) was additionally treated with 1% Triton X-100. Although the buffer conditions of extract 3 provided the best Seb4 precipitation efficiency, the detergent is not compatible with the gelfiltration column. Hence, the

buffer and method of extract 2 (lane 2) offered the optimal conditions (Bioruptor, no detergent) for gelfiltration – a compromise between the precipitation efficiency (Bioruptor-lysis) and the buffer conditions compatible with gelfiltration (no detergent). For the gelfiltration experiments the method was further modified at several steps. The samples (bioruptor or douncer homogenized lysates) applied to the column were either crude lysates of neurula embryos in a small volume, or lysates in a larger starting volume with subsequent ammoniumsulfate precipitation (and dialysis). The standard method of assessing the resolution of a chromatographic separation is to monitor the elution profile with a UV detector for absorbance at 280nm, which provides a rough measurement of total protein eluting in a given fraction (Figure 17B; extract 2). According to the absorbance curve in Figure 17B, the fractions containing total protein above threshold were fraction A14 to C8. The fractions from A14 up to C8 were analyzed by SDS-PAGE and Western blotting against Seb4 (Figure 17C). All different generated protein extracts delivered the same results, represented in Figure 17C. Seb4 is found in the fractions between C4 and C7 (around 29kDa) with a peak in C5 and C6 (< 29kDa), which shows that Seb4 elutes with proteins of a size just below 29kDa. Thus, Seb4 behaves largely as a monomer and is not bound within a complex of higher molecular weight under all tested conditions.

3.4.2 Seb4 – an RNA-binding protein?

Gene regulatory networks require many levels of coordination, one also that links transcriptional and post-transcriptional processes. RNA-binding proteins (RBPs) act on the post-transcriptional level, which could be pre- or post-translational. Due to the amino acid sequence of Seb4, harbouring an RRM domain, we assume an RNA-binding function for Seb4.

With the aim of finding associated RNA targets of Seb4, I developed a technology for purifying endogenously formed RBP–mRNA complexes from embryo extracts, by modifying and optimizing existent protocols for RNP investigations.

To identify Seb4 associated RNAs several approaches were applied (Figure 18). RNA-Co-Immunoprecipitation (RIP) attempted to reveal endogenous Seb4-RNA complexes (red+blue) from lysates of *Xenopus* embryos. In a first step the protein-IP efficiency was controlled by Western blot analysis (18A). Next, putative RNA-target candidates were tested by RT-PCR (18B; data not shown). Finally, targets were screened by hybridizing *Xenopus laevis* total RNA with radioactively labelled cDNA derived from RNA extracted from the co-immunoprecipitated material under RNA-preserving conditions (18C).

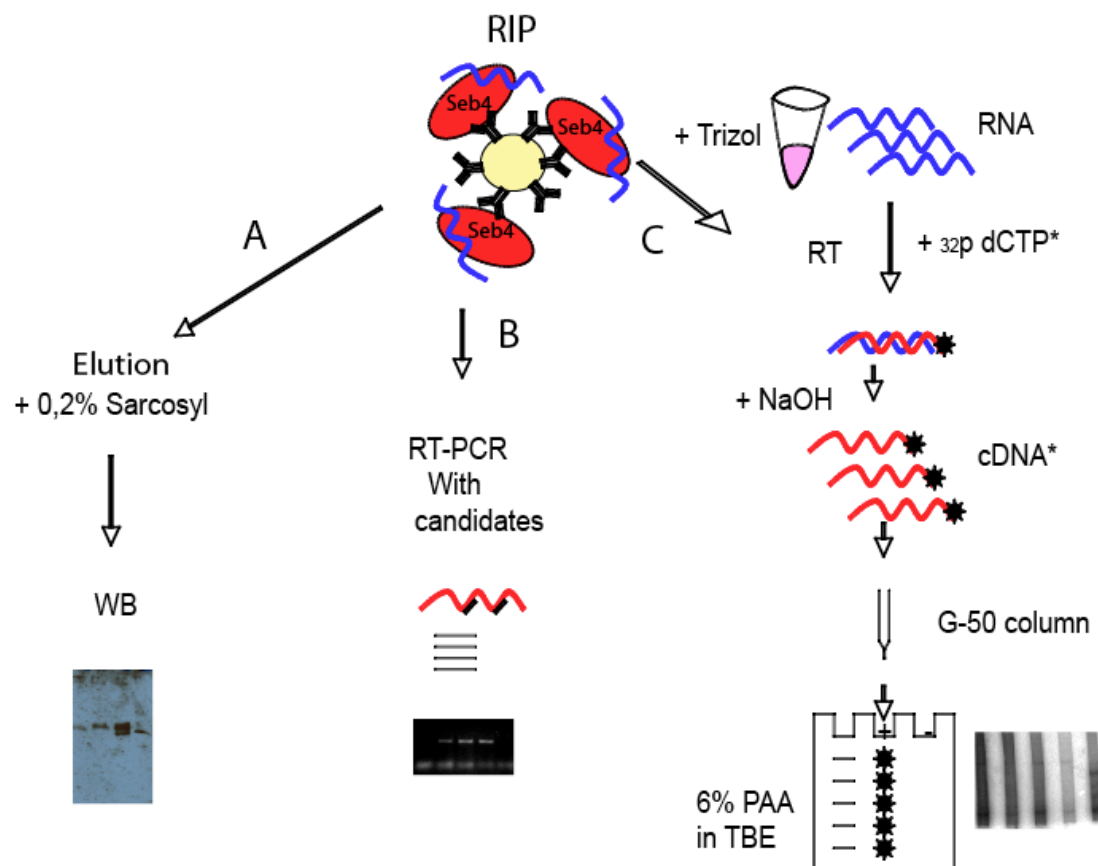


Figure 18: Flowchart of RNA-co-immunoprecipitation (RIP) experiments to identify Seb4 associated RNA targets. RIP: Immunoprecipitation of endogenous Seb4 from embryo extracts with the 6E5 antibody coupled to protein G sepharose beads under RNA preserving conditions, followed by (A) an „efficiency-check“ WB after elution of immunoprecipitated Seb4 by 0.2% sarcosyl; (B) „candidate approach“ by RT-PCR to visualize putative candidates; (C) „fishing approach“ by hybridizing labelled cDNA deriving from co-immunoprecipitated transcripts after RNA preparation with Trizol, to total RNA.

3.4.2.1 RNA-preserving-conditions ensure high protein-IP efficiency

Despite the challenge lacking a positive control for the RNP-preserving conditions (see 2.7.7), it is even of greater importance to control the other steps of the procedure. The main reaction on which every following step depends on is the protein-immunoprecipitation. Hence, it was absolutely necessary to optimize the IP-conditions and to control the efficiency by Western blot analysis (Figure 19). After elution of the beads-antibody complex, more than 25% of total (input) Seb4 could be immunoprecipitated (compare Figure 19 lane 2 and 7). In the contrary, neither the beads control nor the antibody 7F11 against MyoD serving as a negative ab control of type IgG2a (19 lane 3, 4, 1) could bind or precipitate any Seb4 protein. Further evidence for successful Seb4 precipitation was provided by Seb4 immunodepletion

effect observed in the embryo extract after Seb4-IP (19 lane 6). After Seb4-RIP, the Seb4 protein content in the embryo extract is strongly decreased compared to the MyoD-RIP (19 lane 5) and the input (19 lane 7). The high amounts of precipitated Seb4 under RNP-preserving conditions suggest that also Seb4 associated RNAs are precipitated.

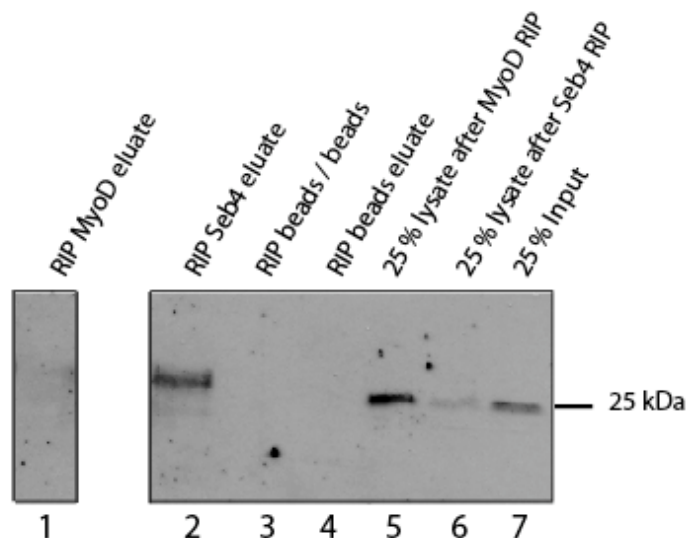


Figure 19: High Seb4 protein precipitation efficiency in RIPs. RIPs with antibodies (coupled to beads) against Seb4 (6E5) and MyoD (7F11), and beads alone. Western blot against Seb4 (6E5, 1:10).

3.4.2.2 Northern blot total RNA screen

The most promising option to screen for unknown RNA targets is a global approach. To identify targets, Seb4 co-immunoprecipitated material was hybridized against total RNA extracted from *Xenopus*. Instead of labelling the cDNA generated from total RNA from embryos an alternative and potentially more sensitive method was carried out. Labelled cDNA probes were generated from the Seb4-co-immunoprecipitated material and were hybridized against total RNA prepared from embryos at the according developmental stage (Figure 20). This method allows detection of rare transcripts, because the signal/noise ratio is much higher by selectively labelling the Seb4 co-immunoprecipitated RNA during the reverse transcription, rather than the total RNA.

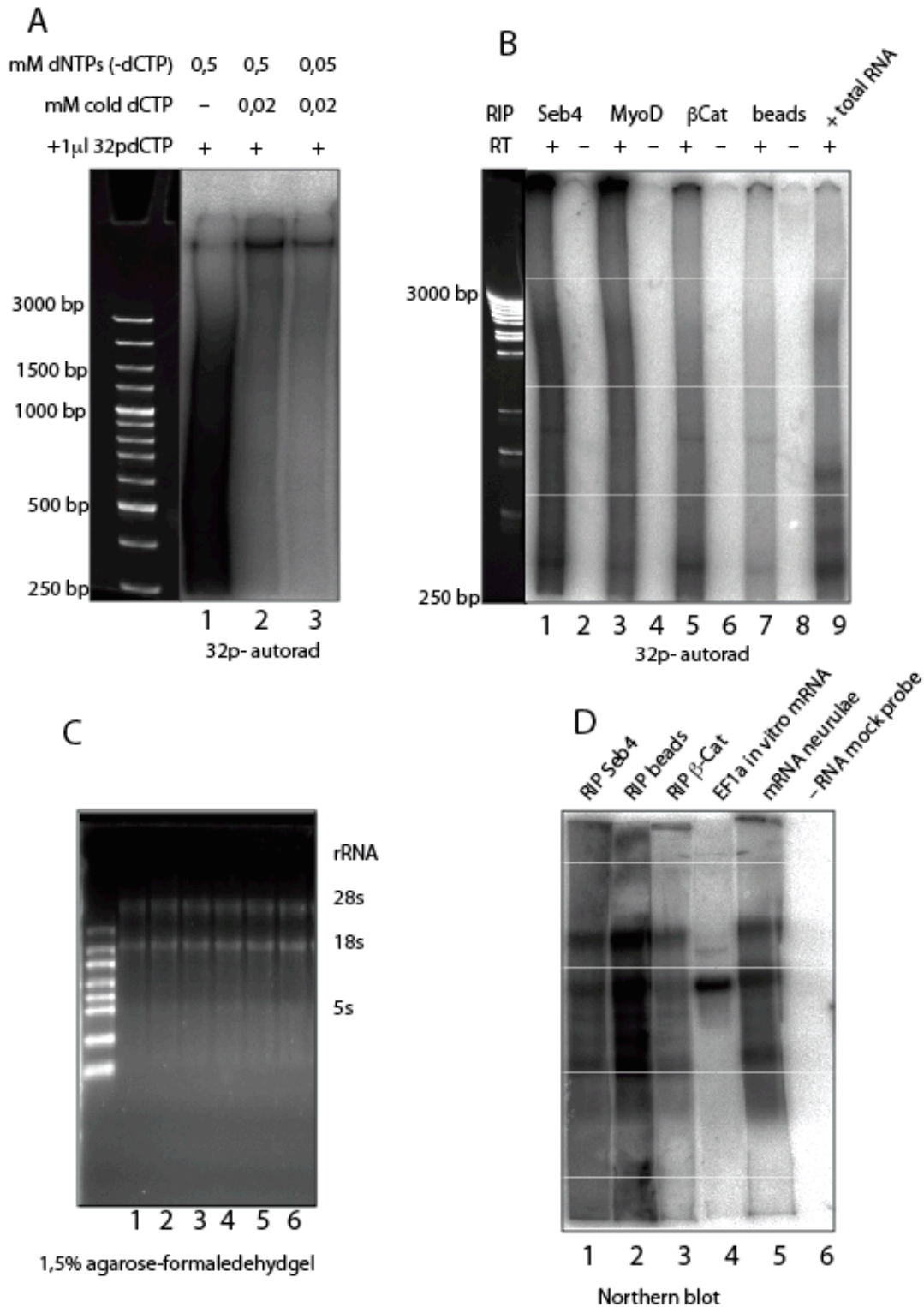


Figure 20: RIP – „Fishing approach“ by hybridization against total neurula RNA. (A), (B) ^{32}p autoradiograph of 6 % PAA gel; loaded samples: ^{32}p dCTP labelled cDNAs, after reverse transcription; 100bp DNA ladder, ethidium bromide stained. (A) Optimizing RT- labelling conditions using total RNA, oligo d(T)-priming. (B) Random hexamer primed cDNA, + and – reverse transcriptase (RT). (C) 1,5% denaturing agarose gel loaded with 20µg total RNA per lane isolated from neurulae. (D) Northern blot hybridising labelled oligo d(T)-primed cDNA from RIP material to total RNA from according lanes from (C); EF1a serves as a positive control, and size marker.

The critical and most important step in the establishment of the protocol for this target-screen was to optimize the labelling reaction for sensitivity (Figure 20A). As expected, the generated cDNA products are represented by a signal smear and not by distinct bands, suggesting that the reverse transcriptase generated first strand cDNA products from all mRNA templates of all sizes in the sample. Additionally, the co-immunoprecipitated RNA molecules were possibly exposed to partial degradation.

The radioactivity of the generated cDNA probes due to incorporation of ^{32}p dCTP is highest amplified by using only radioactively labelled dCTP without unlabelled dCTP and by adding the highest concentration of dNTPs lacking dCTP, resulting in a higher signal intensity in the autoradiograph (Figure 20A). cDNAs in a wide range from 250bp to 3000bp can be detected as a dark smear.

The RIP samples of several conditions using different antibodies against Seb4, MyoD and β -Cat were efficiently labelled during reverse transcription (as described above, 20A lane 1), and analyzed by phosphor-imaging (20B). Control reactions from which the reverse transcriptase was omitted, showed explicitly no labelled products, indirectly indicating the presence of some RNA in the co-immunoprecipitated material (20B). After Seb4 RIP, the co-immunoprecipitated RNA appears mainly as a smear, with few distinct bands. Unfortunately, all signals derived from the RNA-co-immunoprecipiations with different antibodies show the same cDNA band pattern probably caused by unspecific binding; no Seb4 specific enrichment of RNAs could be found by RIP.

In the next experiment cDNA probes were generated from oligo-d(T)primed and labelled co-immunoprecipitated RNA, and were hybridized against total cellular RNA. The pattern of total RNA isolated from neurulae is shown in Figure 20C. Equal amounts of RNA were loaded on a denaturing agarose gel visualizing the typical rRNA pattern as indicated in Figure 20C. The cellular RNA was blotted on a nylon membrane and in the following step hybridized against the RIP probes and analyzed by phosphor-imaging (Figure 20D). Elongation factor EF1a (Frydenberg et al, 1991) served as a positive control for the experimental procedure (reverse transcription of probes, Northern blot hybridization), as well as a size marker (sizes 3kb and 1,5kb; 20D lane 4). It shows that specific mRNAs, albeit an abundant mRNA, can be visualized by this technique. Nevertheless, no enrichment of specific RNAs in the Seb4-RIP sample can be detected.

In spite of RNA-preserving conditions, assuming the coherence of RNP-complexes, and an efficient RT-labelling-reaction producing cDNAs in a wide range of sizes, no selective Seb4-associated RNAs could be enriched.

3.5 Localization of Seb4

As demonstrated in the previous chapters, Seb4 is a highly conserved and very abundant protein, but so far no interaction partners of Seb4 could be determined by protein-IP, gelfiltration and RNA-IP. Therefore, Seb4 could influence a diverse array of global biological processes including cell growth, cell structure and differentiation, acting in concert with a broad range of unknown factors to mediate important regulatory effects. This leads to the suggestion that Seb4 might function as a general regulator in the cell interacting with many targets (e.g. tissue specific RNAs).

Proteins with general, regulatory roles (e.g. splicing factors) are often localized to specific cellular compartments, such as the nucleus, nuclear bodies or cytoplasmic aggregates. Investigating the specific localization of an unknown factor can provide crucial information about the function of the protein. So, I used a different approach to gain a better understanding of the function of Seb4 by analyzing its localization *in vivo* by fluorescence microscopy.

3.5.1 Seb4 is distributed in equal amounts to the cytoplasm and the nucleus

Subcellular fractionation allows cells to be fractionated into compartment-enriched fractions, utilizing differential centrifugation. In this case, separating the nuclear from the cytoplasmic compartment gives information about in which potential regulatory steps of the RNA metabolism Seb4 might be involved.

In the following experiment, the nuclear compartment was separated from the cytoplasmic compartment by isolating the nuclei from neurulae embryos by sucrose density centrifugation. Subsequently, the nuclear fraction was further separated into a soluble fraction and into an insoluble nuclear pellet. The subcellular fractions were analyzed by Western blotting and Coomassie staining (Figure 21). In the Coomassie stained gel (Figure 21, right panel) the varying protein compositions of all three fractions are visualized. The cytoplasm (lane 1) has the highest general protein content and a different protein composition than the nuclear fractions. The cytoplasmic fraction is characterized by high amounts of α -Tubulin, an abundant cytoskeletal protein, whereas Histone H3, a nuclear, DNA bound protein, is solely found in the insoluble nuclear fraction. Intriguingly, Seb4 is localized in comparable amounts in the cytoplasm and in the soluble portion of the nucleus, but is not bound to DNA.

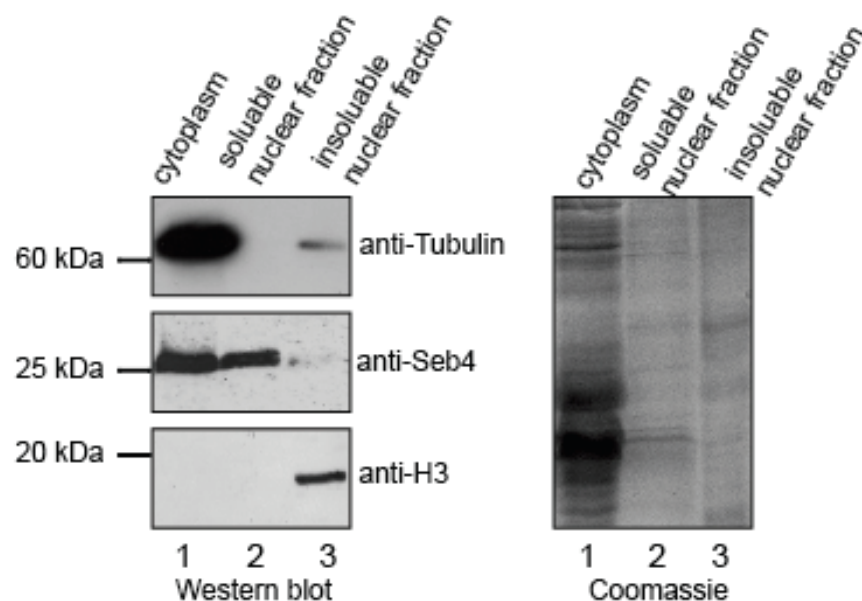


Figure 21: Subcellular fractionation of Seb4 protein by preparation of tailbud nuclei and cytoplasm. Equivalents of 7 embryos loaded per lane. Antibodies are indicated on the right side. Coomassie stained gel serves as loading/separation control.

In conclusion, Seb4 is a soluble protein localized in equal amounts in both compartments in the cell — the cytoplasm as well as the nucleus.

3.5.2 Seb4 is expressed in the *Xenopus* cell lines A6 and XTC

Another way to gain more insights into the localization and the linked function of Seb4 is to investigate Seb4 in another system. For this approach, two *Xenopus* derived cell lines, A6 *Xenopus* adult kidney cell line, and XTC *Xenopus* tadpole cell line were analyzed for Seb4 expression. At first, Seb4 expression was investigated in A6 and in XTC, on the RNA level by performing RT-PCR utilizing primers against *seb4*, *seb4R* and *histone H4* (Figure 22A), and secondly, on the protein level by Western blot analysis (Figure 22B).

To make sure that the Seb4 primers do not amplify Seb4R, because of the high sequence similarity, both primer sets were tested on their own and the other target, respectively (Figure 22A lane 5, 6 and 7). Seb4R appears to be strongly expressed in both *Xenopus* cell lines, even more than in a neurula embryo st.18, normalized by H4 expression. This might be an add-on effect since the Seb4R primers also detect Seb4 to a small extent (22A lane 5). The Seb4 primers, however, operate specifically and recognize only Seb4 and not Seb4R (22A lane 7). Seb4 is expressed in A6 as well as in XTC cells (upper signal in 22A lane 2 and 3), but with a lower expression rate than in a neurula embryo (22A lane 4), as well as lower than Seb4R is expressed in both cell lines judged by the H4 expression.

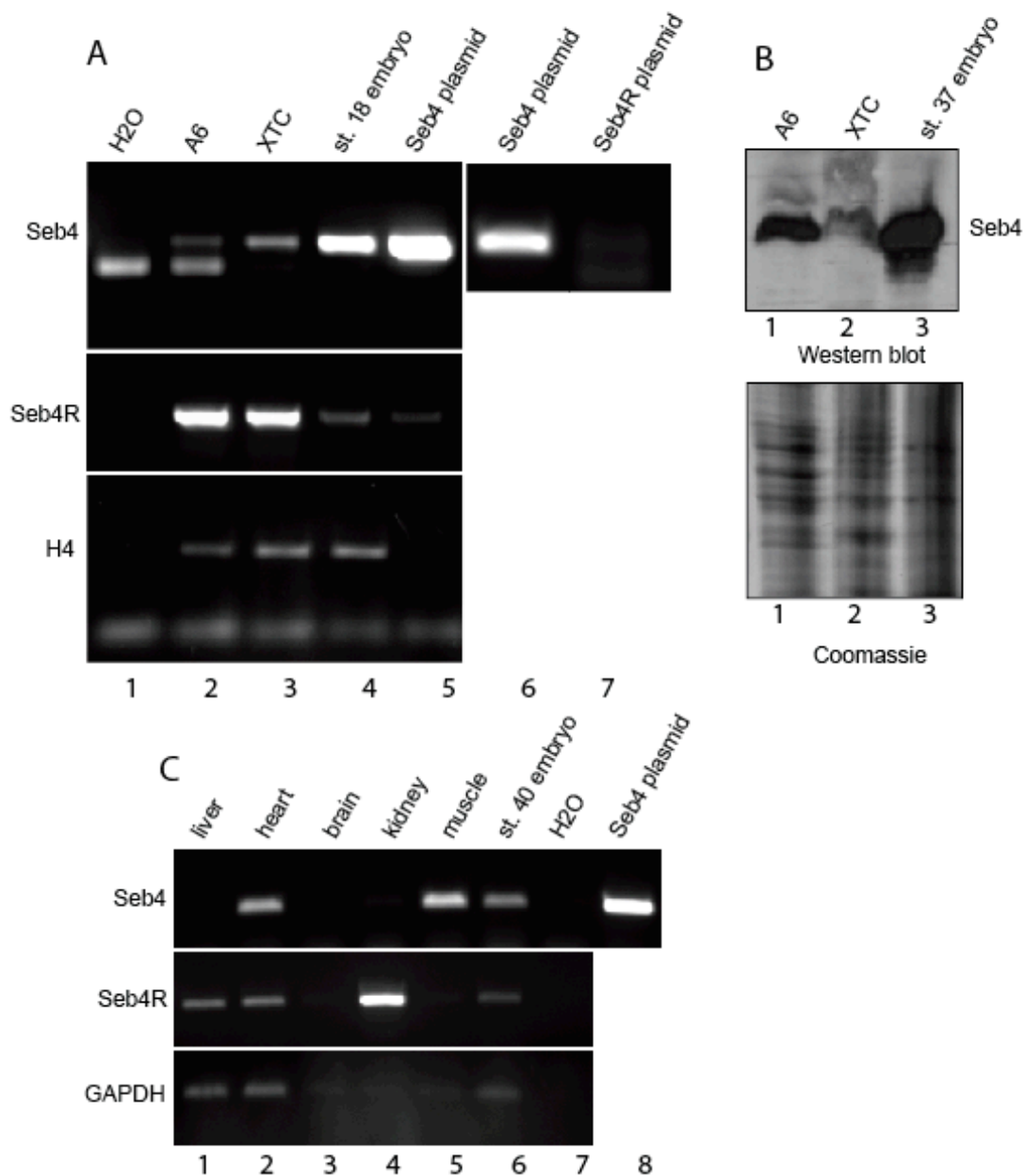


Figure 22: Seb4 expression in A6 and XTC *Xenopus* cell lines. (A) RT-PCR showing Seb4 and Seb4R mRNA expression in different samples compared to histone H4 control. (B) Western blot detecting Seb4 protein in cells and embryos st. 37; Coomassie stained gel shows protein extracts used for WB. (C) Seb4 and Seb4R mRNA expression in different adult *Xenopus* tissues shown by RT-PCR.

On the protein level, Seb4 behaves differently (Figure 22B). Coomassie staining reveals equal loading for the Western blot above. Unexpectedly, Seb4 protein is expressed to a higher extent in A6 cells than in XTC cells (Figure 22B).

Even if Seb4 expression is strongest in the embryo (22B lane 3), the A6 kidney cell line shows Seb4 expression.

In the experiment depicted in Figure 22C, the expression levels of Seb4 and Seb4R are compared in different adult frog organs by RT-PCR. Tissue samples of liver, heart, brain, kidney and muscle were analyzed. Similar to the tadpole embryo (st. 40), Seb4 is expressed in the adult heart and even stronger in muscle tissue. In contrast, Seb4R expression is found weakly in the liver and heart, but mainly in the kidney.

Although Seb4 is neither expressed in the embryonic pronephros nor the adult kidney, it is strongly expressed in A6 cells derived from kidney tissue. The strong Seb4 expression in the A6 cell line make it a very suitable and easy model to study Seb4 localization in detail.

3.5.3 Subcellular localization of Seb4 in the embryo and in A6 cells

After determining the protein expression pattern of Seb4 in whole mount embryos by ICC (Figure 13B), the following experiments were performed to support former results and to learn more about the Seb4 distribution within different embryonic tissues and in A6 cells.

3.5.3.1 *Seb4 localization in different embryonic tissues is mainly nuclear*

On paraffin sections of tailbud embryos the tissues known to be Seb4 positive (chapter 3.2.3) were investigated in detail by immunofluorescence (IF) illustrated in Figure 23. The aligned myocytes from the somites (skeletal muscle) clearly show Seb4 positive signals (in the sagittal sections in panel C and C'), which supports the results from Figure 13B and 13C. In myocytes, the Seb4 protein is mainly found in the nuclei, rather than in the cytoplasm, as judged by the signal-overlap (pink) between the red (Seb4) and blue (DNA) channels. The cross sections through the somitic myocytes (23D and D') demonstrate the density and the proximity of the myocytes positive for Seb4. The whole myotome consisting of stacked myocytes between the epidermis (right) and the notochord (left) express Seb4, whereas other cell types, e.g. epidermis and notochord, do not have any Seb4 protein expression. Interestingly, all cells that express Seb4 show a distinct protein distribution inside the nuclei. Within the Seb4 positive nuclei, a circular region devoid of Seb4 is surrounded by a high content of Seb4 protein. These Seb4-negative structures within the nuclei are also DAPI-free, which were confirmed by later experiments to be the nucleoli.

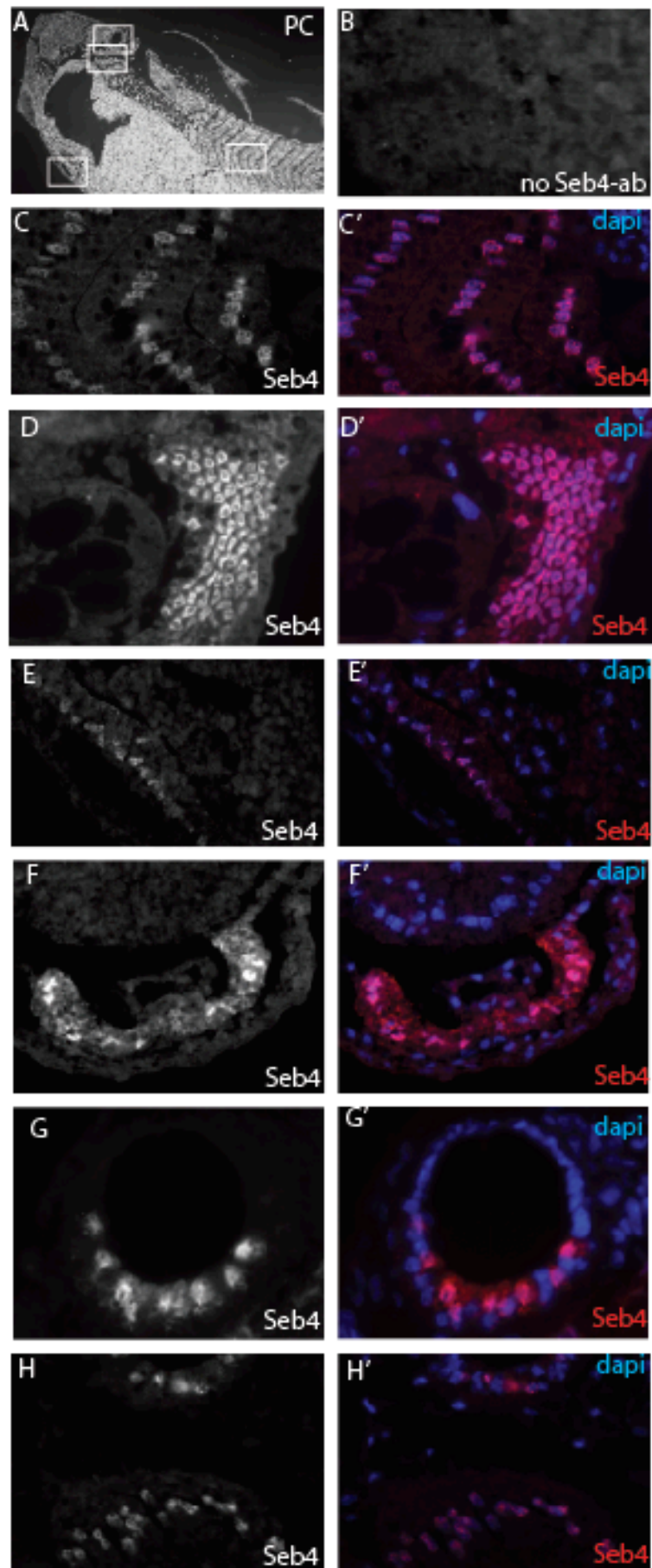


Figure 23: Seb4 protein localization in *Xenopus* embryos by immunofluorescence. (A-H) Immunofluorescence using undiluted Seb4 monoclonal antibody in sections of st. 27 embryos (40x magnification), (D, D', F, F') cross sections, (A-C', E, E', G-H') sagittal sections. (') Merge panels. DNA stain shown in blue by DAPI and Seb4 protein signal in red. (A) Phase contrast of embryo section st. 27 (10x magnification). White squares indicate the location of the areas shown enlarged in panel C-H (40x magnification). (B) IF anti-rat control without Seb4-ab (40x magnification). (C-D) Detail of myotome; (E-F) section through heart, Seb4 signal in the myocardium; (G) otic vesicle; (H) facial placodes.

In panel E and E' a small detail of a sagittal section through the heart is shown. Seb4 is expressed solely within the myocardium, the muscular and multilayered tissue responsible for the contraction of the heart (23F and F'). Seb4 is co-localizing with the DAPI stained nuclei, suggesting mainly nuclear localization of Seb4. The structures surrounding the myocardium contain the epidermis, the pericardium, a double-walled sac that contains the heart and the epicardium (not distinguishable from another in these sections). These tissues do not show any Seb4 expression. The endocardium, the innermost layer of tissue lines the chambers of the heart is also not visible in these sections (23E and F). The oval single cell layered structure surrounded by the myocardium could represent truncated blood vessels, which also show no Seb4 expression. In conclusion, Seb4 expression in the heart is restricted to the myocardium.

Another tissue highly expressive for Seb4 is the ectodermal derived ear placode (compare Figure 13B). Strikingly, Seb4 protein is exclusively expressed in the ventral region of the ear precursor tissue (23G and G'). Accompanied, in the ventral part of the otic vesicle Seb4 protein (G and G') is not co-localizing with the DAPI signal in the nuclei. Seb4 protein seems to be localized to the cytoplasm. In contrast, the cell layers below the ear (23H and H'), most likely cells belonging to other facial placodes like the lateral line primordia, express Seb4 protein within the nucleus, overlapping with DAPI stained DNA.

Since Seb4 is a key regulator of the myogenic programme, the Seb4 distribution within the myocytes was analyzed in more detail in the following experiment. Immunofluorescence of Seb4 can reveal two possible results of the Seb4 protein localization in myocytes, most likely due to the IF procedure. Depending on unknown technical parameters, the Seb4 protein distribution is reproducibly either exclusively nuclear (Figure 24A) and/or strongly cytoplasmic (Figure 24B). The distribution of Seb4 inside the nucleus (24A-A'') appears irregularly dotted, with local enrichments and different signal intensities. Per nucleus one to four Seb4 free regions are visible, which may be the nucleoli. The cytoplasmic Seb4

distribution in B-B'' is rather diffuse than spotty, although distinct dots can also be observed in the nuclei. In the cytoplasm Seb4 is enriched at the termini of the myocytes, morphologically easily recognized by the extracellular gap (dark line, Seb4 negative) between two myocytes in one row. In around 50% (represented by the close up shown in B''), Seb4 co-localizes with striated structures (compared to A''). These regular lines proceed vertically to the longitudinal cell axis. The whole striated structure is located parallel between two cells along the nucleus represented in B''.

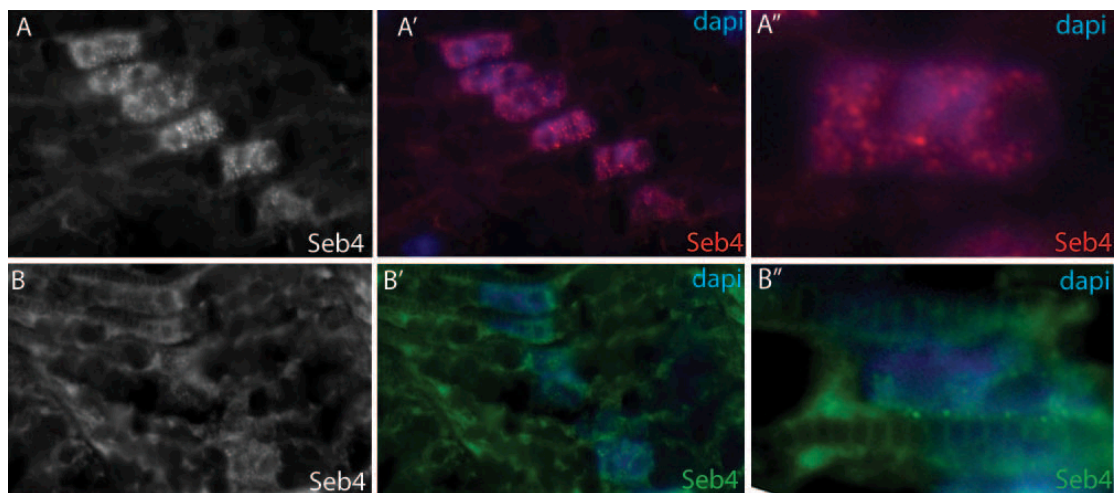


Figure 24: Nuclear and cytoplasmic localization of Seb4 in myocytes. Immunofluorescence on sagittal embryo sections with undiluted Seb4 monoclonal antibody 6E5. Detailed figure of myocyte nuclei (''). (A) Nuclear Seb4 signal in red; (B) Cytoplasmic and nuclear signal in green. DAPI signal in blue.

IF experiments in the embryo confirmed the Seb4 expression in the striated musculature, the myocardium and the myotome, and also in cranial placodes, like the otic vesicle. In most tissues, apart from the ear, Seb4 is mainly co-localizing with DAPI. The Seb4 distribution in myocytes is cytoplasmic and nuclear. In the nucleus Seb4 is localized in a distinct spotty pattern similar to several nuclear bodies (e.g. splicing speckles, etc.). In the contrary, Seb4 distribution in the cytoplasm is rather diffuse with local enrichments at the myocyte termini. The variable Seb4 protein distribution in different tissues suggests multiple functions for Seb4.

3.5.3.2 *Seb4* knock-down leads to an efficient loss of *Seb4* protein in embryonic myocytes

Similar to the *Seb4* knock-down experiments in chapter 3.3 (see Figure 14), here, the specificity of the immunofluorescence signal given by the antibody-antigen complex was tested by *Seb4* Morpholino injections. This experiment should also reveal if the *Seb4* distribution in the cell (cytoplasmic and/or the nuclear protein population) upon *Seb4* depletion was altered. For an internal control, the embryos were unilaterally injected with MO (right side of the notochord) and cross sections were generated, which were subsequently analyzed by immunofluorescence (Figure 25).

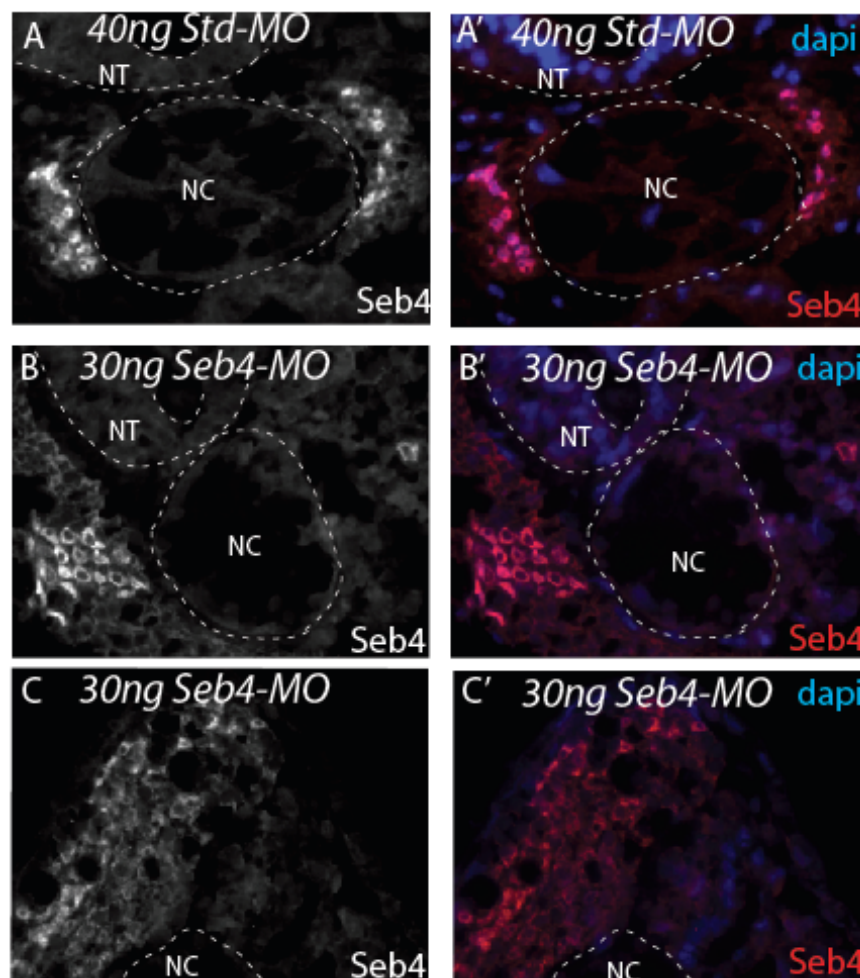


Figure 25: *Seb4* depletion by unilateral Morpholino injections leads to loss of *Seb4* in myocytes. Immunofluorescence using undiluted *Seb4* monoclonal antibody (red signal) in cross sections of st. 27 embryos. (A, A') Control embryo injected (right side) with 40ng of standard MO; (B, C) *Seb4*-MO injected embryo (right side). Abbreviations: NT neural tube, NC notochord.

Injections of high doses of standard control MO had not changed the Seb4 expression and localization pattern in myocytes (compare injected side in the right half of the panel to the uninjected side; Figure 25A and A'): Seb4 is strongly expressed in the nuclei (except the nucleoli) of the myocytes adjacent to the notochord. Upon Seb4 depletion by injection of 30ng of Seb4 MO, a loss of Seb4 protein in most cells was achieved (right side) in both compartments, the nuclei (25B and B') and the cytoplasm (25C and C').

These evidences confirm, that Seb4 expression is depleted extensively in myocytes by Seb4 MO injections. Seb4 knock-down causes equal depletion of both Seb4 proteins, the cytoplasmic and the nuclear subpopulations. This result also verifies that the signals in both compartments correspond to Seb4 protein.

3.5.3.3 In A6 cells Seb4 is localized mainly to the cytoplasm

As shown before in chapter 3.5.2 Seb4 is strongly expressed in *Xenopus* A6 cells. In regard to the variable protein pattern in embryonic myocytes, the next puzzling question was how Seb4 is distributed in A6 cells. Analysis of Seb4 localization in a single cell (of a cell line) by IF is technically easier to analyze and could additionally disclose new aspects of the cellular distribution of Seb4 (Figure 26).

Interestingly, in A6 cells Seb4 protein is clearly localized to the cytoplasm enriched outside the nucleus (26C and C'). The cytoplasmic Seb4 protein appears diffusely localized in a very fine dotted pattern. In a few cells, distinct spots of Seb4 protein are also detectable in the nucleus (26D and D'). Like in the somitic myocytes, the nucleoli are devoid of Seb4 (26D and D').

The most striking contrast of the cellular distribution of Seb4 protein comparing myocytes and A6 cells is that Seb4 is localized in A6 cells mainly to the cytoplasm.

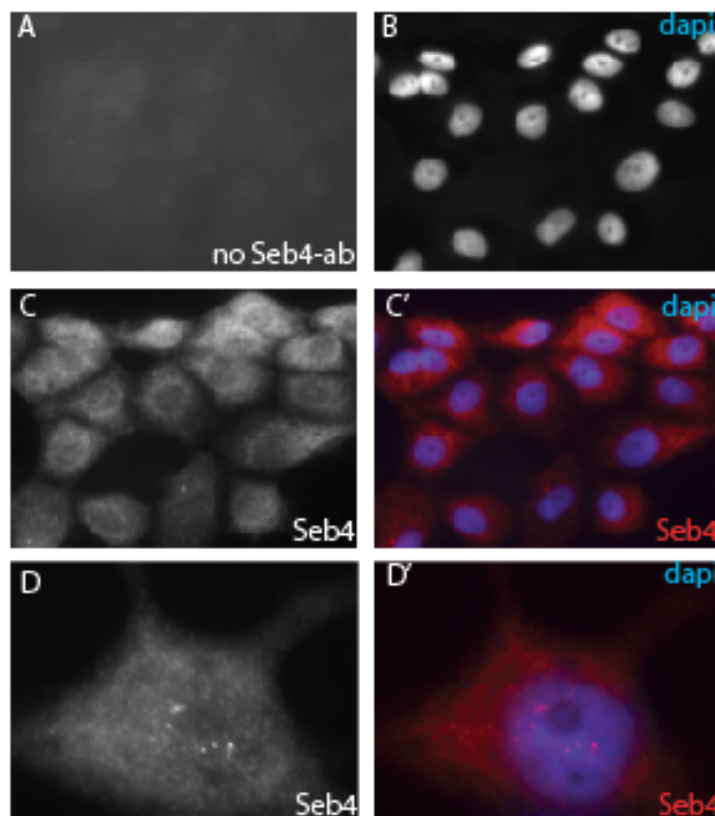


Figure 26: Seb4 protein localizes mainly to the cytoplasm in A6 *Xenopus* cells. Immunofluorescence using undiluted Seb4 monoclonal antibody in A6 cells. (A-C') 40x magnification; (D and D') 60x magnification with oil. (A) IF control, no Seb4-ab. (B) DNA stain by DAPI in blue and Seb4 protein signal in red (C, C', D, D').

3.5.4 Co-localization experiments by IF

The Seb4 distribution pattern alone does not indicate a possible function for the Seb4 protein. Since all steps of RNA metabolism are occurring at specific subcellular compartments or in dynamic bodies within the cell, the co-localization of Seb4 with marker proteins for different cellular regions is one step towards elucidating the function of Seb4 from a different angle.

3.5.4.1 Secondary antibody compatibility tests

Prior to perform sensitive co-localization experiments it is absolutely necessary to titrate the best compatible combination and dilution of secondary antibodies to achieve the highest sensitivity. Figure 27 shows the main results from the secondary antibody titration and compatibility tests. To minimize cross-reactivity among the fluorescently labelled antibodies, the following rules were obeyed.

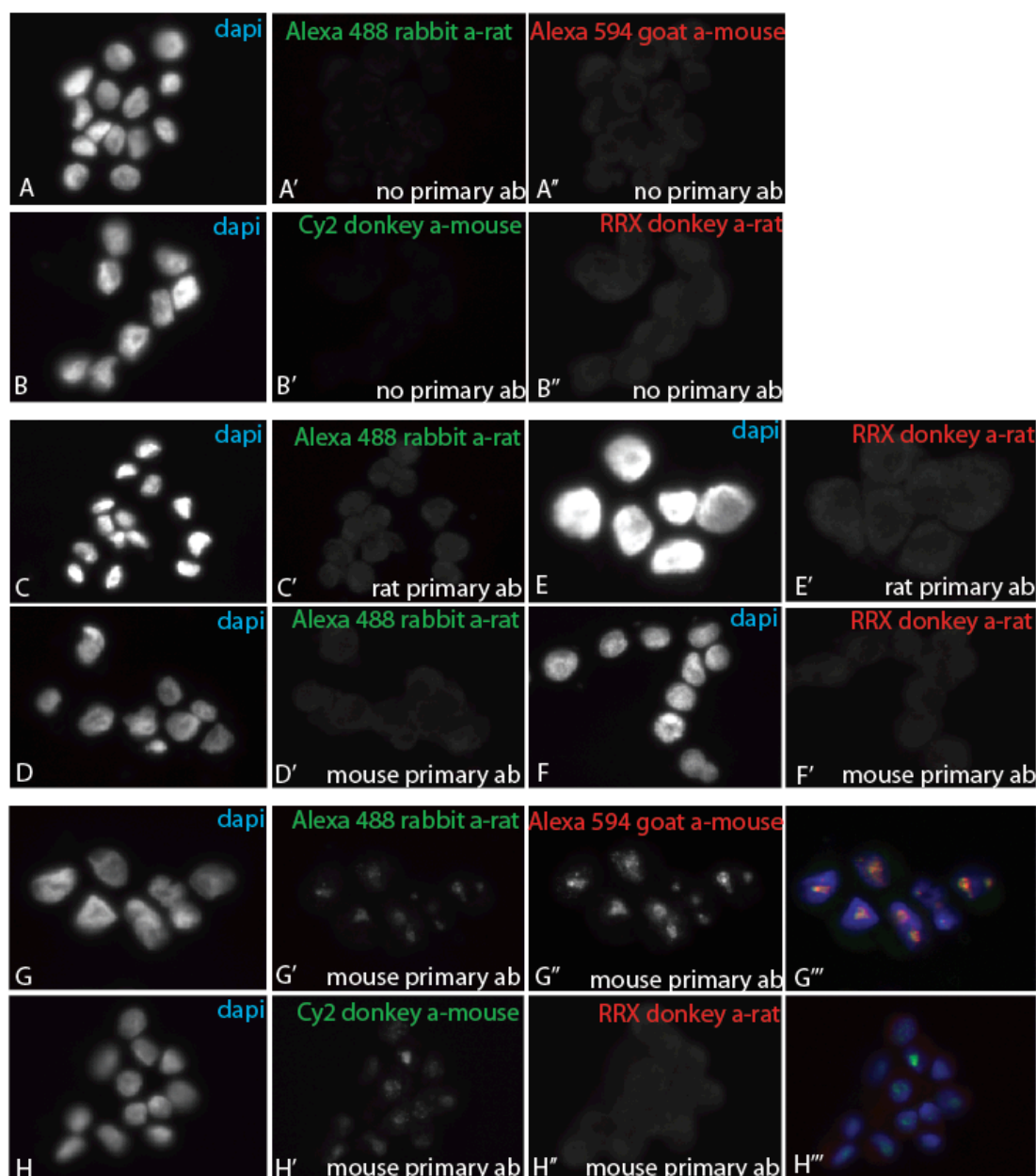


Figure 27: Pretesting of secondary antibodies in A6 cells. (A, B) Background controls of secondary antibodies; (C-F) single IF (G, H), co-IF. (A-H) DNA staining with DAPI. Secondary antibodies used: Alexa fluor 488 (green), Alexa fluor 594 (red), Dianova Cy-2 (green), Dianova RRX (red). (') Green channel, different secondary antibodies, as indicated in the panels. (") Red channel, different secondary antibodies, as indicated in the panels. (""') Merge. (C-H) Primary antibodies used: mouse anti-treacle; rat anti-Seb4.

When two secondary antibodies against two host species (of the primary antibodies) were used, they were always chosen from one company as recommended (dianova and molecular probes). As primary antibodies, a monoclonal mouse antibody against treacle, a nucleolar marker, and the monoclonal rat antibody 6E5 against Seb4 were used to test the optimal secondary antibody combination. To start with, all secondary antibodies were tested for background signals in absence of

primary antibodies (Figure 27A-A'' and B-B''). In the next step, species specificity and minimal cross reaction of the anti-rat secondary antibodies were evaluated by their use together with either the rat primary (27C' and E'') or the mouse primary (27D' and F') antibody. But when two secondary antibodies against mouse and rat were used together in one experiment with either one (27G-G''' and H-H''') or two primary antibodies (data not shown), the Alexa fluor antibodies from molecular probes cross reacted (27G-G''', data not shown). The Alexa anti-rat antibody recognizes the other secondary Alexa anti-mouse antibody bound to the primary mouse antibody, creating false signals (27G' and G''). This cross-reaction leads to the illusion that the Alexa anti-rat antibody would recognize the primary mouse antibody, which was ruled out before (27D'). This combination of Alexa antibodies is therefore inaccurate. In contrast, the dianova secondary antibodies do not show any cross reaction with another component of the reaction (27H-H''', data not shown).

From these initial experiments it could be concluded that the Alexa fluor secondary antibody against rat (and mouse, data not shown) show cross reaction and is therefore inaccurate for the co-immunofluorescence experiments. The dianova antibodies, however, are suitable due to their high specificity, lack of cross-reactivity, and are therefore chosen for the following experiments.

3.5.4.2 Markers for co-localization studies

The proper secondary antibody combination displays only one important tool to study co-localization. Just as important is the choice of markers that should cover a reasonable range of suborganelles and cellular structures and integrate the previous data. The antibodies chosen for the following experiments meet all claims. On one hand, they combine a putative function of Seb4 in the RNA metabolism due to its RNA-binding motif with the localization data gained by other methods and the availability of the antibodies, on the other hand.

In embryonic myocytes Seb4 expression in the nucleus appears in a spotted pattern (see Figure 23). This finding suggests further investigation of nuclear suborganelles that are linked to the RNA life cycle.

Such suborganelles are for example speckles. Speckles are subnuclear structures that are enriched in pre-messenger RNA splicing factors and are located in the interchromatin regions of the nucleoplasm (see 1.3.2.1). At the fluorescence-microscope level they appear as punctate structures, which vary in size and shape. Speckles are dynamic structures, and both their protein and RNA-protein components can cycle continuously between speckles and other nuclear locations, including sites of active transcription (Lamond & Spector, 2003). In order to analyze if

Seb4 is located in speckles or associated with spliceosomes, two markers for speckles, DRSP and SF3b, were analyzed.

DRS protein (also called Pinin) is associated with desmosomes and co-localizes with splicing factors in nuclear speckled domains. Nuclear DRSP binds to spliced mRNPs and participates in mRNA processing and export via interaction with RNPS1 (Li et al, 2003).

The splicing factor SF3b is a multiprotein complex essential for the accurate excision of introns from pre-messenger RNA. As an integral component of the U2 small nuclear ribonucleoprotein (snRNP) and the U11/U12 di-snRNP, SF3b is involved in the recognition of the pre-messenger RNA's branch site within the major and minor spliceosomes (Golas et al, 2003).

Another interesting nuclear functional structure/complex is at the start of the RNA life cycle, the transcription unit. This unit is formed of large multifunctional complexes, called transcriptosomes, in which the biosynthesis of mature mRNAs is coordinated. The essential key player that builds the platform for these complexes is the RNA polymerase II (RNAP II). RNAP II and its associated factors interact with a diverse collection of nuclear proteins during the course of precursor messenger RNA synthesis. Throughout the transcription cycle the carboxy-terminal domain (CTD) of the largest subunit of RNAP II undergoes a variety of covalent and structural modifications, which can in turn modulate the interactions and functions of processing factors during transcription initiation, elongation and termination. Besides the CTD, proteins involved in pre-mRNA processing can interact with general transcription factors and transcriptional activators, which associate with polymerases at promoters (Howe, 2002). The antibody WGPoI II against total RNAP II makes a good marker for all sites where either active (phosphorylated CTD) or inactive (unphosphorylated CTD) RNAP II is located. Another antibody against active RNAP II (phosphorylated CTD at Serin2) was tested in single localization experiments but was not found to show any signal overlap with Seb4 (data not shown).

The most prominent nuclear subcompartment in the nucleus is the nucleolus, the site of ribosome biogenesis. The protein Treacle e.g. functions in ribosomal DNA gene transcription and is recruited to NOR (nucleolar organizing regions) chromatin. Treacle is a phosphoprotein encoded by the TCOF1 gene and belongs to the factors involved in linking transcription with pre-rRNA modification (Prieto & McStay, 2007).

Another nucleolar marker, which was used, is NO38 protein. It is an abundant nucleolar Histone chaperone and a member of the nucleoplasmin family

(Namboodiri et al, 2004). The nucleolar markers can be used as negative controls, since Seb4 was shown to be absent from the nucleolus (see 3.5.3.1).

As a marker for the nucleoplasm an antibody against *Xenopus* acidic nucleoplasmic DNA-binding protein AND-1 was used. AND-1 is a widespread, soluble, ubiquitous protein accumulated in the nucleoplasm of oocytes and various other cells. AND-1 appears as an oligomer, probably a homodimer, and has been localized throughout the entire interchromatic space of the interphase nucleoplasm, whereas during mitosis it is transiently dispersed over the cytoplasm (Kohler et al, 1997).

Nuclear lamins form a highly insoluble structure, the nuclear lamina, which is associated with the nuclear envelope. Lamin A/C belongs to type V intermediate filaments and constitutes the nuclear lamina and nuclear matrix, where a variety of nuclear activities occur. The antibody against Lamin A marks the nuclear envelope.

In addition to all these nuclear markers I chose α -Tubulin for the main cytoplasmic structure, the cytoskeleton, consisting of microtubules built from basic α/β -Tubulin blocks.

3.5.4.3 Co-IF in embryonic myocytes

The nuclear portion of Seb4 in embryonic myocytes is localized in a spotted pattern. Therefore, it appeared very interesting to test, whether Seb4 co-localizes with SF3b and DRSP (Figure 28C and D). DRSP as well as SF3b are irregularly dispersed over the nucleus, except for the nucleolus, in a rather diffuse way with dense areas. Co-localization experiments of the speckles markers with Seb4 revealed, that the local areas in which DRSP and SF3b (28C and D) are enriched, show partly slight Seb4 localization. Despite suboptimal resolution, Seb4 protein, however, is predominantly located in regions devoid of DRSP and SF3b, resulting in no co-localization.

Next, the nuclear distribution of total RNAP II was analyzed in correlation to Seb4 (28E). RNAP II accumulates in distinct spots at many sites dispersed all over the nucleoplasm, similar to the Seb4 distribution pattern. Nevertheless, in the merge of RNAP II and Seb4 signals it becomes clear, that the sites enriched with either of the proteins are not identical; the signal-overlap appears rather random. Seb4 shows no co-localization with total RNAP II.

Finally, the cytoskeletal marker α -Tubulin was investigated (28F). α -Tubulin is localized in the cytoplasm, in an irregular manner and not in a filamentous network. Seb4 is localized mainly to the nucleus, so no co-localization between α -Tubulin and Seb4 could be observed.

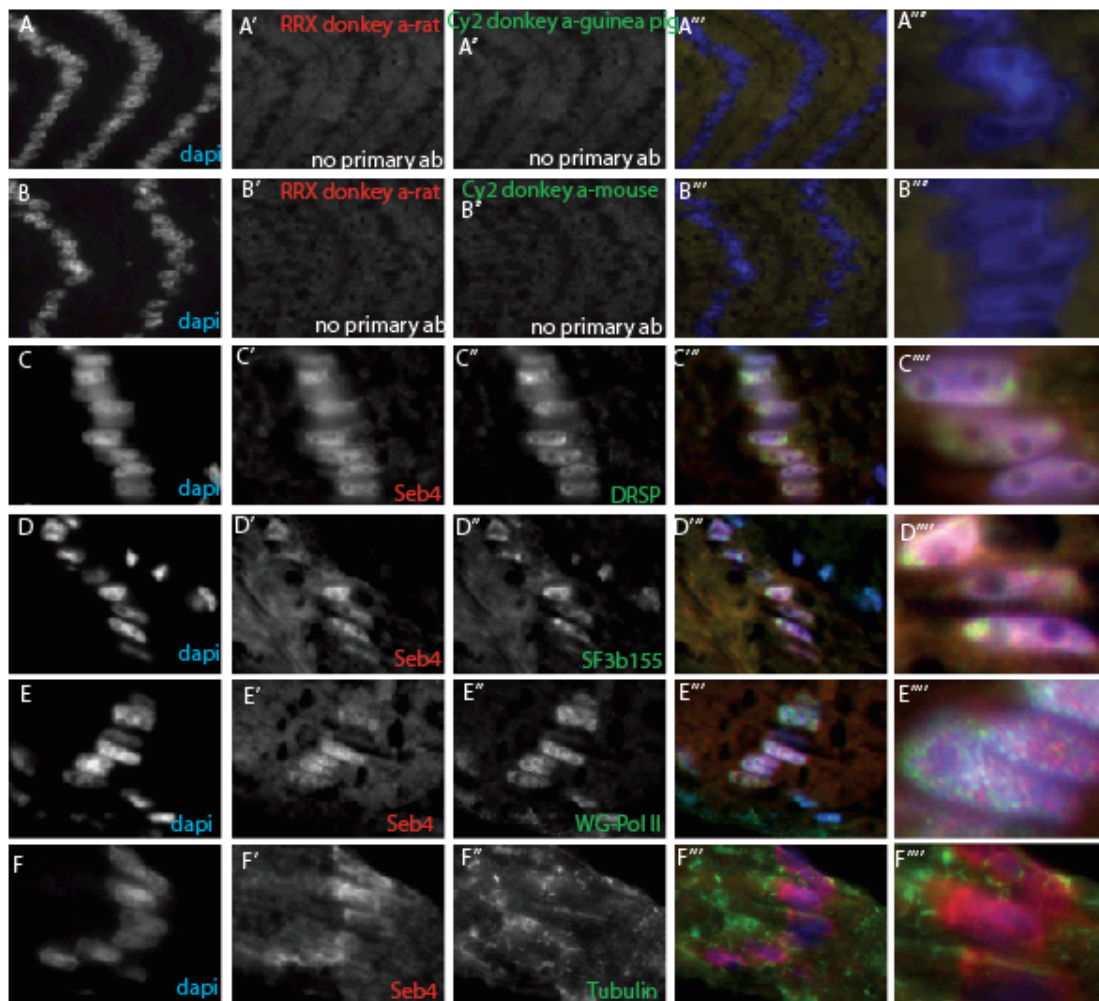


Figure 28: Co-localization of Seb4 protein and selected nuclear and cytoplasmic marker proteins in embryonic sections through myocytes. Co-IF of Seb4 protein with nuclear (C-G), and cytoplasmic (H-I) proteins. (A-B) Background controls, shows secondary antibodies RRX donkey a-rat in red and Cy2 donkey a-mouse in green. (A-I) DAPI stained DNA, (') red channel shows Seb4 signal, (") green channel shows marker signal. (""') merge. (""") Detail of (""').

3.5.4.4 Co-IF in A6 cells

In contrast to the embryonic myocytes Seb4 protein is restricted to the cytoplasm in A6 cells. Nevertheless, it appeared very interesting to analyze the nuclear markers in this cellular background (Figure 29).

Lamin serves as a marker for the nuclear envelope because its boundary is more precise than the one from the DAPI counterstain (Figure 29C). The other question if Seb4 is perhaps enriched inside or at the periphery around the nuclear envelope could be answered by analyzing the co-localization of Seb4 with lamin. The lamin dense region, seems devoid of Seb4 or at least of lower concentration.

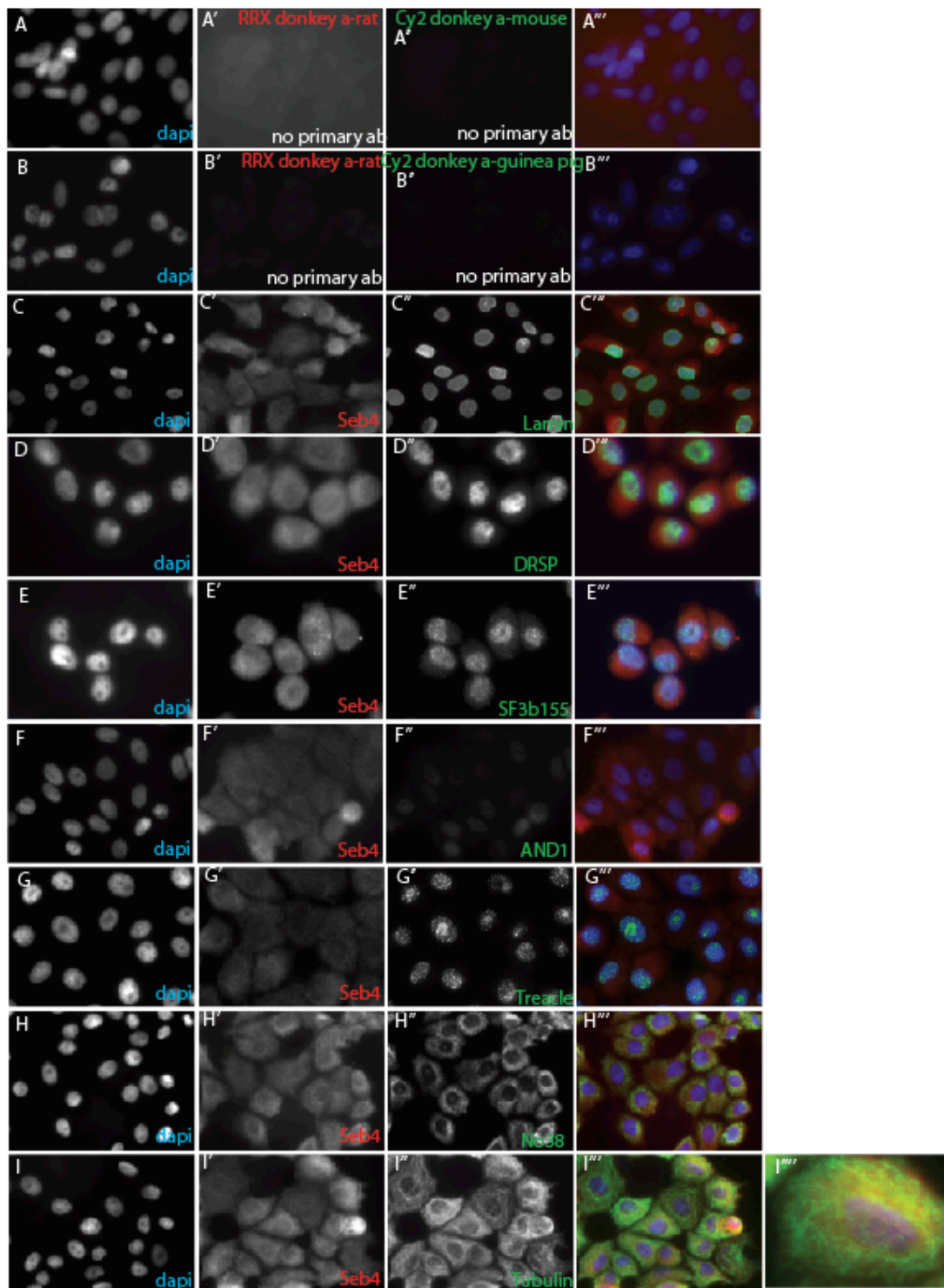


Figure 29: Co-localization of Seb4 protein and selected nuclear and cytoplasmic marker proteins in A6 cells. Co-IF of Seb4 protein with nuclear (C-E) and cytoplasmic (F) marker proteins. (A-B) Background controls, show secondary antibodies RRX donkey a-rat in red and Cy2 donkey a-mouse, and Cy2 donkey a-guinea pig. (A-F) DAPI stained DNA; (') red channel shows Seb4 signal; (") green channel shows co-IF signal; (""') merge; (""") detail of (""').

Seb4 does not co-localize with lamin at the inside of the nuclear envelope, suggesting that Seb4 is localized outside the nucleus.

The antibodies against SF3b and DRSP mark the position of the splicing speckles in the nucleus (29D and E). As shown by the merges, the Seb4 protein signal does not overlap with the speckles markers, because it is located in the cytoplasmic compartment (29D and E).

In Figure 29F the nuclearplasm fluoresces via AND-1 detection. Additionally to the presence of the nucleus, the signal of AND-1 confirms, that the A6 cells do not undergo mitosis (see 3.5.4.2). Though the AND-1 signal is very weak, it is clear that AND-1 and DAPI overlap, whereas Seb4 is located to the cytoplasm.

Treacle protein is detected in Figure 29G. It is concentrated in the nucleolus as well as in these dotted nuclear entities. There is no Seb4 co-localization with Treacle. NO38 shows, besides its nucleolar localization a cytoplasmic distribution, where Seb4 is also localized (29H). Upon overlay of both signals, the cytoplasmic NO38 protein is located not directly adjacent to the nucleus, resulting in a gap of an exclusively Seb4-positive ring around the nucleus. Yet, the structure of the cytoplasmic NO38 does not correlate to the diffuse signal of Seb4 in the cytoplasm.

As mentioned above, Seb4 is localized in A6 cells primarily to the cytoplasm. So, it was very interesting to see if it co-localized with α -Tubulin (Figure 29I). In most cells the densities of both Seb4 and α -Tubulin signals are correlated. In those cytoplasmic areas where Seb4 is enriched, a more concentrated α -Tubulin structure (e.g. both cells at the top right) was detected. This result is confirmed by the yellow signal colour in the overlay. Nevertheless, Seb4 does not show the precise filamentous protein pattern, like α -Tubulin does.

Concluding from the co-localization experiments, nuclear Seb4 is not located to the nucleoli, splicing speckles, or sites of transcription. In regard to its cytoplasmic distribution, Seb4 does not appear to be associated with the cytoskeleton.

4 Discussion

In the last decades, a large amount of developmental studies have been devoted to the identification and characterization of growth factors and transcription factors expressed in the early embryo. In the complex series of events involved in cellular differentiation and organogenesis, also post-transcriptional mechanisms constitute an additional layer of regulatory control over gene expression and are employed to modulate differentiation programmes regulated by growth and transcription factors. Indeed, a lot of evidence indicates that numerous developmental processes are regulated at the level of RNA processing, stability, localization, and translation by non-coding RNAs and/or RNA-binding proteins. MicroRNAs, a class of non-coding RNA molecules, function in potent inhibition of individual key targets or coordinated regulation of target clusters, fine-tuning of target activity, and the reversibility of some aspects of microRNA-mediated repression (Bushati & Cohen, 2007).

RBPs coordinate functionally related sets of mRNAs through binding with their RNA-binding domains to sequence elements in the mRNA. Considering the hundreds of RBPs encoded in eukaryotic genomes, post-transcriptional control may be even comparable in its richness and complexity to transcriptional regulatory systems. Although they are not generally as well characterized as signalling and transcriptional networks yet, the number of RBPs known today to be involved in vertebrate development is growing and provides an additional level of coordination.

The highly conserved, RRM containing protein Seb4 was described first in *Xenopus laevis* by Heinrich Jasper from our laboratory in 1998, as a direct target of MyoD (Jasper, 1998), and later by the Bouwmeester laboratory (Fetka et al, 2000) as a tissue-specific putative RNA-binding protein identified in an RNA *in situ* screen for genes showing time-specific expression patterns. However, the role of Seb4 and its biochemical properties have not been published, yet.

In this study, I have characterized Seb4 in the early development of *Xenopus laevis* by various biological and biochemical approaches. Firstly, I analyzed the Seb4 mRNA and protein expression pattern and its subcellular localization. Next, I addressed the biological function of Seb4 revealing the skeletal and cardiac muscle differentiation pathways, in which Seb4 is involved, and the skeletal muscle and lens differentiation pathway, for which Seb4 is required. Thirdly, I attempted to identify RNA and protein interaction partners of Seb4 via RIP, IP and gel filtration.

4.1 Molecular tools

The following chapters serve to discuss and accent the quality of the biochemical analyses and the L-o-F approaches employed here.

4.1.1 Antibodies

Many applications aiming at the identification of the biochemical properties of a special protein take advantage of the antibody-antigen interaction. Thus, a major part of protein biochemistry is the use of antibodies.

Polyclonal sera contain a mixture of antibodies binding to various epitopes found on the target protein. Therefore, the avidity of polyclonal sera for the antigen is usually high. The polyclonal origin of the antibodies present in the antisera implies that they are prone to cross-react with unrelated proteins. By contrast, monoclonal antibodies bind only one epitope of the antigen. This results in high specificity and in rather low background, but also lower avidity.

Here, for broader applications, we have generated both monoclonal antibodies in rats and polyclonal antibodies in rabbits against the full-length Seb4 peptide. These were tested individually with regard to their cross-reactivity. Regarding their applicability, the monoclonal 6E5 antibody turned out to be an excellent tool of very high specificity exclusive of cross-reactions and unspecific binding. It was successfully applied in many experimental approaches like Western blot, immunocytochemistry, immunofluorescence, and immunoprecipitation, which were of fundamental importance for the biochemical characterization of Seb4.

The monoclonal antibody 6E5 recognizes endogenous and *in vitro* translated full-length Seb4 protein, both in native and SDS-denatured conformation. However, the delta C deletion protein (RRM-domain mainly) is recognized only in its denatured form, but not as a native peptide. The RRM domains of Seb4 and Seb4R are virtually identical in sequence and, consequently, *in vitro* translated Seb4R is recognized by the 6E5 antibody – both in its native and denatured states. Endogenous Seb4R protein from embryo lysates, however, is not detected, which suggests that the epitope of Seb4R is inaccessible, either by an associated factor or by modification.

These observations indicate that the epitope is located within the conserved RRM domain. Though, in some cases, unnatural folding may prevent exposure of the epitope to the antibody, which explains, for example, why the delta C peptide is not recognized. Also in case of Seb4R, it appears that the epitope of endogenous Seb4R is masked, either by complex formation with interacting factors,

or it is not accessible due to modifications. Most importantly, endogenous Seb4 and Seb4R could be distinguished.

The polyclonal serum 7600 showed a lower signal/noise ratio in WB and ICC, but a higher efficiency in IP than the monoclonal 6E5 did. For future experiments this polyclonal serum could be of great value if it was further processed by affinity purification to minimize cross-reactions. An additional advantage is the different host species against which the polyclonal serum had been generated (anti-rabbit), as it would allow double-immunofluorescent analysis with rat-antibodies, which can be applied to demonstrate co-localization.

4.1.2 Morpholinos

Gain-of-function studies (G-o-F) provide useful information about the potential function of a protein. However, only the loss-of-function (L-o-F) studies can reveal the essential function of a protein. Researchers working on RNA-binding proteins with several RRM domains have successfully constructed dominant-negative versions of RBPs, by generating truncated constructs, missing one or two RRMs (Akamatsu et al, 1999; Anderson et al, 2000). However, because Seb4 only contains one RRM, I could not use such a strategy. Previously in our laboratory, deletion and point mutation constructs were generated, which lacked biological activity and were in consequence not dominant-negative. The most successful method used for L-o-F experiments in *Xenopus* is to reduce protein levels by inhibiting mRNA translation by microinjection of specific antisense MO oligonucleotides (Heasman et al, 2000). This method is well established in *Xenopus* and offers many advantages like high specificity, easy target selection, high biological stability, and high efficiency. Its greatest advantage compared to genetic knock-out mutants (in other organisms) is that phenotypes can be rapidly observed in the same generation of animals (F0). The degree of depletion depends on many parameters, including the abundance and stability of the protein that is present at the time of MO introduction, the amount of diffusion, the localization of the targeted mRNA, and the amount of *de novo* transcription. The penetrance of the phenotype obtained by a specific MO is quite variable ranging from low (e.g. *smad5*) to high percentages (e.g. *no tail*) (Heasman, 2002). Furthermore, the expressivity of a specific phenotype can vary immensely, e.g. from only partial protein depletion (may cause only minor defects) to complete lack of protein (Heasman, 2002). The severity of the phenotype is dependent on the injected dose of MO oligonucleotides and the stability of the MO. Subsequently, the concentration of Seb4 MO played an important role for the penetrance and severity of the phenotype; the higher the dose of injected Seb4 MO the more efficient was the

down-regulation of Seb4 protein, as observed in Western blots, consequently leading to an even more severe phenotype (see 3.3.1).

Another consideration specific to *Xenopus laevis* is that due to its allotetraploidy both gene copies of *seb4*, *seb4a* and *seb4b*, have to be targeted by the MO to achieve an efficient knock-down. Therefore, the MO was designed against the conserved coding region at the start site of both gene copies.

Nevertheless, there are limitations to the MO technique. Several authors report toxic effects after MO injections in zebrafish. It has not been resolved whether these side effects are non-specific or due to the MO being complementary to an unknown target. These side effects include widespread cell death, defects in epiboly, and neural degeneration (Imai & Talbot, 2001; Karlen & Rebagliati, 2001; Lele et al, 2001; Nasevicius & Ekker, 2000). None of these phenotypes was observed in *Xenopus* after Seb4 MO injection. The results of the Seb4 MO L-o-F experiments complemented and substantiated the presumptions achieved from the previous overexpression studies (data not shown, chapter 1.3.4). Notably, rescue experiments are left here to mention, which would also demonstrate the specificity of a MO.

Overall, the antisense morpholino oligonucleotides represent a great tool to study many aspects of Seb4 protein function (as shown in Figure 4, 6, 7, and 18). Thus, the knock-down experiments using MO against Seb4 emerged as a very successful approach leading to profound results concerning the role of Seb4.

4.2 Spatio-temporal expression of Seb4 in *Xenopus* embryos

4.2.1 Seb4 is an abundant protein expressed in early development

In this study, Seb4 protein is shown to be expressed throughout early larval development from the unfertilized egg to late tailbud stages. Since zygotic transcription only starts during the mid-blastula transition, Seb4 protein in the earlier stages, from egg to blastula, is either due to the translation of maternal *seb4* RNA or represents maternally contributed Seb4 protein. Maternal Seb4 was located in the animal half of the embryo, which suggests a regulated localization for either Seb4 mRNA or protein. After zygotic transcription has commenced at MBT, the level of zygotic Seb4 remains equally until neurula stage. During neurogenesis, protein expression increases strongly, reaching a constant level at st. 19 neurulae until late tailbud stages.

In order to estimate the Seb4 protein abundance, semi-quantitative Western Blot analysis was performed. Assuming that a tailbud embryo contains 10^6 cells with roughly 10% expressing Seb4, we calculate an average abundance of 10^5 Seb4 protein copies per cell (see calculation in 3.2.1). In comparison, a mammalian dividing cell contains up to 10^7 ribosomes. In the *Xenopus* oocyte even 10^{12} ribosomes accumulate (Cooper, 2000). Histones, for example, are with 3×10^8 molecules one of the most prevalent proteins in the cell, whereas other protein types only exist in up to 1000 copies per cell (Müller-Esterl, 2004). Actually, the abundance of different proteins varies widely, from the quite rare cell-surface receptor protein that binds the hormone insulin (20,000 molecules) to the abundant structural protein actin with 5×10^8 molecules (Lodish et al, 2000).

Thus, the Seb4 protein content with 10^5 copies per cell is in a range just below the most frequent proteins and is therefore a very abundant protein, suggesting broad, perhaps general roles for Seb4.

Besides the high abundance of Seb4, another interesting feature is that in all analyzed stages endogenous Seb4 from embryo extracts migrates as a double band at 25kDa. The migration size correlates with the estimated molecular weight of 24,75kDa, but the origin of the doublet appears puzzling. One explanation is that Seb4 exists in two isoforms, as it was shown before in human, mouse and *Xenopus*, where alternative splice variants exist for many proteins. In human, there is evidence that the RNPC1 gene, which is the human homologue of Seb4, encodes at least two isoforms of an RNA-binding protein through alternate splicing at the C-terminus. Both isoforms, RNPC1a with 239aa and RNPC1b with 212aa, are identical in their N-terminal RRM domain. RNPC1 is induced by the p53 family and by DNA damage in a p53-dependent manner, whereby RNPC1a is capable of inducing G1 arrest and binds to the 3' UTR of the p21 transcript regulating its stability (Shu et al, 2006).

By knocking-down Seb4 selectively with MO (seven mismatches to Seb4R) it was ruled out that the endogenous ortholog Seb4R is detected by the monoclonal 6E5 antibody, concluding that Seb4 exists in two forms. It is possible that either both gene copies Seb4a (calculated MW 24,75kDa) and Seb4b (calculated MW 24,97kDa), two splice variants of Seb4a/b or two protein forms display different migration behaviour due to post-translational modification with the doublet signal representing the steady state equilibrium between the two forms. SR proteins, e.g. those containing one or two RRMs, are extensively phosphorylated at their SR domains and can exist in differentially phosphorylated (hypo- and hyperphosphorylated) states. For proper execution of splicing activity, cycles of phosphorylation and dephosphorylation of SR proteins are important.

Phosphorylation of SR proteins also dictates their nuclear import (Graveley, 2000; Lai et al, 2001; Shi et al, 2006).

The ability of Hu proteins to stabilize their mRNA targets is also regulated by post-translational modifications of the Hu proteins themselves. For instance, the stabilization of the SIRT1 mRNA appears to be modulated by phosphorylation of HuR (Abdelmohsen et al, 2007), whereas the arginine methylation of HuD by coactivator-associated arginine methyltransferase 1 (CARM1) affects mRNA turnover of p21cip1/waf1 mRNA (Fujiwara et al, 2006).

Therefore, phosphorylation as the most common post-translational modification, as shown above, was experimentally tested here, but turned out not to play a role for Seb4 protein migration and doublet recognition indicating that Seb4 protein is not modified by phosphorylation. As it was shown for HuD, for example, it could be tested if arginine methylation, is responsible for the two Seb4 protein states detected.

4.2.2 Seb4 expression in mesodermal and ectodermal derivatives

In the embryo, Seb4 is expressed in a tissue and stage specific pattern in cells belonging to the mesodermal and ectodermal lineages. In gastrula stage embryos, Seb4 expression is first induced in the mesoderm in prospective myoblasts that also strongly express MyoD and Myf5, but Seb4 is restricted to two small regions flanking the organizer. At neurula stage, the expression domains of Seb4 and MyoD are identical in the paraxial mesoderm. Additionally to Seb4 expression in other tissues (see below), at later stages, Seb4 and MyoD expression overlap in differentiating myocytes of the skeletal muscle. The *in situ* analyses strongly confirm the data gained from the *in vitro* screen, where Seb4 was found as a direct target of MyoD protein (Jasper, 1998). Conclusively, endogenous Seb4 expression in the mesoderm is directly controlled by MyoD during muscle differentiation *in vivo*. Thus, Seb4 may be involved in the determination phase of the muscle lineage.

As development proceeds, Seb4 is also expressed in the myocardium (heartmuscle) and in neuroectodermal derivatives like the eye (neuronal), the ventral part of the otic vesicle, some cranial placodes and developing lateral line primordia. All of these tissues lack MyoD expression suggesting that the Seb4 promotor receives multiple inputs and Seb4 transcription responds tissue-dependently to other transcription factors than MyoD.

Moreover, *in situ* expression analyses revealed that the patterns of Seb4 mRNA and protein expression are identical with the exception of the eye. There, Seb4 mRNA expression seems not to correlate with the Seb4 protein localization.

Seb4 mRNA can be detected firstly in the retina at tailbud stage 23. As development proceeds, the retinal Seb4 RNA expression is lost, but found again later in the lens. Seb4 protein behaves the other way around. Firstly, Seb4 protein is detected in the lens and is later solely found in the retina. This paradoxical observation and the poor correlations generally reported in the literature between the mRNA and protein can be explained by several reasons, that may not be mutually exclusive (Greenbaum et al, 2003).

First, there are various post-transcriptional mechanisms involved in turning mRNA into protein that may disturb protein or mRNA detection. Second, proteins may differ substantially in their *in vivo* half-lives compared to their mRNAs. The impression can impose that mRNA and protein are expressed differently, if the mRNA is only transiently expressed, whereby the protein is very stable. In the stages where Seb4 mRNA is detected, but no Seb4 protein, it could be explained by a higher stability of Seb4 mRNA compared to the protein. Since not all continuous stages were analyzed, it is possible that the missing stages would show an overlap of Seb4 mRNA and protein expression.

Another explanation for the indirect correlation of Seb4 RNA and protein expression in the eye could be due to non-specific cross-reactions of the 6E5 antibody accompanied with masking of the Seb4 epitope. Since Seb4R harbours the same epitope recognized by the 6E5 antibody *in vitro*, it could become the target protein, because it is expressed in the retina (Boy et al, 2004). A conformational change or the dissociation of a bound factor, for example, could suddenly make the Seb4R epitope accessible.

The option that Seb4 protein is transported from the retina to the lens and later from the lens to the retina is rather unlikely.

The possibility that Seb4 RNA was not detected despite it was expressed, is ruled out by the ISH procedure, which destroys all RNA secondary structures leading to free access of all RNAs to the antisense probes.

Nevertheless, in regard to the eye, the disparate correlation between the observed Seb4 mRNA and protein expression remains cryptic and requires further investigation. But in all other tissues, muscle, heart, ear, and neural placodes the expression of Seb4 mRNA and protein is identical.

4.3 Nuclear and cytoplasmic localization of Seb4

Immunolocalization experiments in the embryo have demonstrated that in striated muscle Seb4 protein is localized to the nucleus and cytoplasm. Regardless of the different volumes of both compartments Seb4 is shown to be distributed in

equal amounts (not concentration) between the nucleus and the cytoplasm. Seb4 contains no classical nuclear localization signal for active transport. Seb4 protein with only 25kDa is small enough to enter the nucleus by passive diffusion through the nuclear pore complex.

On the other hand, passive diffusion would imply an equal protein concentration in both compartments. Taking in consideration that the volume of the nucleus is much smaller than of the cytoplasm, Seb4 concentration in the nucleus is much higher (even when the protein amounts are equal in both compartments). This supports the hypothesis of an active import mechanism for Seb4. This finding suggests a role for Seb4 in the early RNA metabolism, a step between the birth of transcripts until they are exported out of the nucleus. In this study however, Seb4 was shown not to localize to the sites of transcription, where nascent transcripts are generated, because no co-localization with total RNA-Polymerase II was found. In the nucleus of myocytes Seb4 is concentrated in distinct foci – structures that bear similarity to nuclear speckles, in which splicing factors accumulate when they are not actively engaged in splicing reactions.

Seb4 may be involved in polyadenylation or a later step in the RNA metabolism implicating a shuttling mechanism. One option to be considered is that Seb4 could exit the nucleus by the piggyback style, as part of RNP complexes dependent on the association to mRNA.

SR proteins, for example, piggyback on mRNA to exit the nucleus. Several members of this family have been shown to bind to exon sequences and to accompany mRNA molecules in transit to the nuclear pores. The association of SR proteins with spliced mRNA could therefore serve as a guide for mature RNAs to cross the nuclear pores (Manley & Tacke, 1996).

U2AF65 and U2AF35 are also shown to shuttle continuously between the nucleus and the cytoplasm by a mechanism that involves carrier receptors and is independent from binding to mRNA. The SR domain of U2AF65 or U2AF35 acts as a nuclear localization signal and is sufficient to target the protein complex to the nuclear speckles. Although Seb4 is enriched in distinct foci, Seb4 does not co-localize with markers for speckles. Furthermore, the presence of an SR domain in either U2AF subunit is sufficient to trigger the nucleocytoplasmic import (Gama-Carvalho et al, 2001). Nucleocytoplasmic shuttling of TIAR and TIA-1 is also mediated by their RNA-binding capacity. The RRM2 and the first half of the auxiliary region were identified as important determinants for TIAR and TIA-1 nuclear accumulation. In contrast, the nuclear export of TIAR and TIA-1 is mediated by RRM3 (Zhang et al, 2005).

Since Seb4 contains no SR domain, possibly an unknown signal patch or peptide in the C-terminal half of the protein is used as a localization signal, or Seb4 transport is dependent on its single RRM, as shown for TIAR and TIA-1 above.

So far, the foci in which Seb4 is concentrated could not be associated to any of the nuclear suborganelles tested here.

Previous studies have shown that other RRM containing RBPs are also present in both the nucleus and cytoplasm. These include the Elav-family, which are required for neuronal differentiation (Perron et al, 1997; Perron et al, 1999). Furthermore, it has been demonstrated that RBPs can exhibit different functions in different cellular compartments. One prominent example is sex lethal, which regulates splicing in the nucleus, but is involved in translational repression in the cytoplasm (Bashaw & Baker, 1997; Kelley et al., 1997).

Another example for post-transcriptional regulation by different subcellular localization is already shown for *myoD*. Early in muscle differentiation, the RBP HuR is localized to the nucleus of myoblasts by active Transportin 2 (TRN2)-mediated import. In differentiated muscle fibers, however, the TRN2-HuR complex is disrupted, leading to the cytoplasmic localization of HuR, as well as to the stabilization of *myoD* and *myogenin* mRNAs (van der Giessen & Gallouzi, 2007).

In embryonic striated muscle the main population of Seb4 protein is shown in this study to be enriched in the nucleus, albeit some of the protein accumulates in the cytoplasm. Seb4 protein that is expressed in the ventral part of the otic vesicle is exclusively localized to the cytoplasm, suggesting a different regulation and functional role for Seb4 in the ear. The ventral pole of the otic vesicle is the pars inferior, serving as anlage for vestibular and auditory structures. As in most vertebrates, inner ear development begins with the invagination of a thickened epithelium near the hindbrain, the otic placode that gives rise to a spherically shaped otic vesicle. In *Xenopus*, induction of the otic placode and specification of the otic vesicle are complete by neural tube stages, establishing that the ear is one of the first organs to be determined during organogenesis (Noramly & Grainger, 2002). The otic placode in early *Xenopus* tailbud embryos starts out as part of a larger dorsoventral placodal area that will later also give rise to individual lateral line placodes (Schlosser & Northcutt, 2000). It has been proposed that this dorsoventral thickening is merely a subset of a much larger primitive ectodermal thickening present at earlier stages that gives rise to all neurogenic placodes, of which some also express Seb4. These observations suggest that all ectodermal expression of Seb4 in different cranial/neurogenic placodes is derived from one origin, the primitive

ectodermal thickening.

In A6 cells, Seb4 is mainly localized to the cytoplasm, distributed diffusely. Cytoplasmic accumulation has been shown to occur in many cases in response to cellular stress. For example, the shuttling proteins CIRP and TIA-1/TIAR migrate to stress granules, which are sites of translational regulation (De Leeuw et al, 2007; Zhang et al, 2005). Unfortunately, it could not be tested whether Seb4 migrates to stress granules upon stress induction, because the only available antibody against TIAR was against human TIAR and did not cross-react with *Xenopus* TIAR.

Instead, it could be shown that cytoplasmic Seb4 is not attached to the microtubuli of the cytoskeleton, indicating that Seb4 is not involved in RNA transport along these microtubuli. Interestingly in myocytes, besides the diffuse cytoplasmic distribution, Seb4 is also organized in regular structures perpendicular to the longitudinal axis of the cell. These structures may represent Z-lines, which are dense protein bands. In a striated muscle fiber, Actin filaments and Titin molecules are anchored to myotendinous junctions and attached to Z-lines, marking the boundaries between adjacent sarcomeres (Luther et al, 2003). α -Actinin is a major component of Z-lines. It cross-links antiparallel Actin filaments from opposite sarcomeres. Z-lines are laterally connected to the extra cellular matrix (ECM). Connecting Z-lines with each other and to the surrounding connective tissue ensures synchronous, uniform muscle contraction (Jani & Schöck, 2007). Seb4 could possibly be attached to Z-lines playing a structural role by maintaining, for example, α -Actinin anchorage at the Z-line. This could be mediated by controlling the localization of α -actinin mRNA to the Z-lines.

4.4 Seb4 is found as a monomer with no associated targets

The protein sequence of Seb4 containing the highly conserved RNA recognition motif RRM reveals the potential to bind macromolecules like nucleic acids and proteins.

A single RRM is known to be sufficient to bind RNA (Scherly et al, 1989), but better target specificity has been demonstrated when several RRMs are present (Kuhn & Pieler, 1996). These data suggest that Seb4 could act through a multi-protein complex or as an oligomer conferring higher specificity. The two additional conserved domains, observed in the C-terminal half of the Seb4 protein sequence, or the RRM itself, could be involved in the formation of this protein complex. The

structural features of Seb4 raise the question on how such a small protein acquires its specificity.

To test whether Seb4 operates as an oligomer or in concert with other cofactors immunoprecipitation assays followed by silver-staining and gelfiltration experiments were performed. Despite the high sensitivity of silver-staining no Seb4 associated proteins were found. Consistent with this result, gelfiltration experiments of embryo extracts also revealed that endogenous Seb4 is not stably bound in a complex, and elutes as a monomer. But multiple copies of Seb4 protein may be binding to a single RNA. In this case, there need to be no physical interaction between individual Seb4 proteins, but to RNA instead.

Ectopic (myc-tagged) Hermes protein, for example, has been shown to pull-down *RINGO/spy*, *mos*, and *xcat2* mRNAs (Song et al, 2007); however, purified Hermes protein does not bind to RNAs *in vitro* in the absence of oocyte extract (Gerber et al., 2002). Immunoprecipitation experiments indicate that multiple copies of Hermes protein are associated with each other within the cell. The fact that the association of Hermes proteins is sensitive to RNase suggests that it is not a simple protein/protein interaction. Thus, Seb4 complex-formation may be based on RNA association serving as a platform for other protein partners, as shown for Hermes.

Of particular interest could be a state of “induced fit”, brought about by association with RNA. This conformational change may allow association of Seb4 with other proteins (homo-oligomerization or hetero-oligomerization). Assembly of most RNP complexes is accompanied by significant conformational changes in both protein and RNA components. In some cases, these conformational changes may occur in a progressive fashion such that early interactions in assembly lead to further conformational rearrangements that uniformly facilitate later steps (Williamson, 2000).

Analysis of the interaction of Seb4 with RNA by immunoprecipitation involves three steps: first, the appropriate experimental conditions allowing natural Seb4-RNA and protein interactions, second, the association of endogenous Seb4 protein bound to its partners with the antibody-beads complex, and third, the visualization of the associated target.

The main challenges in the RIP experiment was, on one hand, the RNA preserving conditions and, on the other hand, the visualization step, which requires a very sensitive and specific technique to detect possible targets and to reduce background contaminations. Most laboratories solve this issue by using the PCR method after reverse transcription of the co-immunoprecipitated RNA. The amplification step facilitates the detection of rare targets. But the major problem is

that the cDNA derived from the immunoprecipitated RNA molecules after RIP are of unknown sequence and may possibly contain variable ends due to degradation, which makes it difficult to design primer sets against these target sequences.

PCR can be applied when certain candidates are speculated to be targets of a specific RBP. For example, in the case of Hermes, knock-down and localization experiments indicated a putative interaction of Hermes with *RINGO/spy*, *mos* and *xcat2*. This interaction could then be demonstrated by RT-PCR (Song et al, 2007). Just recently, after assuming an interaction of maternal Seb4R with VegT by the co-localization of both factors in the vegetal pole it was also confirmed by RT-PCR. Ectopic Seb4R associates with *vegT* mRNA controlling its stability and translation (Souopgui et al, 2008).

Here, several experiments led to the conclusion that Seb4 is not only a direct target of MyoD, but also an upstream regulator of MyoD. Therefore, *myoD* became a putative candidate for an RNA target of Seb4. Despite the efforts of generating several primer sets against MyoD, an interaction of Seb4 protein with *myoD* RNA could not be shown in RT-PCR (data not shown). Because of the lack of indications on RNA candidates interacting with Seb4, a more general approach was chosen. For Northern blotting, the Seb4-co-immunoprecipitated RNA was labelled during reverse transcription and hybridized to total RNA from *Xenopus* neurulae. The attempt to accumulate Seb4 targets by this strategy was not possible. Several reasons may be responsible for this. On one hand, the sensitivity of the technique could be too low to discover rare targets or, on the other hand, endogenous interactions without cross-linking may not be stable enough. In most laboratories RNA interactions are shown by either *in vitro* binding assays, like for Fox-1 and HuR (Figueroa et al, 2003; Zhou & Lou, 2008) or with an ectopically expressed, tagged version of the protein, like Hermes and Seb4R (Song et al, 2007; Souopgui et al, 2008). Another common method is to fix the RNP with UV-crosslinking (Luo & Reed, 2003).

Hermes was shown to bind RNA only *in vivo*. The possibility that a protein co-factor is required for Hermes to bind RNA efficiently may explain why neither protein-protein interactions nor protein-RNA interactions are observed by using Hermes protein that has been translated *in vitro*. Therefore the major aim of the target screen was to be as close as possible to the physiological conditions *in vivo* and to find an interaction with the endogenous Seb4 in the embryo. The biological relevance of *in vitro* experiments, frequently including artefacts and false-positives, has to be confirmed by all means by *in vivo* data.

In contrast, the interaction of Seb4 with RNA could also be of transient

nature and, therefore, very challenging to identify.

Another explanation for the negative outcome of the RIP experiments could be of functional nature. Many RBPs have been reported to interact with thousands of RNAs, in a structural and not sequence-specific manner (Halbeisen et al., 2008). For example, to address the question of whether the splicing factors U2AF65 and PTB associate with mature mRNAs, a genome-wide analysis of transcripts that were immunoprecipitated with U2AF65 and PTB was performed. This analysis resulted in over 5000 targets for both RBPs. A detection of Seb4 targets by RIP and Northern blotting would be impossible if Seb4 associated with many targets, like e.g. U2AF65 and PTB, unselectively. Consistent with this view, Seb4 could control generally mRNA on the post-transcriptional level.

The U2AF65-associated mRNA population is highly enriched in mRNAs encoding transcription and cell cycle regulators, whereas PTB-associated mRNAs contain a large proportion of transcripts encoding proteins that are involved in intracellular transport and vesicle trafficking. An additional group of genes related to ubiquitination and signalling through small GTPase molecules exhibits significant enrichment in both U2AF65- and PTB-associated mRNA populations. These data illustrate, that these RBPs bind subsets of related gene groups (Gama-Carvalho et al., 2006). This finding in combination with the results presented here, could suggest not only a global function for Seb4 at a particular step in differentiation, but a regulatory role for tissue-specific transcripts, possibly even causing enhanced differentiation.

4.5 Seb4 functions as a myogenic regulator

After Seb4 was identified as a direct target of MyoD in our laboratory (Jasper, 1998), overexpression studies revealed that Seb4 induced ectopic skeletal muscle gene expression (Authaler & Rupp, unpublished results). Here in this study, a function for Seb4 as a regulator of the myogenic programme was verified. Loss of function experiments demonstrated that dose-dependent Seb4 depletion caused a very severe muscle phenotype. This included unstructured somites, reduction to loss of muscle-specific gene expression, reduced body size, head and tailbud ablations, indicating loss of muscle tissue. These data strongly suggest that Seb4 is involved in myogenesis controlling the onset of myogenic regulators and perhaps structural properties (Z-lines) of myocyte differentiation.

Intriguingly, the expression of *myoD*, one of the upstream regulators of *Seb4*, was decreased immensely upon *Seb4* depletion. Several growth factor signalling cascades like sonic hedgehog, FGF, Wnt or TGF- β have been implicated to be important for the determination of the muscle lineage (Chanoine & Hardy, 2003). Furthermore, epigenetic mechanisms like histone deacetylase activities have been shown to be involved in the induction of MyoD (Steinbach et al, 2000). At the mid-blastula transition (MBT), which demarcates the onset of zygotic transcription, MyoD is transiently expressed at low levels (Rupp & Weintraub, 1991). This basal gene expression is necessary for the — formerly supposed autocatalytic — upregulation of the expression in the preinvolted mesoderm at the early gastrula stage (Steinbach et al, 1998). It is important to note that in the case of MyoD the induction occurs on an active rather than an inactive locus. Subsequently, during the neurula and the following tailbud stage, MyoD expression is maintained in the paraxial mesoderm and in myocytes, respectively (Hopwood et al, 1989). The competence phase for the upregulation of the *myoD* transcription occurs in a narrow time window of about 90min during the mesodermal competence phase (Steinbach et al, 1998). The window of mesodermal and myogenic competence is terminated by the replacement of the maternal linker histones B4 by somatic linker histones at the end of the gastrulation (Steinbach et al, 1997).

The results achieved here, demonstrate that *Seb4* functions not only downstream but also upstream of *myoD* indicating a feedback loop between both factors at the determination step of the myogenic pathway. *In situ* data revealed, that *seb4* expression is located within the *myoD* expression domain, suggesting that after MyoD induction by FGF, for example, *Seb4* is induced and feeds back on MyoD thereby enhancing the myogenic response in a “wave”, starting in the cells that involute first and are later found most anterior. After complete involution, *Seb4* is expressed in the paraxial mesoderm, correlating exactly with the MyoD expression domain, suggesting a role for *Seb4* in MyoD maintenance expression.

Seb4 regulation of *myoD*, operating either directly or indirectly over one or several factors, is anticipated to occur post-transcriptionally, implying another mode of controlling muscle determination. As mentioned before, one example of post-transcriptional regulation is already shown for *myoD*. During determination, the RRM containing protein HuR causes the stabilization of *myoD* and *myogenin* mRNAs of myoblasts *in vitro* (van der Giessen & Gallouzi, 2007).

Taking these evidences together, the effect of *Seb4* on *myoD* transcription supports the model that at least one role of *Seb4* is maintaining MyoD, thereby enhancing positive feed back loops, altogether boosting the differentiation process

for example via translational activation/stability, like it is shown for VegT regulation by Seb4R (Souopgui et al, 2008).

The early myogenic phenotype of Seb4 depleted embryos has lasting consequences, resulting in dose-dependent impairment of late skeletal muscle differentiation and reduction of skeletal muscle tissue. In accordance with this loss of muscle the body size is greatly reduced. The observed myogenic effects of Seb4 are considered cell autonomous, and are not due to secondary effects of diminished neurogenesis.

In addition to the pro-myogenic role, Seb4 is also required for lens differentiation. Though Seb4 is also strongly expressed in the myocardium during heart development, Seb4 expression is not required (at high levels) for heart differentiation. These results demonstrate that Seb4 is involved in various differentiation processes in *Xenopus* including lens and ear (ectodermal) and skeletal muscle (mesodermal) formation. These findings suggest that Seb4 is controlled by different upstream regulators tissue-specifically, which leads to different outputs, but possibly by a general mechanism.

All these observations suggest a global function for Seb4 operating in fine-tuning the differentiation programme of multiple cell lineages promoting differentiation.

4.6 Conclusions

Seb4 was identified as a direct transcriptional target of MyoD protein, in the early development of *Xenopus*. In this study, I investigated the function of this putative RNA-binding protein Seb4 in *Xenopus*. Seb4 is a small, single RRM-domain protein, which is a member of a subfamily of RNA-binding proteins conserved in human, mouse, fish and *C.elegans*. My results provide evidence that Seb4 is essentially required for myogenesis and lens differentiation in *Xenopus*. Unexpectedly, I found that in embryonic cells Seb4 protein is very abundant. Consistent with this, RNA-coimmunoprecipitation assays have failed to reveal selective RNA-binding of Seb4-specific target RNAs, which could provide information on Seb4 functions. Furthermore, this protein, which I found to be localized in both cytoplasmic and nuclear compartments, elutes as a monomer from Superose6 gelfiltration columns, which so far precluded the identification of interacting partner proteins. Given its tissue-specific expression pattern, the high protein abundance and the fact that no specific targets could be found, I consider Seb4 to have a more

general function in the RNA metabolism of differentiating cells, rather than a selective function in the myogenic regulatory circuit.

4.7 Outlook

In the scope of this work, the RBP Seb4, which is involved in few early differentiation processes in *Xenopus laevis* was characterized. By the means of various biochemical and biological approaches this unexplored protein was examined from many different angles. Besides many successful experiments and fruitful observations, the attempt to identify Seb4 target partners turned out to be very challenging.

The currently available data suggest that a multifunctional nature is more likely to be the rule than the exception among RBPs (Moore, 2005). Dissecting the cellular roles of multifunctional regulators of gene expression through classical approaches involving knock-down or mRNA over-expression is not an easy task, because the upstream functions of the processes such as transcription and splicing cannot be observed. Thus, searching for the functions of Seb4, forces us to integrate new approaches in the future like microarray analyses, e.g. RIP-on-Chip. This begins with Seb4 specific RNA-immunoprecipitations performed with the monoclonal 6E5 antibody. The cDNA copies are then fluorescently labelled and hybridized to DNA microarrays. Putative Seb4 mRNA targets identified through the microarray analysis could be subsequently confirmed by independent RT-PCR analysis, arguing for the specificity of the results obtained. Also expression profiles comparing Seb4-depleted tissue to wildtype tissue could reveal the consequences downstream of Seb4.

Another interesting future experiment would be to discover the implications within a Seb4 expressing cell, in which the subcellular localization of Seb4 was manipulated. Whether a change in its localization behaviour has any functional relevance still has to be determined, but could possibly reveal different functions for Seb4 in the different compartments. This, for instance, could be achieved by mapping the sequence stretch responsible for the right localization and inserting deletions or point mutations into it, in case RNA-binding is uncoupled from localization. Another option is to study the consequences when several nuclear localization signals have been attached to Seb4. Or what happens if Seb4 was tethered to the membrane; would other proteins follow? In the course of this study, the precise localization of Seb4 could also be further analyzed by testing for co-localization with additional markers for subcellular structures, like p-bodies, cajal

bodies or stress granules, to eventually associate a putative role for Seb4. The main challenge here would be the availability of appropriate *Xenopus* antibodies, and the limitations in the cross-reactivity of antibodies from other species.

Furthermore, it would be of great interest, whether the specificity of Seb4 and Seb4R, which show a high degree of similarity, arises from their tissue-specific expression or from protein-functional differences. To address this question, it was shown by overexpression during retinogenesis, that both genes cause the same effects in the retina, suggesting that Seb4, at least when overexpressed in the retina, can interact with the same targets than Seb4R (Boy et al, 2004). The next question to investigate in this context could be if Seb4R when overexpressed in muscle tissue caused the same effects as Seb4. Moreover, could overexpression of Seb4R rescue the Seb4 depletion phenotype obtained by Seb4-MO injection?

Another unresolved and very important issue regards the role of Seb4 during myogenesis. Indeed, several key observations strongly support an active role of Seb4 in this process, most notably the fact that Seb4 is trans-activated by MyoD in proliferating prospective myoblasts and that muscle differentiation is impaired in the absence of Seb4. In addition, I also showed that Seb4 also feeds back on MyoD, implicating that Seb4 is involved in the maintenance of MyoD expression. But what other steps of myoblast determination does Seb4 control? And how is the putative RNA-binding activity linked to myogenesis?

Recent works, including many examples discussed in this study, indicate that the post-transcriptional control of gene expression is much more elaborate and extensive than previously thought, with essentially every step of mRNA metabolism being subject to regulation in a mRNA-specific manner. Thus, a comprehensive understanding of gene expression requires an appreciation for how the lives of mRNAs are influenced by a wide array of diverse regulatory mechanisms carried out by RBPs. Particularly, in the embryo RBPs gain more and more importance as developmental regulators, as gene expression has begun to be regarded as a regulatory network rather than a linear progression of single events.

It will be a future challenge to link developmental programmes with post-transcriptional regulatory networks mediated by RBPs to fully reveal their physiological implications.

Abbreviations

aa	amino acid
ab	antibody
bHLH	basic helix-loop-helix
bp	base pairs
cDNA	complementary DNA
co-IP	coimmunoprecipitation
d	day/days
DEPC	diethylpyrocarbonate
ddH ₂ O	double-distilled water
DNA	deoxyribonucleic acid
e	embryo
e.g.	exempli gratia, for example
et al.	et alii, and others
etc.	et cetera
g	gram
GFP	green fluorescent protein
G-o-F	gain-of-function
GST	glutathione S-transferase
h	hour/hours
HMG	high mobility group
hpf	hours post fertilization
ICC	immunocytochemistry
IF	immunofluorescence
IgG	immunoglobulin
IP	immunoprecipitation
ISH	<i>in situ</i> hybridization
l	liter
kDa	kilodaltons
L-o-F	loss-of-function
min	minutes
M	molar
MBT	mid-blastula transition
ml	milliliter

mM	millimolar
MO	Morpholino
mRNA	messenger ribonucleic acid
mut	mutant
ng	nanogram
nm	nanometer
NTPs	nucleotide triphosphate mixture containing adenosine, guanine, uridine and cytosine
OD	optical density
o/N	over night
PAA	polyacrylamide
PCR	polymerase chain reaction
pmol	picomol
pol	RNA-polymerase II
RBP	RNA-binding protein
RBD	RNA-binding domain
RIP	RNA-immunoprecipitation
RNA	ribonucleic acid
RNP	ribonucleoprotein complex
rpm	revolutions per minute
RRM	RNA-recognition motif
rt	room temperature
RT	reverse transcription
RT-PCR	reverse transcription polymerase chain reaction
SDS	sodium dodecyl sulfate
SDS-PAGE	sodium dodecyl sulfate polyacrylamide gelelectrophoresis
sec	seconds
st.	<i>Xenopus</i> developmental stages according to the normal table of staging of <i>Xenopus laevis</i> (Daudin) after (Niewkoop & Faber, 1994)
std.	standard/control
TNT	transcription and translation
UV	ultraviolet
WB	Western blot analysis
WT	wildtype
µg	microgram
µl	microliter
µM	micromolar

References

Abdelmohsen K, Pullmann R, Jr., Lal A, Kim HH, Galban S, Yang X, Blethrow JD, Walker M, Shubert J, Gillespie DA, Furneaux H, Gorospe M (2007) Phosphorylation of HuR by Chk2 regulates SIRT1 expression. *Mol Cell* **25**(4): 543-557

Adam SA, Nakagawa T, Swanson MS, Woodruff TK, Dreyfuss G (1986) mRNA polyadenylate-binding protein: gene isolation and sequencing and identification of a ribonucleoprotein consensus sequence. *Mol Cell Biol* **6**(8): 2932-2943

Akamatsu W, Okano HJ, Osumi N, Inoue T, Nakamura S, Sakakibara S, Miura M, Matsuo N, Darnell RB, Okano H (1999) Mammalian ELAV-like neuronal RNA-binding proteins HuB and HuC promote neuronal development in both the central and the peripheral nervous systems. *Proc Natl Acad Sci U S A* **96**(17): 9885-9890

Anantharaman V, Koonin EV, Aravind L (2002) Comparative genomics and evolution of proteins involved in RNA metabolism. *Nucleic Acids Res* **30**(7): 1427-1464

Anderson KD, Morin MA, Beckel-Mitchener A, Mobarak CD, Neve RL, Furneaux HM, Burry R, Perrone-Bizzozero NI (2000) Overexpression of HuD, but not of its truncated form HuD I+II, promotes GAP-43 gene expression and neurite outgrowth in PC12 cells in the absence of nerve growth factor. *J Neurochem* **75**(3): 1103-1114

Aoki K, Matsumoto K, Tsujimoto M (2003) Xenopus cold-inducible RNA-binding protein 2 interacts with ElrA, the Xenopus homolog of HuR, and inhibits deadenylation of specific mRNAs. *J Biol Chem* **278**(48): 48491-48497

Arnold HH, Winter B (1998) Muscle differentiation: more complexity to the network of myogenic regulators. *Curr Opin Genet Dev* **8**(5): 539-544

Auweter SD, Fasan R, Reymond L, Underwood JG, Black DL, Pitsch S, Allain FH (2006) Molecular basis of RNA recognition by the human alternative splicing factor Fox-1. *EMBO J* **25**(1): 163-173

Baneyx F (1999) Recombinant protein expression in Escherichia coli. *Curr Opin Biotechnol* **10**(5): 411-421

Barreau C, Paillard L, Osborne HB (2005) AU-rich elements and associated factors: are there unifying principles? *Nucleic Acids Res* **33**(22): 7138-7150

Berglund JA, Abovich N, Rosbash M (1998) A cooperative interaction between U2AF65 and mBBP/SF1 facilitates branchpoint region recognition. *Genes Dev* **12**(6): 858-867

Berkes Ch, Tapscott S. (2005) MyoD and the transcriptional control of myogenesis. *Cell & Dev Biol* **16**, 585-595

- Borello U, Buffa V, Sonnino C, Melchionna R, Vivarelli E, Cossu G (1999) Differential expression of the Wnt putative receptors Frizzled during mouse somitogenesis. *Mech Dev* **89**(1-2): 173-177
- Boudjelida H, Muntz L (1987) Multinucleation during myogenesis of the myotome of *Xenopus laevis*: a qualitative study. *Development* **101**(3): 583-590
- Boy S, Souopgui J, Amato MA, Wegnez M, Pieler T, Perron M (2004) XSEB4R, a novel RNA-binding protein involved in retinal cell differentiation downstream of bHLH proneural genes. *Development* **131**(4): 851-862
- Brennan CM, Steitz JA (2001) HuR and mRNA stability. *Cell Mol Life Sci* **58**(2): 266-277
- Brown T, Mackey K, Du T (2004) Analysis of RNA by Northern and Slot Blot Hybridization. *Current Protocols in Molecular Biology*. Unit 4.9
- Brunekreef GA, van Genesen ST, Destree OH, Lubsen NH (1997) Extralenticular expression of *Xenopus laevis* alpha-, beta-, and gamma-crystallin genes. *Invest Ophthalmol Vis Sci* **38**(13): 2764-2771
- Bushati N, Cohen SM (2007) MicroRNA Functions. *Ann. Rev. Cell Dev. Biol* **23**: 175-205
- Callis TE, Deng Z, Chen JF, Wang DZ (2008) Muscling through the microRNA world. *Exp Biol Med (Maywood)* **233**(2): 131-138
- Chanoine C, Hardy S (2003) *Xenopus* muscle development: from primary to secondary myogenesis. *Dev Dyn* **226**: 12-23
- Chen A, Ginty D, Fan C. (2005) Protein kinase A signalling via CREB controls myogenesis induced by Wnt proteins. *Nature*; (**433**) 317-322
- Cheng S, Gallie DR. (2007) IF4G, eIF4G, and eIF4B bind the poly(A)-binding protein through overlapping sites within the RNA recognition motif domains. *J Biol Chem.* **282** (35): 25247-58
- Clements D, Friday RV, Woodland HR (1999) Mode of action of VegT in mesoderm and endoderm formation. *Development* **126**(21): 4903-4911
- Clery A, Blatter M, Allain FH (2008) RNA recognition motifs: boring? Not quite. *Curr Opin Struct Biol* **18**(3): 290-298
- Colegrove-Otero LJ, Devaux A, Standart N (2005) The *Xenopus* ELAV protein ElrB represses Vg1 mRNA translation during oogenesis. *Mol Cell Biol* **25**(20): 9028-9039
- Conlon FL, Sedgwick SG, Weston KM, Smith JC (1996) Inhibition of Xbra transcription activation causes defects in mesodermal patterning and reveals autoregulation of Xbra in dorsal mesoderm. *Development* **122**(8): 2427-2435
- De Leeuw F, Zhang T, Wauquier C, Huez G, Kruys V, Gueydan C (2007) The cold-inducible RNA-binding protein migrates from the nucleus to cytoplasmic stress granules by a methylation-dependent mechanism and acts as a translational repressor. *Exp Cell Res* **313**(20): 4130-4144

Della Gaspera B, Sequeira I, Charbonnier F, Becker C, Shi DL, Chanoine C. (2006) Spatio-temporal expression of MRF4 transcripts and protein during *Xenopus laevis* embryogenesis. *Dev Dyn.* Feb; **235**(2):524-9.

Deo RC, Bonanno JB, Sonenberg N, Burley SK (1999) Recognition of polyadenylate RNA by the poly(A)-binding protein. *Cell* **98**(6): 835-845

Deshler JO, Highett MI, Schnapp BJ (1997) Localization of *Xenopus* Vg1 mRNA by Vera protein and the endoplasmic reticulum. *Science* **276**(5315): 1128-1131

Ding J, Hayashi MK, Zhang Y, Manche L, Krainer AR, Xu RM (1999) Crystal structure of the two-RRM domain of hnRNP A1 (UP1) complexed with single-stranded telomeric DNA. *Genes Dev* **13**(9): 1102-1115

Dosch R, Gawantka V, Delius H, Blumenstock C, Niehrs C (1997) Bmp-4 acts as a morphogen in dorsoventral mesoderm patterning in *Xenopus*. *Development* **124**(12): 2325-2334

Dreyfuss G, Swanson MS, Pinol-Roma S (1988) Heterogeneous nuclear ribonucleoprotein particles and the pathway of mRNA formation. *Trends Biochem Sci* **13**(3): 86-91

Drysdale TA, Tonissen KF, Patterson KD, Crawford MJ, Krieg PA (1994) Cardiac troponin I is a heart-specific marker in the *Xenopus* embryo: expression during abnormal heart morphogenesis. *Dev Biol* **165**(2): 432-441

Fan XC, Steitz JA (1998) Overexpression of HuR, a nuclear-cytoplasmic shuttling protein, increases the in vivo stability of ARE-containing mRNAs. *EMBO J* **17**(12): 3448-3460

Fetka I, Radeghieri A, Bouwmeester T (2000) Expression of the RNA recognition motif-containing protein SEB-4 during *Xenopus* embryonic development. *Mech Dev* **94**(1-2): 283-286

Figuroa A, Cuadrado A, Fan J, Atasoy U, Muscat GE, Munoz-Canoves P, Gorospe M, Munoz A (2003) Role of HuR in skeletal myogenesis through coordinate regulation of muscle differentiation genes. *Mol Cell Biol* **23**(14): 4991-5004

Finn RD, Mistry J, Schuster-Bockler B, Griffiths-Jones S, Hollich V, Lassmann T, Moxon S, Marshall M, Khanna A, Durbin R, Eddy SR, Sonnhammer EL, Bateman A (2006) Pfam: clans, web tools and services. *Nucleic Acids Res* **34**(Database issue): D247-251

Frydenberg J, Poulsen K, Petersen AK, Lund A, Olesen OF (1991) Isolation and characterization of the gene encoding EF-1 alpha O, an elongation factor 1-alpha expressed during early development of *Xenopus laevis*. *Gene* **109**(2): 185-192

Fujiwara T, Mori Y, Chu DL, Koyama Y, Miyata S, Tanaka H, Yachi K, Kubo T, Yoshikawa H, Tohyama M (2006) CARM1 regulates proliferation of PC12 cells by methylating HuD. *Mol Cell Biol* **26**(6): 2273-2285

Gama-Carvalho M, Barbosa-Morais NL, Brodsky AS, Silver PA, Carmo-Fonseca M (2006) Genome-wide identification of functionally distinct subsets of cellular mRNAs associated with two nucleocytoplasmic-shuttling mammalian splicing factors. *Genome Biol* **7**(11): R113

- Gama-Carvalho M, Carvalho MP, Kehlenbach A, Valcarcel J, Carmo-Fonseca M (2001) Nucleocytoplasmic shuttling of heterodimeric splicing factor U2AF. *J Biol Chem* **276**(16): 13104-13112
- Gebauer F, Hentze MW (2004) Molecular mechanisms of translational control. *Nat Rev Mol Cell Biol* **5**(10): 827-835
- Gerber WV, Vokes SA, Zearfoss NR, Krieg PA (2002) A role for the RNA-binding protein, hermes, in the regulation of heart development. *Dev Biol* **247**(1): 116-126
- Gerber WV, Yatskievych TA, Antin PB, Correia KM, Conlon RA, Krieg PA (1999) The RNA-binding protein gene, hermes, is expressed at high levels in the developing heart. *Mech Dev* **80**(1): 77-86
- Gilbert SF (2000) *Developmental Biology, 6th Edition*, Sunderland, Massachusetts: by Sinauer Associates, Inc.
- Glisovic T, Bachorik JL, Yong J, Dreyfuss G (2008) RNA-binding proteins and post-transcriptional gene regulation. *FEBS Lett* **582**(14): 1977-1986
- Golas MM, Sander B, Will CL, Luhrmann R, Stark H (2003) Molecular architecture of the multiprotein splicing factor SF3b. *Science* **300**(5621): 980-984
- Good PJ, Abler L, Herring D, Sheets MD (2004) Xenopus embryonic poly(A) binding protein 2 (ePABP2) defines a new family of cytoplasmic poly(A) binding proteins expressed during the early stages of vertebrate development. *Genesis* **38**(4): 166-175
- Graveley BR (2000) Sorting out the complexity of SR protein functions. *RNA* **6**(9): 1197-1211
- Greenbaum D, Colangelo C, Williams K, Gerstein M (2003) Comparing protein abundance and mRNA expression levels on a genomic scale. *Genome Biol* **4**(9): 117
- Gritsman K, Talbot WS, Schier AF (2000) Nodal signalling patterns the organizer. *Development* **127**(5): 921-932
- Grunz H, McKeehan WL, Knochel W, Born J, Tiedemann H (1988) Induction of mesodermal tissues by acidic and basic heparin binding growth factors. *Cell Differ* **22**(3): 183-189
- Guo X, Hartley RS (2006) HuR contributes to cyclin E1 deregulation in MCF-7 breast cancer cells. *Cancer Res* **66**(16): 7948-7956
- Gurdon JB, Dyson S, St Johnston D (1998) Cells' perception of position in a concentration gradient. *Cell* **95**(2): 159-162
- Halbeisen RE, Galgano A, Scherrer T, Gerber AP (2008) Post-transcriptional gene regulation: from genome-wide studies to principles. *Cell Mol Life Sci* **65**(5): 798-813
- Hamilton L (1969) The formation of somites in Xenopus. *J Embryol Exp Morphol* **22**(2): 253-264

Handa N, Nureki O, Kurimoto K, Kim I, Sakamoto H, Shimura Y, Muto Y, Yokoyama S (1999) Structural basis for recognition of the tra mRNA precursor by the Sex-lethal protein. *Nature* **398**(6728): 579-585

Handwerger KE, Gall JG (2006) Subnuclear organelles: new insights into form and function. *Trends Cell Biol* **16**(1): 19-26

Hargous Y, Hautbergue GM, Tintaru AM, Skrisovska L, Golovanov AP, Stevenin J, Lian LY, Wilson SA, Allain FH (2006) Molecular basis of RNA recognition and TAP binding by the SR proteins SRp20 and 9G8. *EMBO J* **25**(21): 5126-5137

Heasman J (2002) Morpholino oligos: making sense of antisense? *Dev Biol* **243**(2): 209-214

Heasman J (2006) Patterning the early *Xenopus* embryo. *Development* **133**(7): 1205-1217

Heasman J, Crawford A, Goldstone K, Garner-Hamrick P, Gumbiner B, McCrea P, Kintner C, Noro CY, Wylie C (1994) Overexpression of cadherins and underexpression of beta-catenin inhibit dorsal mesoderm induction in early *Xenopus* embryos. *Cell* **79**(5): 791-803

Heasman J, Kofron M, Wylie C (2000) Beta-catenin signalling activity dissected in the early *Xenopus* embryo: a novel antisense approach. *Dev Biol* **222**(1): 124-134

Hopwood ND, Pluck A, Gurdon JB (1989) MyoD expression in the forming somites is an early response to mesoderm induction in *Xenopus* embryos. *EMBO J* **8**(11): 3409-3417

Hopwood ND, Pluck A, Gurdon JB (1991) *Xenopus* Myf-5 marks early muscle cells and can activate muscle genes ectopically in early embryos. *Development* **111**(2): 551-560

Hopwood ND, Pluck A, Gurdon JB, Dilworth SM (1992) Expression of XMyoD protein in early *Xenopus laevis* embryos. *Development* **114**(1): 31-38

Houseley J, LaCava J, Tollervey D (2006) RNA-quality control by the exosome. *Nat Rev Mol Cell Biol* **7**(7): 529-539

Howe KJ (2002) RNA polymerase II conducts a symphony of pre-mRNA processing activities. *Biochim Biophys Acta* **1577**(2): 308-324

Huang Y, Gattoni R, Stevenin J, Steitz JA (2003) SR splicing factors serve as adapter proteins for TAP-dependent mRNA export. *Mol Cell* **11**(3): 837-843

Hyde CE, Old RW (2000) Regulation of the early expression of the *Xenopus* nodal-related 1 gene, *Xnr1*. *Development* **127**(6): 1221-1229

Imai Y, Talbot WS (2001) Morpholino phenocopies of the *bmp2b/swirl* and *bmp7/snailhouse* mutations. *Genesis* **30**(3): 160-163

Jani K, Schöck F, (2007) Zasp is required for the assembly of functional integrin adhesion sites. *J Cell Biol.* **179**(7): 1583–1597

- Jasper H (1998) Identifizierung eines Zielgens des Transkriptionsfaktors MyoD mittels subtraktiver cDNA-Hybridisierung. Eberhard-Karls-Universität Tübingen
- Karlen S, Rebagliati M (2001) A morpholino phenocopy of the cyclops mutation. *Genesis* **30**(3): 126-128
- Kassar-Duchossoy L, Gayraud-Morel B, Gomes D, Rocancourt D, Buckingham M, Shinin V. (2004) Mrf4 determines skeletal muscle identity in Myf5:MyoD double-mutant mice. *Nature* **431**, 466-71
- Kedersha N, Stoecklin G, Ayodele M, Yacono P, Lykke-Andersen J, Fritzler MJ, Scheuner D, Kaufman RJ, Golan DE, Anderson P (2005) Stress granules and processing bodies are dynamically linked sites of mRNP remodeling. *J Cell Biol* **169**(6): 871-884
- Keene JD (2007) RNA regulons: coordination of post-transcriptional events. *Nat Rev Genet* **8**(7): 533-543
- Khokha MK, Yeh J, Grammer TC, Harland RM (2005) Depletion of three BMP antagonists from Spemann's organizer leads to a catastrophic loss of dorsal structures. *Dev Cell* **8**(3): 401-411
- Kielkopf CL, Rodionova NA, Green MR, Burley SK (2001) A novel peptide recognition mode revealed by the X-ray structure of a core U2AF35/U2AF65 heterodimer. *Cell* **106**(5): 595-605
- Kim-Ha J, Kerr K, Macdonald PM (1995) Translational regulation of oskar mRNA by bruno, an ovarian RNA-binding protein, is essential. *Cell* **81**(3): 403-412
- Kimelman D, Kirschner M (1987) Synergistic induction of mesoderm by FGF and TGF-beta and the identification of an mRNA coding for FGF in the early Xenopus embryo. *Cell* **51**(5): 869-877
- Kimelman D, Schier AF (2002) Mesoderm induction and patterning. *Results Probl Cell Differ* **40**: 15-27
- Kloc M, Etkin LD. RNA localization mechanisms in oocytes. (2005) *J Cell Sci.* **15** (118):269-82.
- Kofron M, Demel T, Xanthos J, Lohr J, Sun B, Sive H, Osada S, Wright C, Wylie C, Heasman J (1999) Mesoderm induction in Xenopus is a zygotic event regulated by maternal VegT via TGFbeta growth factors. *Development* **126**(24): 5759-5770
- Kofron M, Wylie C, Heasman J (2004) The role of Mixer in patterning the early Xenopus embryo. *Development* **131**(10): 2431-2441
- Kohler A, Schmidt-Zachmann MS, Franke WW (1997) AND-1, a natural chimeric DNA-binding protein, combines an HMG-box with regulatory WD-repeats. *J Cell Sci* **110** (Pt 9): 1051-1062
- Kosaka K, Kawakami K, Sakamoto H, Inoue K (2007) Spatiotemporal localization of germ plasm RNAs during zebrafish oogenesis. *Mech Dev* **124**(4): 279-289
- Kuhn U, Pieler T (1996) Xenopus poly(A) binding protein: functional domains in RNA binding and protein-protein interaction. *J Mol Biol* **256**(1): 20-30

- Kunz M, Herrmann M, Wedlich D, Gradl D (2004) Autoregulation of canonical Wnt signalling controls midbrain development. *Dev Biol* **273**(2): 390-401
- Lai MC, Lin RI, Tarn WY (2001) Transportin-SR2 mediates nuclear import of phosphorylated SR proteins. *Proc Natl Acad Sci U S A* **98**(18): 10154-10159
- Lamond AI, Spector DL (2003) Nuclear speckles: a model for nuclear organelles. *Nat Rev Mol Cell Biol* **4**(8): 605-612
- Lee MH, Schedl T (2006) RNA-binding proteins. *WormBook*: 1-13
- Lele Z, Bakkars J, Hammerschmidt M (2001) Morpholino phenocopies of the swirl, snailhouse, somitabun, minifin, silberblick, and pipetail mutations. *Genesis* **30**(3): 190-194
- Li C, Lin RI, Lai MC, Ouyang P, Tarn WY (2003) Nuclear Pnn/DRS protein binds to spliced mRNPs and participates in mRNA processing and export via interaction with RNPS1. *Mol Cell Biol* **23**(20): 7363-7376
- Lodish, Berk, Zipursky, Matsudaira, Baltimore, Darnell (2000) *Molecular Cell Biology*, Fourth Edition Freeman edn.: W. H. Freeman and Company.
- Lou H, Neugebauer KM, Gagel RF, Berget SM (1998) Regulation of alternative polyadenylation by U1 snRNPs and SRp20. *Mol Cell Biol* **18**(9): 4977-4985
- Luo MJ, Reed R (2003) Identification of RNA binding proteins by UV cross-linking. *Curr Protoc Mol Biol* **Chapter 27**: Unit 27 22
- Luther PK, Padron R, Ritter S, Craig R, Squire JM (2003) Heterogeneity of Z-band structure within a single muscle sarcomere: implications for sarcomere assembly. *J Mol Biol* **332**(1): 161-169
- Manley JL, Tacke R (1996) SR proteins and splicing control. *Genes Dev* **10**(13): 1569-1579
- Maris C, Dominguez C, Allain FH (2005) The RNA recognition motif, a plastic RNA-binding platform to regulate post-transcriptional gene expression. *FEBS J* **272**(9): 2118-2131
- Martin BL, Harland RM (2001) Hypaxial muscle migration during primary myogenesis in *Xenopus laevis*. *Dev Biol* **239**(2): 270-280
- Maruyama K, Sato N, Ohta N (1999) Conservation of structure and cold-regulation of RNA-binding proteins in cyanobacteria: probable convergent evolution with eukaryotic glycine-rich RNA-binding proteins. *Nucleic Acids Res* **27**(9): 2029-2036
- McMahon AP, Moon RT (1989) Ectopic expression of the proto-oncogene int-1 in *Xenopus* embryos leads to duplication of the embryonic axis. *Cell* **58**(6): 1075-1084
- Melton DA (1987) Translocation of a localized maternal mRNA to the vegetal pole of *Xenopus* oocytes. *Nature* **328**(6125): 80-82
- Mohun TJ, Brennan S, Dathan N, Fairman S, Gurdon JB (1984) Cell type-specific activation of actin genes in the early amphibian embryo. *Nature* **311** 716-721

- Mollet S, Cougot N, Wilczynska A, Dautry F, Kress M, Bertrand E, Weil D (2008) Translationally Repressed mRNA Transiently Cycles through Stress Granules during Stress. *Mol Biol Cell* **10**:4469-79
- Monecke T, Schell S, Dickmanns A, Ficner R (2008) Crystal Structure of the RRM Domain of Poly(A)-Specific Ribonuclease Reveals a Novel m(7)G-Cap-Binding Mode. *J Mol Biol* **382**(4):827-34
- Moore MJ (2005) From birth to death: the complex lives of eukaryotic mRNAs. *Science* **309**(5740): 1514-1518
- Müller-Esterl W (2004) *Biochemie*: Elsevier Spektrum.
- Muntz L (1975) Myogenesis in the trunk and leg during development of the tadpole of *Xenopus laevis* (Daudin 1802). *J Embryol Exp Morphol* **33**(3): 757-774
- Namboodiri VM, Akey IV, Schmidt-Zachmann MS, Head JF, Akey CW (2004) The structure and function of *Xenopus* NO38-core, a histone chaperone in the nucleolus. *Structure* **12**(12): 2149-2160
- Nasevicius A, Ekker SC (2000) Effective targeted gene 'knockdown' in zebrafish. *Nat Genet* **26**(2): 216-220
- Nicolas N, Gallien CL, Chanoine C (1998) Expression of myogenic regulatory factors during muscle development of *Xenopus*: myogenin mRNA accumulation is limited strictly to secondary myogenesis. *Dev Dyn* **213**(3): 309-321
- Nieuwkoop PD, Faber, J. (1967) Normal Tables of *Xenopus laevis*, Amsterdam, North Holland.
- Nieuwkoop PD, Faber J (1994) Normal Table of *Xenopus laevis* (daudin), Vol. Second edition, reprint, New York & London: GARLAND PUBLISHING ,INC.
- Nishikawa A, Hayashi H (1994) Isoform transition of contractile proteins related to muscle remodeling with an axial gradient during metamorphosis in *Xenopus laevis*. *Dev Biol* **165**(1): 86-94
- Noramly S, Grainger RM (2002) Determination of the embryonic inner ear. *J Neurobiol* **53**(2): 100-128
- Parker R, Song H (2004) The enzymes and control of eukaryotic mRNA turnover. *Nat Struct Mol Biol* **11**(2): 121-127
- Pascale A, Amadio M, Quattrone A (2008) Defining a neuron: neuronal ELAV proteins. *Cell Mol Life Sci* **65**(1): 128-140
- Perron M, Bourlito P, Wegnez M, Theodore L (1997) Subcellular distribution of *Xenopus* XEL-1 protein, a member of the neuron-specific ELAV/Hu family, revealed by epitope tagging. *DNA Cell Biol* **16**(5): 579-587
- Perron M, Furrer MP, Wegnez M, Theodore L (1999) Misexpression of the RNA-binding protein ELRB in *Xenopus* presumptive neuroectoderm induces proliferation arrest and programmed cell death. *Int J Dev Biol* **43**(4): 295-303

- Prieto JL, McStay B (2007) Recruitment of factors linking transcription and processing of pre-rRNA to NOR chromatin is UBF-dependent and occurs independent of transcription in human cells. *Genes Dev* **21**(16): 2041-2054
- Reed R, Cheng H (2005) TREX, SR proteins and export of mRNA. *Curr Opin Cell Biol* **17**(3): 269-273
- Richter K, Good PJ, Dawid IB (1990) A developmentally regulated, nervous system-specific gene in *Xenopus* encodes a putative RNA-binding protein. *New Biol* **2**(6): 556-565
- Rosa F, Roberts AB, Danielpour D, Dart LL, Sporn MB, Dawid IB (1988) Mesoderm induction in amphibians: the role of TGF-beta 2-like factors. *Science* **239**(4841 Pt 1): 783-785
- Roth JF, Shikama N, Henzen C, Desbaillets I, Lutz W, Marino S, Wittwer J, Schorle H, Gassmann M, Eckner R. (2003) Differential role of p300 and CBP acetyltransferase during myogenesis: p300 acts upstream of MyoD and Myf5. *EMBO J*; (**22**) 5186–5196.
- Rupp, RA and Weintraub, H (1991) Ubiquitous MyoD transcription at the midblastula transition precedes induction-dependent MyoD expression in presumptive mesoderm of *X. laevis*. *Cell* **65**: 927-937.
- Rupp RA, Snider L, Weintraub H (1994) *Xenopus* embryos regulate the nuclear localization of XMyoD. *Genes Dev* **8**(11): 1311-1323
- Sambrook J, Fritsch EF, Maniatis T (1989) *Molecular Cloning. A laboratory manual*, 2nd edn. New York: Cold Spring Harbour Laboratory Press.
- Sartorelli V, Caretti G (2005) Mechanisms underlying the transcriptional regulation of skeletal myogenesis. *Curr Opin Genet Dev.* **15**(5): 528–535.
- Scales JB, Olson EN, Perry M (1990) Two distinct *Xenopus* genes with homology to MyoD1 are expressed before somite formation in early embryogenesis. *Mol Cell Biol* **10**(4): 1516-1524
- Scherly D, Boelens W, van Venrooij WJ, Dathan NA, Hamm J, Mattaj IW (1989) Identification of the RNA binding segment of human U1 A protein and definition of its binding site on U1 snRNA. *EMBO J* **8**(13): 4163-4170
- Schlosser G, Northcutt RG (2000) Development of neurogenic placodes in *Xenopus laevis*. *J Comp Neurol* **418**(2): 121-146
- Schohl A, Fagotto F (2003) A role for maternal beta-catenin in early mesoderm induction in *Xenopus*. *EMBO J* **22**(13): 3303-3313
- Schwartz SP, Aisenthal L, Elisha Z, Oberman F, Yisraeli JK (1992) A 69-kDa RNA-binding protein from *Xenopus* oocytes recognizes a common motif in two vegetally localized maternal mRNAs. *Proc Natl Acad Sci U S A* **89**(24): 11895-11899
- Shamoo Y, Abdul-Manan N, Patten AM, Crawford JK, Pellegrini MC, Williams KR (1994) Both RNA-binding domains in heterogenous nuclear ribonucleoprotein A1 contribute toward single-stranded-RNA binding. *Biochemistry* **33**(27): 8272-8281

- Shamoo Y, Abdul-Manan N, Williams KR (1995) Multiple RNA binding domains (RBDs) just don't add up. *Nucleic Acids Res* **23**(5): 725-728
- Shi Y, Reddy B, Manley JL (2006) PP1/PP2A phosphatases are required for the second step of Pre-mRNA splicing and target specific snRNP proteins. *Mol Cell* **23**(6): 819-829
- Shu L, Yan W, Chen X. RNPC1, an RNA-binding protein and a target of the p53 family, is required for maintaining the stability of the basal and stress-induced p21 transcript. *Genes Dev.* **20**(21):2961-72
- Showell C, Binder O, Conlon FL (2004) T-box genes in early embryogenesis. *Dev Dyn* **229**(1): 201-218
- Simpson PJ, Monie TP, Szendroi A, Davydova N, Tyzack JK, Conte MR, Read CM, Cary PD, Svergun DI, Konarev PV, Curry S, Matthews S (2004) Structure and RNA interactions of the N-terminal RRM domains of PTB. *Structure* **12**(9): 1631-1643
- Skrisovska L, Bourgeois CF, Stefl R, Grellscheid SN, Kister L, Wenter P, Elliott DJ, Stevenin J, Allain FH (2007) The testis-specific human protein RBMY recognizes RNA through a novel mode of interaction. *EMBO Rep* **8**(4): 372-379
- Slack JM, Darlington BG, Heath JK, Godsave SF (1987) Mesoderm induction in early *Xenopus* embryos by heparin-binding growth factors. *Nature* **326**(6109): 197-200
- Slevin MK, Gourronc F, Hartley RS (2007) ElrA binding to the 3'UTR of cyclin E1 mRNA requires polyadenylation elements. *Nucleic Acids Res* **35**(7): 2167-2176
- Song HW, Cauffman K, Chan AP, Zhou Y, King ML, Etkin LD, Kloc M (2007) Hermes RNA-binding protein targets RNAs-encoding proteins involved in meiotic maturation, early cleavage, and germline development. *Differentiation* **75**(6): 519-528
- Souopgui J, Rust B, Vanhomwegen J, Heasman J, Henningfeld KA, Bellefroid E, Pieler T (2008) The RNA-binding protein XSeb4R: a positive regulator of VegT mRNA stability and translation that is required for germ layer formation in *Xenopus*. *Genes Dev* **22**(17): 2347-2352
- Spadaccini R, Reidt U, Dybkov O, Will C, Frank R, Stier G, Corsini L, Wahl MC, Luhrmann R, Sattler M (2006) Biochemical and NMR analyses of an SF3b155-p14-U2AF-RNA interaction network involved in branch point definition during pre-mRNA splicing. *RNA* **12**(3): 410-425
- St Johnston D (2005) Moving messages: the intracellular localization of mRNAs. *Nat Rev Mol Cell Biol* **6**(5): 363-375
- Steinbach OC, Ulshofer A, Authaler A, Rupp RA (1998) Temporal restriction of MyoD induction and autocatalysis during *Xenopus* mesoderm formation. *Dev Biol* **202**(2): 280-292
- Steinbach OC, Wolffe AP, Rupp RA (1997) Somatic linker histones cause loss of mesodermal competence in *Xenopus*. *Nature* **389**(6649): 395-399
- Steinbach OC, Wolffe AP, Rupp RA (2000) Histone deacetylase activity is required for the induction of the MyoD muscle cell lineage in *Xenopus*. *Biol Chem* **381**(9-10): 1013-1016

- Stewart M (2007) Ratcheting mRNA out of the nucleus. *Mol Cell* **25**(3): 327-330
- Theze N, Hardy S, Wilson R, Allo MR, Mohun T, Thiebaud P (1995) The MLC1f/3f gene is an early marker of somitic muscle differentiation in *Xenopus laevis* embryo. *Dev Biol* **171**(2): 352-362
- van der Giessen K, Gallouzi IE (2007) Involvement of transportin 2-mediated HuR import in muscle cell differentiation. *Mol Biol Cell* **18**(7): 2619-2629
- Vermaak D, Steinbach OC, Dimitrov S, Rupp RA, Wolffe AP (1998) The globular domain of histone H1 is sufficient to direct specific gene repression in early *Xenopus* embryos. *Curr Biol* **8**(9): 533-536
- Wang X, Tanaka Hall TM (2001) Structural basis for recognition of AU-rich element RNA by the HuD protein. *Nat Struct Biol* **8**(2): 141-145
- Wessely O, De Robertis EM (2000) The *Xenopus* homologue of Bicaudal-C is a localized maternal mRNA that can induce endoderm formation. *Development* **127**(10): 2053-2062
- Williamson JR (2000) Induced fit in RNA-protein recognition. *Nat Struct Biol* **7**(10): 834-837
- Wilmore HP, McClive PJ, Smith CA, Sinclair AH (2005) Expression profile of the RNA-binding protein gene hermes during chicken embryonic development. *Dev Dyn* **233**(3): 1045-1051
- Wolpert L (1998) *Principles of Development*, Oxford: Current Biology.
- Wu S, Romfo CM, Nilsen TW, Green MR (1999) Functional recognition of the 3' splice site AG by the splicing factor U2AF35. *Nature* **402**(6763): 832-835
- Xanthos JB, Kofron M, Tao Q, Schaible K, Wylie C, Heasman J (2002) The roles of three signalling pathways in the formation and function of the Spemann Organizer. *Development* **129**(17): 4027-4043
- Xanthos JB, Kofron M, Wylie C, Heasman J (2001) Maternal VegT is the initiator of a molecular network specifying endoderm in *Xenopus laevis*. *Development* **128**(2): 167-180
- Yisraeli JK (2005) VICKZ proteins: a multi-talented family of regulatory RNA-binding proteins. *Biol Cell* **97**(1): 87-96
- Yokota C, Kofron M, Zuck M, Houston DW, Isaacs H, Asashima M, Wylie CC, Heasman J (2003) A novel role for a nodal-related protein; Xnr3 regulates convergent extension movements via the FGF receptor. *Development* **130**(10): 2199-2212
- Youn BW, Malacinski GM (1981) Comparative analysis of amphibian somite morphogenesis: cell rearrangement patterns during rosette formation and myoblast fusion. *J Embryol Exp Morphol* **66**: 1-26
- Zearfoss NR, Chan AP, Wu CF, Kloc M, Etkin LD (2004) Hermes is a localized factor regulating cleavage of vegetal blastomeres in *Xenopus laevis*. *Dev Biol* **267**(1): 60-71

Zhang J, Houston DW, King ML, Payne C, Wylie C, Heasman J (1998) The role of maternal VegT in establishing the primary germ layers in *Xenopus* embryos. *Cell* **94**(4): 515-524

Zhang T, Delestienne N, Huez G, Krays V, Gueydan C (2005) Identification of the sequence determinants mediating the nucleo-cytoplasmic shuttling of TIAR and TIA-1 RNA-binding proteins. *J Cell Sci* **118**(Pt 23): 5453-5463

Zhou HL, Lou H (2008) Repression of prespliceosome complex formation at two distinct steps by Fox-1/Fox-2 proteins. *Mol Cell Biol* **28**(17): 5507-5516

Zorio DA, Blumenthal T (1999) Both subunits of U2AF recognize the 3' splice site in *Caenorhabditis elegans*. *Nature* **402**(6763): 835-838